

DEVELOPMENT OF AN ALGAL OPTICAL DENSITY SENSOR

A Thesis

by

YAO YAO

Submitted to the Office of Graduate and Professional Studies
Texas A&M University
in partial fulfillment of the requirements for the degree of

MASTER OF SCIENCE

Chair of Committee,	Yufeng Ge
Committee Members,	Ruixiu Sui
	Ronald E. Lacey
	Timothy P. Devarenne
Head of Department,	Stephen W. Searcy

December 2013

Major Subject: Biological and Agricultural Engineering

Copyright 2013 Yao Yao

ABSTRACT

Algae, which are high in lipids productivity and photosynthesis rate, have the potential to be one of the major sources for large scale biodiesel production due to the lack of the fossil fuel. Optical density (OD) which is directly related to algal density in culture media is a key parameter for the automation of production systems. In order to save labor, cost, and realize a fully automatic algal production system, an OD sensor was developed. To evaluate its performance, current to voltage amplifiers, LED drivers and the system power were designed and built to drive the LEDs in the sensor and process the signal. Also, a program was created for the data-acquisition system used with the sensor to record and plot the output data. The sensor was calibrated and tested under both lab and raceway environments. During the tests, more issues were discovered, such as temperature drift, unstable output signal, and noise problems during the tests. In order to achieve a more robust and repeatable output, a new sensor was developed based on the original sensor. First, the sensor housing was redesigned to accommodate a new optical measurement configuration. Second, a constant current LED driver circuit was built to stabilize the LEDs illumination output. Third, a feedback temperature control mechanism was built to control the temperature of LEDs in order to reduce output temperature drift. Finally, a logarithmic IC chip was used for processing of raw outputs from photodiodes. All the parts were assembled and enclosed in a specially modified box. Then, the new sensor was calibrated and tested in the lab and raceway production environments. The results showed that the performance of the sensor was improved.

ACKNOWLEDGEMENTS

This project could not be possible without the support from U.S. Dept. of Energy through National Alliance for Advanced Biofuels and Bio-Products (NAABB). Also, thanks are given to Air Force Research Laboratory through General Atomics for the initial sensor development.

I would like to thank Dr. Ron Lacey for allowing me use his lab to test the sensor, his research associate Scott Emsoff, graduate students Derek Kovalcik, Phillip Luedecke to assist me on the raceway testing. Also, thanks should go to Mathew Shimek of BAEN machine shop for manufacturing the design of the sensor housing; Viktor Vlassov of the Texas Engineering Experiment Station for helping construct electronic circuits and sensor housing.

Thanks to Dr. Thomasson allowing me to participate in this project; my committee Chair, Dr. Ge, and my committee member Dr. Sui, Dr. Lacey, and Dr. Devarenne for their guidance and support throughout this research. Thanks also go to my friends and colleagues and the department faculty and staff for their support and help. Also, thank TI for providing me sample electronic chips. Finally, I would give special thanks to my family for their encouragement, love and support.

TABLE OF CONTENTS

	Page
ABSTRACT	ii
ACKNOWLEDGEMENTS	iii
TABLE OF CONTENTS	iv
LIST OF FIGURES.....	vi
LIST OF TABLES	x
1. INTRODUCTION AND LITERATURE REVIEW.....	1
1.1 Introduction	1
1.1.1 Composition of Algae	1
1.1.2 Benefits of Algae Production	2
1.1.3 Requirements of Mass Algae Production.....	4
1.2 Literature Review.....	6
1.2.1 Biomass Determination Methods	6
1.2.2 OD Sensors.....	9
1.3 Objectives.....	14
2. ORIGINAL SENSOR	16
2.1 Design and Construction of the Original Sensor System.....	16
2.1.1 Review of the Operation Theory and Structure of the Original Sensor	16
2.1.2 Overall View of Sensor System Structure.....	18
2.1.3 Circuits Design.....	19
2.1.5 Calibration of Temperature Monitoring Unit.....	25
2.1.6 Software.....	27
2.2 Preliminary Tests.....	29
2.2.1 Initial Tests and Calibration Procedure	30
2.2.2 Main Tests and Calibration Procedure	32
2.2.3 Sensor System Temperature Stability Tests.....	33
3. REDESIGNED SENSOR	35
3.1 Design and Construction of the Redesigned Sensor System	35
3.1.1 Overall Modifications.....	35
3.1.2 Design of the Circuits.....	36
3.1.3 Redesign and Assembly of the Sensor System Housing.....	50

3.1.4 Software.....	59
3.2 Tests of the Redesigned Sensor.....	60
3.2.1 Initial Test.....	60
3.2.2 Test of the Sensor Temperature Stability in BEST Lab.....	61
3.2.3 Main Tests and Calibration Procedure of the Redesigned Sensor	61
4. RESULTS.....	65
4.1 Tests Results of the Original Sensor	65
4.1.1 Results of Initial Tests in BEST Lab.....	65
4.1.2 Results of the Main Tests in Algae Cultivation Lab	68
4.1.3 Results from Sensor System Temperature Stability Tests	71
4.2 Tests Results of the Redesigned Sensor.....	74
4.2.1 Results of the Redesigned Sensor Initial Tests in the BEST Lab	74
4.2.2 Results of Redesigned Sensor System Temperature Stability Tests	78
4.2.3 Main Tests Results of Redesigned Sensor	80
5. CONCLUSIONS AND DISCUSSIONS	87
5.1 Original Sensor.....	87
5.2 Redesigned Sensor	87
5.3 Practical Application.....	88
5.4 Issues Regarding Usage of the System	89
5.5 Future Research.....	90
REFERENCES.....	91
APPENDIX A	94
APPENDIX B	107
APPENDIX C	117
APPENDIX D	120
APPENDIX E.....	122

LIST OF FIGURES

	Page
Figure 1: Diagram of the steps for the sensor development (Steps: 1. Design the circuit, power for the original sensor; 2. test the original sensor in the lab and indoor raceway; 3. evaluate the issues regarding the original sensor; 4. redesign, build and assemble the sensor according to the issues; 5. test the new design in lab and indoor raceway.)	15
Figure 2: The simplified figure which showed the sensor's basic measurement principle	16
Figure 3: Prototype algal-properties sensor and data-acquisition system (the green arrow pointing at the sensor head and the red arrow pointing at the DAQ).....	18
Figure 4: LEDs PCB plate (left) with the LEDs and detector PCB plate (right) with the detectors	18
Figure 5: OD sensor system block diagram (The signal from the photo diode was sent to the amplifier to process; after converting and amplification, the signal was sent to the DAQ to be recorded; the LEDs driver circuit sent to drive the LEDs in the sensor head; and the DC power should provide +12 volts and -12volts voltage to power the pump on the sensor head and the amplifiers. And the ambient temperature monitor unit was added to evaluate the sensor system temperature performance)	19
Figure 6: Power, amplification and LEDs driver schematic (The highlighted circuit on the top was the pump circuit; the middle part was the LEDs driver circuit; and the bottom part was the current inverter and amplification circuit for both channels: left was NIR channel and the right one is the red channel.).....	23
Figure 7: Prototype board with all components soldered (above) and the enclosure box (below).....	24
Figure 8: Amplification, built in power supply in the 8"x11.5"x3.25" enclosure box (arrow 1 pointed to the power supply module; arrow 2 pointed to the amplification and LED driver circuit)	25
Figure 9: Calibration curve for both RTD water and air temperature sensor probes	27
Figure 10: Flow chart of the program on the DAQ.....	29
Figure 11: New sensor design block diagram (There are four major modules in the system: TEC module, optical module, electronics module, and DAQ).....	35

Figure 12: TEC control circuit block diagram	38
Figure 13: The current limit circuit schematic	39
Figure 14: The control chip with its circuit and the feedback loop.....	40
Figure 15: H-bridge circuit and LC filter circuit.....	41
Figure 16: The logarithmic circuit schematic.....	43
Figure 17: Minimum Value of Compensation Capacitor (the I1 refers to the current signal from the reference detector and the I2 is from the sample detector)	45
Figure 18: Constant current LED driver schematic.....	47
Figure 19: New printed circuit board (TEC control, LED driver and logarithmic circuit).....	49
Figure 20: Calibration equation of the thermistor	50
Figure 21: 3D design of the sensor housing in AutoCAD (Picture on the top is the left side view of the sensor housing: the top level is the reference housing and the bottom level is the sample level. Part 1 is the top level detector plate. Part 2 is the detector widow where detector mounted in. Part 3 is the top plate together with the Part 5 bottom plate to hold the flow cell which is part 4. The part numbers referred to different levels. Picture on the bottom is the right side view of the sensor housing. Part 6 is the LED plate which has Part 7 is LED holder to hold the LEDs in place. Part 8 are the back side plates which secure the flow cell in length. In the figure, the front side plates are not shown to give the better view of the flow cells.).....	53
Figure 22: Sensor housing assembly with TEC and heat sink (1: Sensor housing; 2: Photodiodes side cold plate; 3: TEC module; 4: LED side cold plate; 5: Detector side heat sink; 6: LED side heat sink.).....	55
Figure 23: PCB and power supply module inside the electronics enclosure	57
Figure 24: Whole sensor enclosure (left: Inside view; middle: Font view; right: Back view. 1: Electronics enclosure; 2. Sensor housing; 3: Ambient temperature monitor; 4: Pump).....	59
Figure 25: Sensor set up in BEST lab for initial test (1. PCB board; 2. Sensor housing; 3. Labjack DAQ system)	61
Figure 26: Main test of the redesigned sensor set up in Dr. Lacey's lab by the raceway.	63

Figure 27: Optical channels voltage output vs. offline OD measurement (Test in the BEST lab with algae <i>Nannochloris oculata</i> in different concentrations).....	66
Figure 28: Initial sensor test result with fixed concentration of algal sample in BEST lab (Above: optical channels output during the 40 minutes test; blow: sensor predicted OD at 750 nm during the 40 minutes test.).....	67
Figure 29: Sensor predicted OD vs. time during test in algae cultivation lab for around 2 days (from 10/18/2010 to 10/20/2010).....	69
Figure 30: Comparison of sensor measured OD and the offline spectrometer OD measurement of the main test on 10/18/2010 in algae cultivation lab	69
Figure 31: Plot of the sensor estimated OD in 7 days period from test on 11/22/2010 with the algal culture in the algae cultivation lab (showing the unstable output).....	71
Figure 32: Results from the test of sensor system temperature stability tests in algae cultivation lab without algae culture (Top: optical channels output during the 3 days test; bottom: Sensor estimated OD ₇₅₀ graph for 3 days during the test in algae cultivation lab).....	73
Figure 33: Correlation between optical channels output and ambient temperature during the temperature stability test in algae cultivation lab for 3 days (Left: NIR channel output vs. ambient temperature; right: red channel output vs. ambient temperature).....	74
Figure 34: Optical channels response to the different concentration of algal samples test in BEST lab with P4B	76
Figure 35: Results of the sensor initial test with different concentration of P4B algal culture in the BEST lab (Top: optical channels long term response under different situations; bottom: temperature long term response).....	77
Figure 36: Results of the redesigned sensor temperature stability test without any algal culture in the BEST lab (Top: optical channels long term response during the test period; bottom: temperature long term response during the test period)	79
Figure 37: Correlation between optical channels output and ambient temperature during the temperature stability test in the BEST lab (Left: NIR channel output vs. ambient temperature; right: red channel output vs. ambient temperature).....	80

Figure 38: Optical channels output response compared to measured offline OD ₇₅₀ sample values (test in algae cultivation lab 06/04/2012).....	82
Figure 39: Sensor predicted OD ₇₅₀ values compared to spectrometer OD ₇₅₀ measurement (test in algae cultivation lab 06/04/2012 with algal culture from the raceway)	82
Figure 40: Test results from the main test in algae cultivation lab with the algal culture from the raceway on 06/04/2012 (Top: optical channels output response during the test period; middle: ambient temperature and regulated temperature during the test period; bottom: sensor predicted OD ₇₅₀ during the whole test time).....	84
Figure 41: Test results from the main test in algae cultivation lab with the algal culture from the raceway from 06/13/2012 to 06/25/2012 (Top: optical channels output response during the test period; middle: ambient temperature and regulated temperature during the test period; bottom: sensor predicted OD ₇₅₀ during the whole test time)	86
Figure 42: The PCB layout of the whole electronic circuit for the new sensor	121
Figure 43: Whole schematic of the new sensor circuits including TEC control circuit, LED drivers and logarithmic circuit	123

LIST OF TABLES

	Page
Table 1: Resistor and Capacitor value for the whole circuit	23
Table 2: Calibration data set for the original sensor (calibrated on 08/16/2010).....	108
Table 3: Validation data set for the original sensor (test on 10/18/2010).....	108
Table 4: Original recorded offline OD measurement and two channels output (test from 06/04/2012 to 06/24/2012 of the redesigned sensor)	109
Table 5: Calibration data set for the redesigned sensor (test from 06/04/2012 to 06/24/2012).....	111
Table 6: Validation data set for the test of the redesigned sensor (test from 06/04/2012 to 06/24/2012).....	113
Table 7: RTD temperature probe calibration data points for the ambient air temperature	114
Table 8: RTD temperature probe calibration data points for the algal culture temperature	115
Table 9: Thermistor calibration data points for monitoring the regulated temperature .	116
Table 10: Regression statistics of the original sensor calibration on 08/16/2010	118
Table 11: Coefficients for the calibration of the original sensor on 08/16/2010	118
Table 12: Regression statistics of the redesigned sensor calibration from the test from 06/04/2012 to 06/24/2012.....	119
Table 13: Coefficients for the calibration of the from 06/04/2012 to 06/24/2012 (tests of the redesigned sensor)	119

1. INTRODUCTION AND LITERATURE REVIEW

1.1 Introduction

1.1.1 Composition of Algae

Algae are a variety of aquatic, eukaryotic, and photosynthetic organisms having structures ranging from micro-level unicellular organisms to very large multicellular organisms [1]. The biochemical composition of algae, much like other photosynthetic organisms, primarily includes: protein, amino acids produced by the cells, polar and nonpolar lipids, fatty acids, carbohydrates, minerals, chlorophyll and carotenoids [2, 3]. The percentage of each composition does, however, vary greatly among species, culture condition, and growth stages [4]. For instance, lipid content in microalgae has attracted interest in the biofuel production field because the transesterification of triglycerides lipid can convert them into biodiesel. *Botryococcus braunii* is an example of algae species proposed for biofuel production due to a relatively high (34% of dry weight) lipid content [2]. But, in other species which are not aimed at biofuel production, such as *Bracteacoccus grandis*, which is used as food source for aqua-culture, have relatively low (9%) lipid content [4]. This indicates variation in lipid composition between different species. While in the study, both nutrient starvation and temperature influence the lipids yield [4, 5]. This indicates that during different growth conditions the percentage of the composition is varied even for the same species.

1.1.2 Benefits of Algae Production

Due to the composition of algae, they are potentially high-value biological products, with many different benefits to different fields. More and more research is being conducted in several different areas.

1.1.2.1 Algae as Sources of Nutrients

The first major area is traditional use of algae for food [6]. Algae are rich in many vitamins such as A1, B1, B2, B6 and C. They can also provide essential iodine, potassium, iron, magnesium and calcium. In addition, because of the amount of high-value ingredients such as protein, carbohydrates, omega-3 fatty acids, pigment and antioxidants in algae, research on industrial-scale algal production for food has been conducted in Japan, the U.S., Germany and other countries since 1950s [7]. During this time, the nutritional value of algae has been paid the most attention, and so consideration has been given to industrial scale production of algae for human consumption as nutrient supplements. Algae have also found use as food sources in aquaculture due to the high value of their nutrients. They are important for rearing marine bivalve mollusks, and larvae of several marine fish. Penaeid shrimp and some marine gastropods feed on algae as well [8].

1.1.2.2 Algae as a Method of Waste Water Treatment

The second major research area is in waste water treatment. Due to increasing agricultural and industrial activities, water pollution problem continues to be a major issue. To effectively reduce the amount of toxic chemicals used for waste water treatment, biological methods have been introduced [6, 9]. Among the biological

methods, it was reported by several researchers that algal-based waste water treatment is a relatively new but efficient method. Compared with conventional methods, algal-based processing can have multiple advantages. One of those advantages is that as industrial effluents are usually treated with chemicals to remove sludge in the first stage of waste water treatment; using algae in this process can reduce chemical usage. Another advantage is that during cultivation, the algae can effectively fix the CO₂; therefore, compared to traditional waste water treatment methods, the greenhouse gas emission is reduced. Another advantage is an improvement over mechanical aeration in traditional methods, which is a high-energy process that provides enough oxygen for bacteria to break down the wastes. During photosynthesis, algae are effective at consuming nutrients while providing oxygen which aerobic bacteria need [9].

1.1.2.3 Algae as a Source of Lipids for Biofuels

A third and final research area involves production of biofuel. Most fuel energy is generated from fossil resources, but this has potential problems such as environmental pollution [10]. With the increasing demand for energy, involving rising oil prices and dependency on imported oil, there is an urgent demand for development of sustainable, clean, economically efficient and environmentally friendly energy sources [11, 12]. Among the dozens of candidates for biofuel, algae are relatively new as a potential type of “biocrude” that has attracted a great deal of interest. Studies of algae as a biofuel are usually focused on the following fields: lipids for biodiesel production and carbohydrates for ethanol production [13]. There are a number of benefits to mass production of algae, which can be summarized in a few sections. First, the production of

biomass rate of algae is high. The microalgae have high photosynthetic yields, which is about 3%-8%. It is much greater than other terrestrial plants, which have only approximately 0.5% of solar energy converted to biomass [14]. Second, the lipid content of algae is greater when compared to other types of biofuel crops. Microalgae are estimated to contain up to 85% lipids by dry weight. Third, algae are also environment friendly. When compared to other biofuel sources, such as soybean, rapeseed, palm, and so on. The use of algae saves the use of land to reduce competition with food crops. In addition, cultivating algae can absorb CO₂ and produce O₂. Fourth, there are a lot of other products that can be produced from the biomass of algae after lipids extraction. These include animal feed, pharmaceuticals, and cosmetic products [15].

1.1.3 Requirements of Mass Algae Production

Nowadays, both bioethanol and biodiesel from algae are still not commercially available. But as previously discussed, algae would be an excellent source of biomass for biofuel. In the near future, due to depletion of traditional fossil energy and also due to the advantages of algal biofuels, large scale algae production has to be established to fulfill the requirement for the commercialization of the biofuel. Since the early 1960's, with the commencement of large scale culture of the microalga *Chlorella* in Japan, more and more countries have begun to be involved in the algal industry and the commercial algae production has grown significantly. One of the main factors that would affect the success of the large scale algae production is to build a cost-effective system [16]. One of the most crucial points is to reduce the cost of production facilities. Traditionally, the

production systems need a relatively large amount of expensive human labor and skilled technicians to support and maintain, which would significantly increase the cost.

Therefore, to reduce the cost of biodiesel, an effective automation system must be implemented in the large-scale algal culture industry.

Development of large scale algae cultivation and commercialization requires precise information including the fertilizing, harvesting and ambient environment condition control to make decision on. Thus, on-line monitoring of growth and environmental parameters is very crucial in order to provide real time information and reduce human labor thus the costs [17]. Based on the environmental and growth variables, sensors have to be developed according to each of the variables to obtain on-line and accurate information to optimize the cultivation process. According to the variables, the sensors that often need to be implemented in algal cultivation production basically includes a pH sensor, a temperature sensor, an ethanol sensor, dissolved oxygen sensor, green fluorescent protein sensor, carbon dioxide sensor and biomass monitoring sensor [18]. Among all the sensors mentioned above, the biomass monitor sensor is used to measure the biomass which is a basic parameter of production procedure. Recently, large scale algae production is mainly in the open-pond raceway for its lower cost and operation convenience. Thus, the development of a sensor which is suitable for a raceway is required, since the conventional and most precise way of measuring biomass, directly counting cell number under a microscope or determining the dry cell weight, is both time consuming and labor intensive. At present, there are several common systems which are based on dissolved oxygen uptake or electrical

properties of the culture media [19]. But the main drawbacks of these sensors during long term operation are that their electrodes are sensitive and fragile. Also, the correlation between those parameters and biomass is complicated [20]. Measurement of absorbance is relatively easy and also the absorbance can be used to measure turbidity which can be related with the total biomass relatively simply. Thus, recently, more and more sensors which monitor algae biomass begin to focus on optical density measurement.

1.2 Literature Review

1.2.1 Biomass Determination Methods

Biomass concentration, which refers to the total amount of biological material in a specific volume, is a key parameter in bioprocessing. Not only is it the variable that determines growth rate, but it can also be used as a reference for other properties. Sonnleitner et al. (1992) reviewed methods of online and offline biomass determination. Gravimetric methods are the classical approach for offline biomass concentration determination. These methods sometimes involve cell lysis but often involve extraction, centrifugation, filtration, washing and drying to separate the biomass from liquids and other materials. Another common offline method involves cell counting with differentiation between all cells and viable cells. Counting methods are conducted with single cell-type suspensions and involve microscopy or Coulter counters or flow cytometers. All these procedures tend to be time consuming and tedious, requiring human labor.

Methods for online biomass determination are often based on optical measurements. Several online methods focus on optical-density (OD) measurement, which can be correlated with total biomass dry weight. Common technologies for OD sensors are based on the measurement of transmission, reflection, or scattering of light or near-infrared energy interacting with the sample suspension. Measurement wavelengths are selected according to the size of the cell, the growth medium's absorption spectrum, and other factors. OD sensors commonly have problems with interference from gas bubbles or other matter inside the media. Degassing procedures are common and include degas chambers, steel screens, etc. Furthermore, OD measurement at high cell density is a critical problem for those sensors because of the inner filtering effect of the cells. The dynamic range of OD sensors is limited by the density of the culture, and thus dilution of the suspension to OD levels between 0 and 0.5 is common. Flow injection analysis systems have been successfully developed for rapid dilution so that high-density suspensions can be measured with a larger dynamic range. When the fraction of the inside cell NAD(P)H was relatively stable compared to the biomass and also large enough, the fluorescence can be used for the indication of it to estimate the biomass. Other sensors based on visible and short-wavelength near-infrared energy have also been developed as indicators of intracellular components such as the metabolic state of the microorganism in order to estimate the biomass concentration.

Acoustic resonance densitometry is another indirect method for biomass estimation and has shown good linearity in the range of 0 to 500 optical density units. Another method involves using electrical properties of viable biomass as an indicator.

This method is based on the fact that intact membranes of live cells are polarized when an electric field is applied, and the amount of polarization can be measured by the capacitance at low frequency. The range of the capacitance has been found to be from 0.1 to 200 pF, and the frequency range could be up to several 100 kHz. However, the limitation of this method was that for the intermediately concentrated media the maximum accepted capacitance for would be easily reached. This method also suffers from interference resulting from gas bubbles and from the conductivity of the culture media. Filtration properties are another ways to determine biomass concentration. An automatic filtration device was developed to monitor the flux of filtration and accumulated filter cake while a sample was filtered through a fresh filter. Measurements taken with a proper model could be used for the calculation of biomass. Another method for online biomass monitoring involved software sensors. Based on common bioreactor measurements such as simple off-gas or base consumption results, the software sensor used models including growth kinetics or statistical methods or neural networks to estimate biomass concentration. Problems with this method include accuracy and what parameters model calculations can be based on [20].

Kivibarju et al. (2007) compared two types of cell density probes that were employed to monitor growth of different yeast and bacterial cultures. One sensor was a near-infrared (NIR), light-absorption, cell-density probe (Trucell, Finesse Instruments, San Jose, CA). Its light source was a laser, and two photodetectors were used for measurement and reference signal. Then, the analog 4-20 mA signal was sent to the computer through a 10-bit conversion. The second sensor was a dielectric spectroscopy

probe that had four annular ring electrodes with a Biomass Monitor 220, which would process the signal from the probe. At a certain frequency range, capacitance and conductivity of the culture suspension were measured with the probe.

The OD of the culture was measured at the 600 nm in the OD range of 0.05 to 0.5 in the diluted samples. For the NIR absorption sensor, the biomass concentration was calculated from the probe measurement and then compared with the OD measurement and the cell dry weight. OD and cell dry weight were linearly correlated within different cultures, the lowest R^2 value above 0.9. For the dielectrics spectroscopy probe, biomass concentrations from different microorganisms were calculated from the Biomass Monitor and compared with cell dry weight values estimated from OD. Also, the actual cell's dry weight measurements as well.

Both sensors were influenced by strong physical and chemical changes (pH, stirring, aeration). But the results showed that the NIR light absorption was more developed and more stable method to use for online biomass concentration monitor than dielectric spectroscopy [21].

1.2.2 OD Sensors

1.2.2.1 Commercially Available OD Sensor

Different types of commercial OD sensors are currently available. Most of the sensors are based on the absorbance measurement or scattering measurement which calculates the biomass using an indirect method.

There is one single NIR optical channel probe (AS16-N, Optek-Danulat, Inc., Germantown, WI) which measures the light attenuation caused by absorption by the

substance in the liquid. This sensor uses the filter which adapts the wavelength from 730 to 970 nm together with six different optical path lengths for different use [22].

A noninvasive OD sensor (BE2100 sensor, BugLab LLC, Danville, CA) has been designed for biomass monitoring. Together with the base unit which provides the power for the sensor and displays the results, it has a current output from 4 to 20 mA. Also, except displaying on the base unit, the results can be sent to the computer through USB/RS232. This sensor outputs a real-time, continuous, online OD measurement with a wide linear range which can be in 0.1 to 300 OD units. To implement this sensor in production, it can be attached to the transparent surface of bioreactors or fermentors [23].

There are a series OD sensors (InPro series, Mettler Toledo LLC, Urdorf, Switzerland) which have been manufactured for usage under different conditions. In these series of OD sensor, InPro 8100 and InPro 8050 are single optical fiber probes based on backward scattering. They can be both used for the cell culture monitoring and waste water environment. They are designed for the high concentration media with a wide linear range. InPro 8200 is a dual optical turbidity/OD sensor which is based on the same principle as previous ones. But this sensor is suitable for the medium to low turbidity with a high resolution. Another flow through model (InPro 8400) which is based on the principle of forward scattered light divided by transmitted light is ideal for very low to medium concentration suspension with particle size $\geq 0.3 \mu\text{m}$. Together with the corresponding transmitter which provides power for the sensor and also can

implement the calibration curve, these sensor can output an analog output from 4 to 20 mA [24].

Several commercial OD sensors are available, but some are used for specific bioreactors, while others are used with specific proprietary analog to digital converter (ADC) systems that increase cost. To fulfill the requirement of monitoring large scale production of algae in an open raceway environment, more research about optical density sensors which are used specifically for algae is required.

1.2.2.2 Algae OD Sensor in Research

A computer-controlled flow-injection analysis system was developed by Meireles (2002) to monitor OD of algal culture in a 2-L bioreactor. The system used a valve to form two sample loops that provided different dilution rates, 1.88 and 4.56. The first loop was suitable for measuring OD levels under 0.8, and the other was used for ODs above that level. Two pumps were used to circulate algal culture from the reactor to the valve and to move the dilution fluid from its reservoir to the dilution loop and then to the detector. The detector was essentially a spectrophotometer equipped with a flow cell, and the measurement wavelength was set to 550 nm. In operation, an algal-culture sample flowed from the bioreactor to a dilution loop where it was diluted at a proper rate and then to the detector where OD was measured. After each measurement a cleaning step would be carried on by the system for 10s. Cell concentration was calculated by calibrating detector response with cell number and ash free dry weight. The flow rate, dilution rate and tube length were optimized to provide a linear correlation for the culture media over entire growth periods. The sensor was tested with the microalga, *P.*

lutheri, at three different growth stages with three replicates. Results were compared with standard offline measurement of the samples, and concentration of the biomass was determined accurately and reproducibly [25].

Sandnes et al. (2005) measured the OD of algal culture flowing inside a tubular photobioreactor system to monitor and control biomass density. The sensor consisted of a five-LED array and photodiode detector positioned on opposite sides of the photobioreactor tube. The LEDs were driven with constant current and emitted near-infrared energy at 880 nm. The main tube was transparent for light collection and 30-mm in diameter, and it was reduced to 10 mm in diameter where the sensor was mounted to increase the transmitted energy from the LEDs. A detector was mounted on the other side of the reduced tube section to measure the intensity of light transmitted through the culture. The sensor was calibrated with cell number and dry weight of the algal biomass. The accuracy of the sensor was within approximately 8% of the total biomass. The output voltage of the detector was logged with a data-acquisition module and transferred to a computer for data processing. The output voltage was also used as a feedback signal to an automatic control system in order to maintain constant OD level. Measurement of the algal culture was done every 10 min. and compared with a reference value. If OD exceeded the reference value, an electronically controlled valve would open to allow a media mix to be pumped into the system to dilute the algal culture and maintain constant OD. This system was successfully tested with *N. oceanic* [26].

Nedbal and Trtilek (2008) modified a commercial photobioreactor (FMT150, Photon System Instrument, Brno, Czech Republic) system in order to more precisely

control photosynthesis of cyanobacteria. Specifically, the modified system was used to monitor diurnal growth dynamics under the presence and absence of nitrate in the growth medium. The system was also operated in the turbidostat and pH-stat modes to compare growth rates of cyanobacteria among certain fixed levels of turbidity and pH. The system involved a flat rectangular cuvette with front and back windows made of glass. The suspension was filled to 0.35 L to optimize the performance, and a pH electrode and a thermocouple were included to monitor growth conditions. The system contained a real-time kinetic fluorometer and dual-wavelength densitometer consisting of a LEDs array with two wavelengths, 680 and 735 nm. The detector was covered with a broad-band optical filter from 665 to 750 nm to limit the spectral-response range, and it was positioned opposite the LEDs across the cuvette glass window. OD of the cyanobacterial suspension was then measured at 735 nm, where the near-infrared energy essentially scatters on the cell structure, and the signal should thus be proportional to total biomass in the liquid. OD was also measured at 680, where both scattering of the cell and absorption of the chlorophyll affect the signal. Sensor test results showed that the sensor can detect OD as low as 0.02. The difference between the ODs at 680 and 735 was used to estimate chlorophyll concentration in the suspension. Results of other analyses showed that cell count and chlorophyll concentration were linearly proportional to OD at 680 when OD was between 0.1 and 1.2 and to OD at 735 when OD was between 0.02 and 0.4. Outside these ranges, a non-linear calibration was needed [27].

1.2.2.3 Sui and Thomasson's Sensor

Thomasson and Sui (2010) built a real-time, online, biomass-concentration monitoring sensor in order to have an accurate signal to control algal production. The system was based on measurement of absorption as an indication of algal-cell concentration. Culture samples of *Nannochloropsis oculata* were analyzed at different OD levels with standard spectrophotometric methods. Absorbance data between 250 and 2500 nm were processed with statistical methods to select wavebands highly correlated with OD as measured with reference methods. A narrow band in the red range and another in the near-infrared range were selected. The sensor output was calibrated with OD at 750 nm as measured with a spectrophotometer (Cary 500, Scan UV-Vis-NIR, Varian, Australia). A small pump forced the algal culture through a flow cell where absorbance was measured with photodetectors to generate an output signal. Detectors and LEDs were positioned to face each other across the flow cell, but inside a housing that blocked outside ambient light. Optical filters for the two bands were used to cover the two detectors, respectively, in order to separate light responses for the two channels. Thomasson and Sui's (2010) sensor was designed originally in a laboratory environment [28].

1.3 Objectives

The final goal of this research is to have a robust algal optical density which can be used in the raceway production. Therefore, the objectives of this research are to:

1. Design and build the electronic circuit for the original sensor;
2. Test the original sensor in the lab and indoor raceway and evaluate the issues regarding the

original sensor; 3. Redesign and build the sensor according to the issues; 4. Test the new design in lab and indoor raceway. Figure 1 shows the steps in order to achieve these specific objectives.

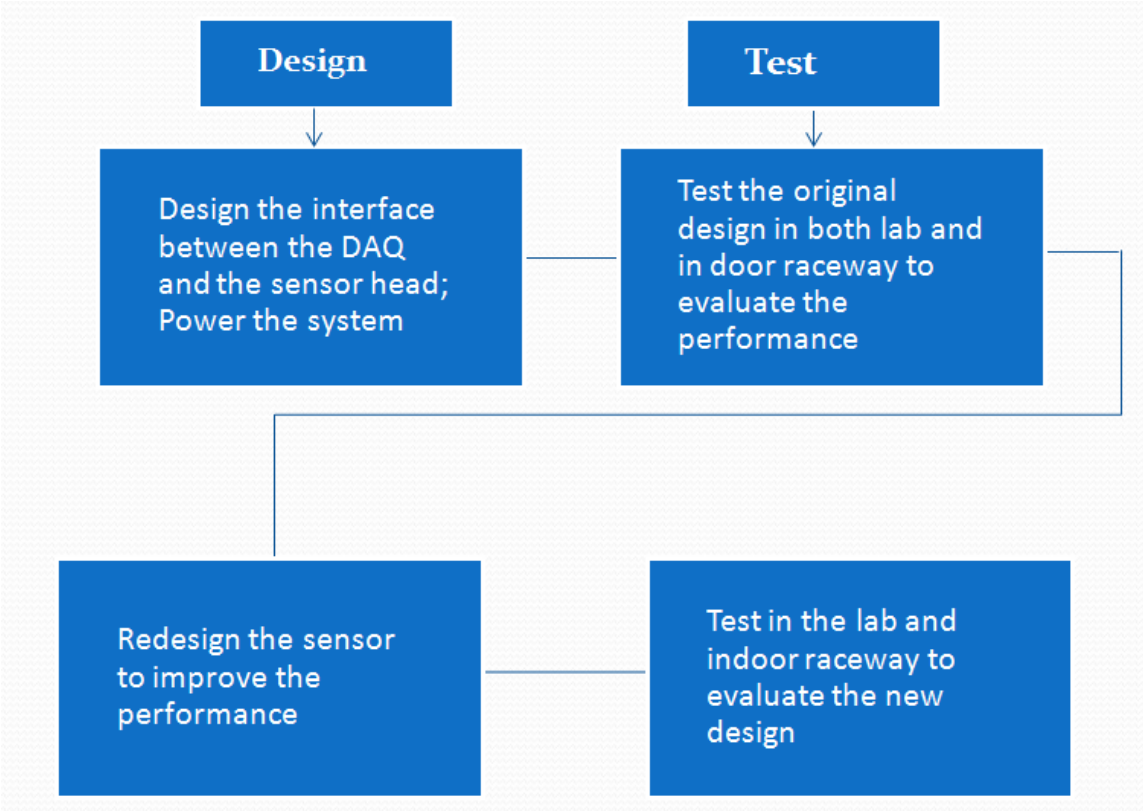


Figure 1: Diagram of the steps for the sensor development (Steps: 1. Design the circuit, power for the original sensor; 2. test the original sensor in the lab and indoor raceway; 3. evaluate the issues regarding the original sensor; 4. redesign, build and assemble the sensor according to the issues; 5. test the new design in lab and indoor raceway.)

2. ORIGINAL SENSOR

2.1 Design and Construction of the Original Sensor System

2.1.1 Review of the Operation Theory and Structure of the Original Sensor

The original OD-measurement system is based on determining light absorbance of an algal culture (Figure 2). When light from an emission source passes through the culture inside a sample container, its intensity is attenuated by the algal cells in the culture. Absorbance (A) is defined as the log ratio between light intensity incident (I_0) on the sample and light intensity transmitted through the sample (I) (Equation 1). As concentration of the algae in the sample varies, the intensity of the light transmitted through the sample varies correspondingly, so absorbance changes. Therefore, differences in OD can be measured as absorbance changes through variation in the output voltages of light detectors.

$$A = -\log_{10}\left(\frac{I}{I_0}\right) \quad (1)$$

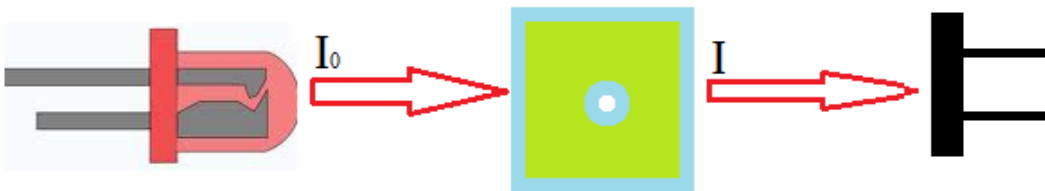


Figure 2: The simplified diagram which showed the sensor's basic measurement principle

An OD sensor for algae was originally designed and built by Dr. Sui and Dr. Thomasson (2010). The sensor (Figure 3) consists of a PVC housing, a flow-through cell, a printed circuit board (PCB) plate for light emitting diodes (LEDs) (Figure 4) used as light sources, and a PCB plate for detectors (Figure 4). The two PCB plates are placed in parallel with the flow-through cell in between. A miniature diaphragm pump with a 12-V DC brush motor (W311-11, Hargraves Technology Corporation, Mooresville, NC) is mounted on top of the sensor housing and used to force the algal culture through the cell. The LEDs include two (L6112-02, Hamamatsu, Hamamatsu City, Japan) of a narrow emission band in the red range and two (L1915-02, Hamamatsu, Hamamatsu City, Japan) of a narrow emission band in the near-infrared (NIR) range. Two silicon photodiode detectors (S3117-33BQ, Hamamatsu, Japan) are used, one for each channel (Red and NIR). Photodiode detectors generate an output signal by detecting the light from the two respective LEDs as it passes through the flow cell. IR cutoff filters at 700nm (NT55-237, Edmund Optics Inc., Barrington, NJ) was placed before the detector window for the Red channel to block light from IR LEDs. . A long pass filter at 750nm (NT55-237, Edmund Optics Inc., Barrington, NJ) was placed before the detector for the NIR channel to prevent the detector from receiving the light from the red LEDs. A data-acquisition system (DAQ) (Figure 3) was programmed to serve as the user interface, to record the output signal, calculate and store the OD level. The DAQ is based on a single-board computer (SBC) (MicroPod, RLC Enterprises Inc., Paso Robles, CA) and accepts -10 to +10 V for analog input. A USB interface was incorporated to transfer data to a computer.

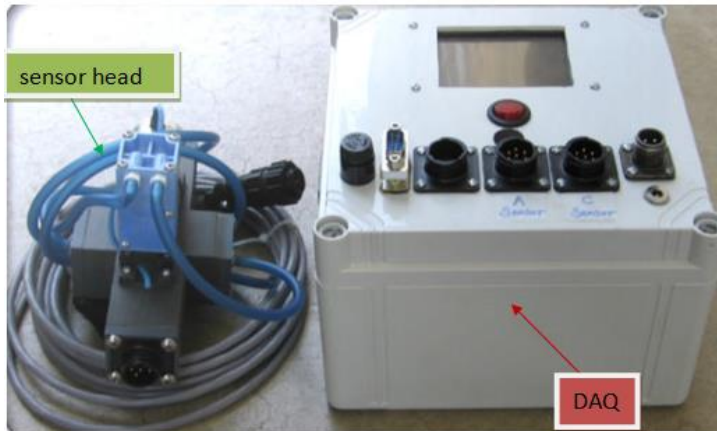


Figure 3: Prototype algal OD sensor and data-acquisition system (the green arrow pointing at the sensor head and the red arrow pointing at the DAQ)

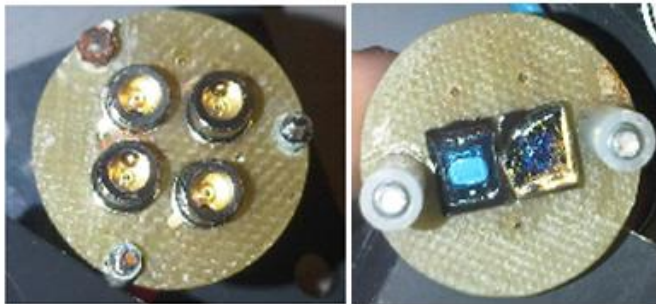


Figure 4: LEDs PCB plate (left) with the LEDs and detector PCB plate (right) with the detectors

2.1.2 Overall View of Sensor System Structure

The silicon photodiode detectors in the sensor head generate current as output. In order to be accepted by the DAQ, the signal would be converted into voltage and then amplified into a proper range. Therefore, a circuit had to be designed to process the current signal (Figure 5). Also, to provide power for the DAQ, the sensor, and the diaphragm pump (Figure 5), a power supply module was required. And after the initial

tests, with the suspicion of the sensor temperature drift, an ambient temperature monitor unit was added to evaluate the system temperature performance.

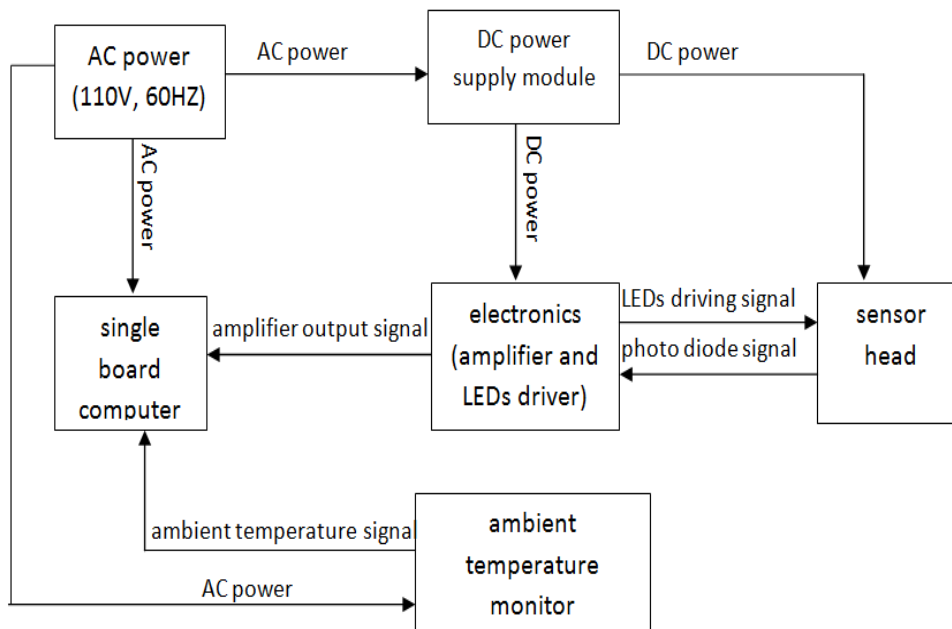


Figure 5: OD sensor system block diagram (The signal from the photo diode was sent to the amplifier to process; after converting and amplification, the signal was sent to the DAQ to be recorded; the LEDs driver circuit sent to drive the LEDs in the sensor head; and the DC power should provide +12 volts and -12volts voltage to power the pump on the sensor head and the amplifiers. And the ambient temperature monitor unit was added to evaluate the sensor system temperature performance)

2.1.3 Circuits Design

2.1.3.1 Transimpedance Amplifier

The initial calculation for design was based on the parameter of the LEDs and detectors to estimate the theoretical output of the detectors under the assumption, that the alignments of the optical components were perfect and there was no energy loss during

the light passing through the air. The radiant flux ϕ_e , which refers to the total amount of light emitted from a LED and the photo sensitivity S of photodiodes will give a theoretical output current of the sensor. Radiant flux ϕ_e is 2.5 mW when forward current is 20 mA for the red channel. For the NIR channel, when the forward current equals to 50 mA, ϕ_e is 4.5 mW. The detector's photo sensitivity is approximately 0.42 A/W for red channel and 0.58 A/W for NIR channel. The transmission η of the filter is approximately 90% and 97% for Red and NIR channel respectively. The following equation described the calculation of the estimated current output:

$$I_{output} = \phi_e \times s \times \eta \quad (2)$$

According to equation 2, the estimated output current from red channel is 0.945mA and 2.5317mA from NIR channel.

There are a number of ways to design a converter, from the transistor level to the integrated circuit chip level. A basic design is preferred for the amplifier used. Based on the estimated current output and the DC output requirement, a simplified design may be sufficient for the signal provided by the photodetectors. A transimpedance amplifier with an operational amplifier (op amp) was selected as the main component of a simple current-to-voltage conversion and processing circuit. The LM 2904 op amp (LM2904N, STMicroelectronics, Geneva, Switzerland) was chosen because it is a low power dual op amp that enables a compact circuit design and low power consumption. Since there are two separate detectors, the similar U1 and U2 amplifier circuits (Figure 6) were used to process the current signals from the NIR and Red channels. Op amp U1B was used to convert the current and amplify the signal. The photodiode was connected between the

negative input and ground of the op amp so that the current signal could go through an inverting configuration. The variable resistor R3 was used as an amplifying element, as its magnitude adjusts the output voltage level. Capacitor C1 forms an active low pass filter to reduce high frequency noise. Op amp U1A works as a voltage buffer that is not involved in the amplification but keeps the output voltage stable for the DAQ. Capacitor C4 attenuates noise and stabilizes the output signal. Equation 3 is the transfer function that describes the relationship between current signal and output voltage. The transfer function shows that capacitor C1 adds a pole at the frequency shown in Equation 3, which is the cutoff frequency of the low-pass filter.

$$V_{out1} = -\frac{I_s R_3}{1 + R_3 C_1 S} \quad (3)$$

$$f_c = \frac{1}{2 * \pi * R_3 * C_1} \quad (4)$$

In the equation 3, I_s is the current output generated by the detector; R_3 is the adjustable resistor. C_1 is the capacitor which filters out the high frequency noises. S is equivalent to $j\omega$, which indicates the frequency response of the circuit.

Once the entire circuit was constructed, it had to be calibrated. For this purpose, variable resistor R3 was included in the NIR channel circuit so that output voltage could be adjusted to the desired level; R3 was adjusted to 200 kΩ during circuit testing to provide a desired maximum output voltage of roughly -3 V. According to Equation 4, a 100 pF capacitor was chosen so that the cutoff frequency could be kept around 7.96 kHz. With this cutoff frequency, the high-frequency electronic noise and the noise caused by vibration of the pump should be largely attenuated. The setup of the red channel was

basically the same as that of the NIR channel, but due to a difference in underlying signal strength, the variable resistor R4 was set at 900 kΩ during calibration. The capacitor C2 was sized at 100 pF, which set the cutoff frequency at approximately 1.77 kHz.

2.1.3.2 LEDs Driver Circuit

The LEDs driver circuit consists of a voltage regulator and resistors. The U3 in a Figure 6 circuit is a fixed voltage output regulator (LM323, STMicroelectronics, Geneva, Switzerland), and it regulates the 12 V input down to 5 V to power the LEDs. Using a voltage regulator also stabilizes the voltage output of the detectors. Therefore, regulating voltage reduces the effects of variation in the power supply that can occur when large current loads turn on or off. Resistors R1 and R2 are current limiting resistors for the NIR and Red LEDs respectively, and their values were determined as in Equation 5, where V_{OUT} is the output of the voltage regulator, and $V_{forward}$ and $I_{forward}$ are forward voltage and current, respectively, of the LEDs; $V_{forward}$ and $I_{forward}$ are found in the manufacturer's datasheet.

$$R = \frac{V_{OUT} - 2 * V_{forward}}{I_{forward}} \quad (5)$$

Figure 6 shows the whole circuit schematic, including the transimpedance amplifiers for the detector, the LED driver and the power supply layout. Each variable mentioned in this section corresponds to a component in this schematic. The value of each component is listed in Table 1. The MG1 device in Figure 6 represents the pump, which is directly powered by the 12-VDC power.

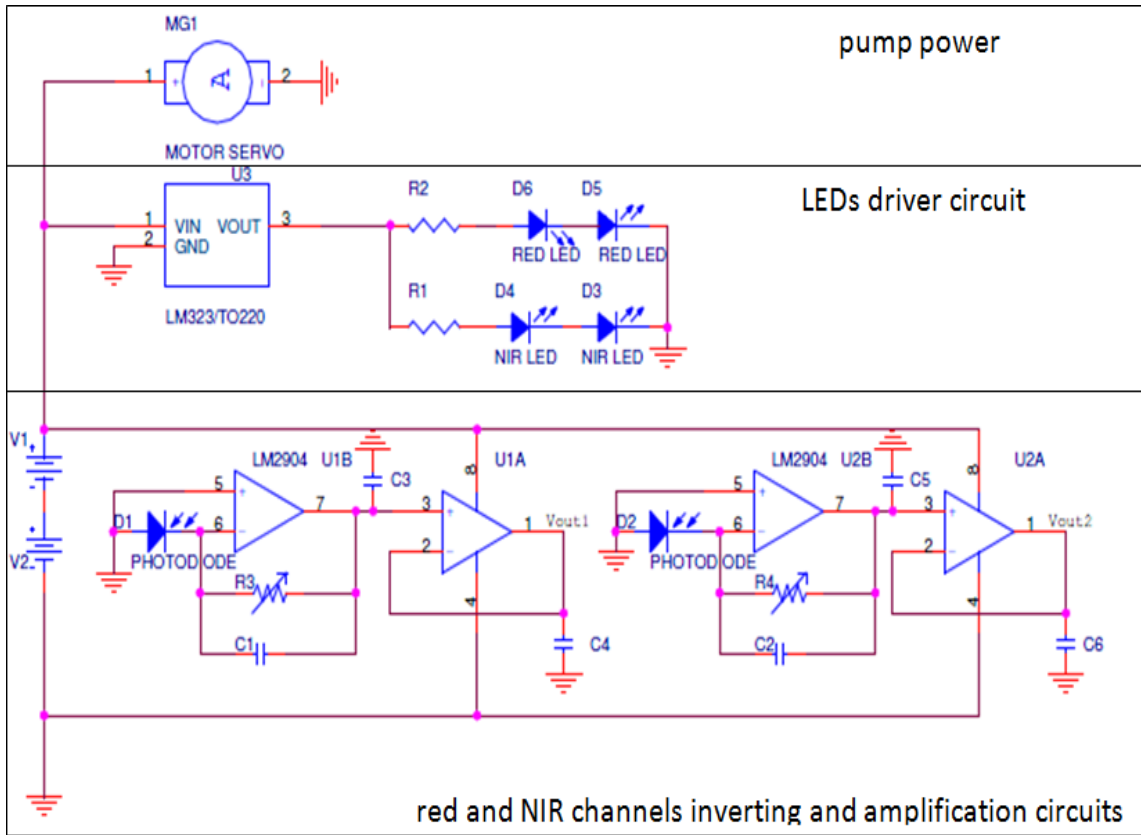


Figure 6: Power, amplification and LEDs driver schematic (The highlighted circuit on the top was the pump circuit; the middle part was the LEDs driver circuit; and the bottom part was the current inverter and amplification circuit for both channels: left was NIR channel and the right one is the red channel.)

Table 1: Resistor and Capacitor value for the whole circuit

Component ID	Value	Units
R1	47	Ω
R2	75	Ω
R3	1	$M\Omega$
R4	1	$M\Omega$
C1	100	pF
C2	100	pF
C3	1	μF
C4	1	μF
C5	1	μF
C6	1	μF

2.1.4 Construction of the Sensor Electronics and Enclosure

After the circuit was designed, it was built and tested in prototype form on a bread board (Figure 7). This prototype circuit board was enclosed inside a 6”x4”x1.8” weather-proof plastic box. Three connectors were required to connect the circuit to the power supply, the sensors, and the DAQ.

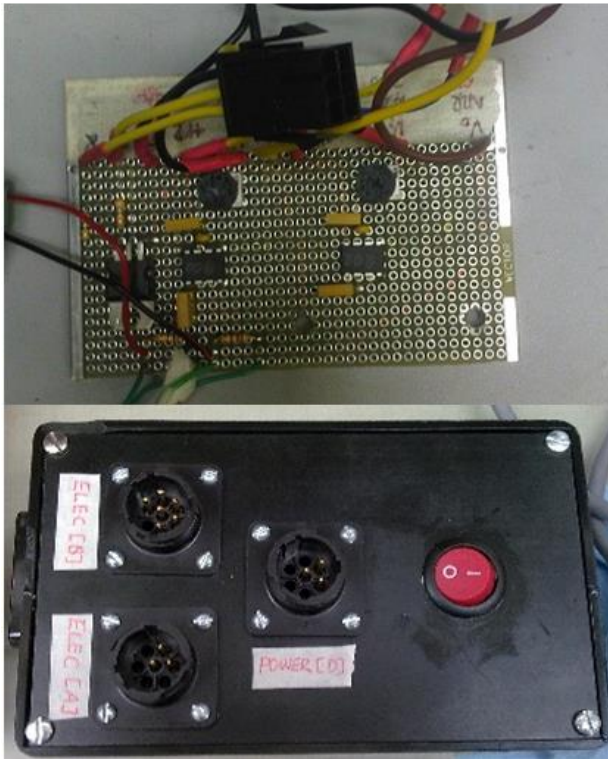


Figure 7: Prototype board with all components soldered (above) and the enclosure box (below)

Initially the DC power of the system was generated from two auto batteries. For the convenient, a power supply module (REL-150-2004, Integrated Power Designs, Wilkes-Barre, PA) was added to the system before the raceway tests. The power module is rated at 150 watts, with high-current dual output, an AC-to-DC integrated power

supply, and two separate outputs of +12 and -12 V. The power module was installed in the enclosure with all other circuits (Figure 8) to maintain the compact design of the system.

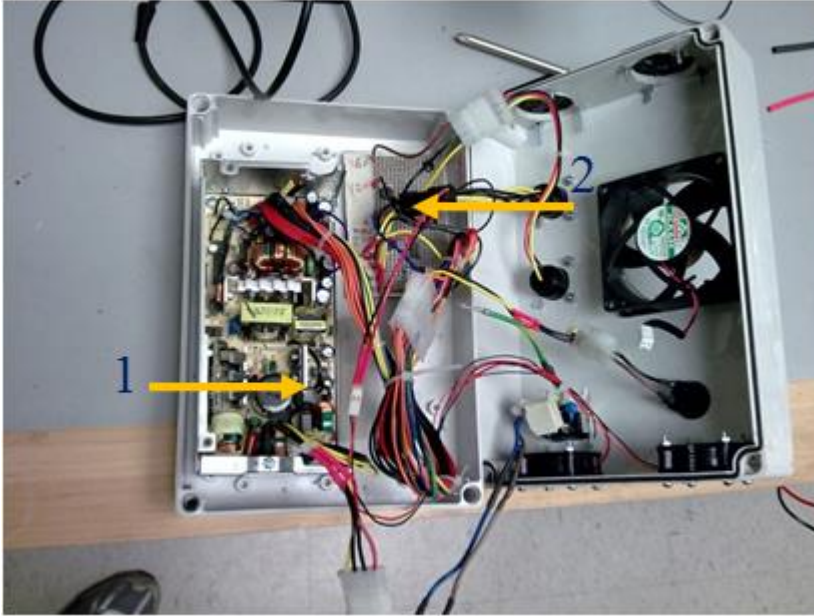


Figure 8: Amplification, built in power supply in the 8”x11.5”x3.25” enclosure box (arrow 1 pointed to the power supply module; arrow 2 pointed to the amplification and LED driver circuit)

2.1.5 Calibration of Temperature Monitoring Unit

Due to temperature drift tendency which was found in the results of initial test of the sensor, a temperature-monitoring system was designed for inclusion in the sensor. Two resistance temperature detectors (RTD) probes, a transmitter (TXDIN70, Omega Engineering Inc., Stamford, CT) that converted RTD output into current, and a transmitter display (TXDIN70-display, Omega Engineering Inc., Stamford, CT) that displayed the temperature measured. One RTD probe (P-L-A-1/8-6-0-T-3, Omega

Engineering Inc., Stamford, CT) was used to monitor ambient air temperature, and the other (P-M-A-1/8-6-0-T-3, Omega Engineering Inc., Stamford, CT) was used for monitoring algal-culture temperature. The latter probe was modified to fit inside the sensor enclosure. The output range of the transmitter was from 4 to 20 mA, so two 200- Ω resistors were included to convert the output into voltage for recording by the DAQ. With the transmitter display, the measured temperature of those RTD probes that was calibrated by the manufacture would be displayed on the LCD screen. Both circuits were calibrated according to the temperature display in order to accurately convert their voltage outputs into degrees Celsius. The calibration of the air temperature consisted of first heating up the oven up to 50°C. While the oven was naturally cooling down, different temperature was measured. Then the displayed temperature with corresponding output voltage from the probe was recorded (Figure 9) for plotting the calibration equation. The water temperature probe had the similar calibration procedure (Figure 9) except that the temperature variation was created in the water. Then the input pin on the DAQ was set in software to the correct input range.

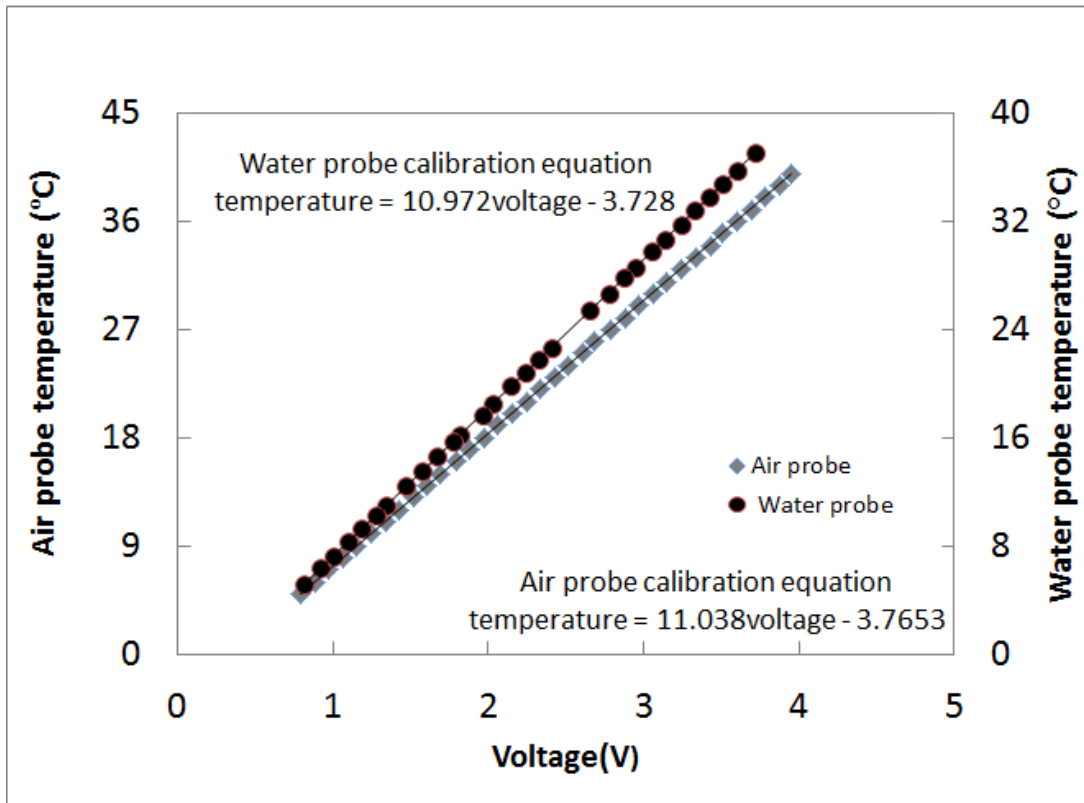


Figure 9: Calibration curve for both RTD water and air temperature sensor probes

2.1.6 Software

The single board computer (SBC) in the DAQ is operated with Windows CE© and runs a custom-developed program to control sensor-system operation (Figure 10).

The program code was written in Visual Basic and has three main functions:

1. Set up and initialize the SBC. This aspect of the program sets the input channels, analog input mode, sampling rate, and the acceptable range of the input channels. For example, the output range of the NIR and Red channel voltages is from -3 V to 0 V, so the input range is set from -5 to 5 V.

2. Log and save data. This aspect of the program has two modes, logging mode and monitoring mode. In logging mode, the output voltage from the circuit is received and stored on a Micro SD card. In monitoring mode the data is displayed but not stored.

3. Calibrate, calculate, and plot. This aspect of the program is used to calibrate the sensor based on a predetermined calibration equation, to calculate the OD from the input voltages on the Red and NIR channels, and to graph the OD on the screen of the SBC after they are calculated.

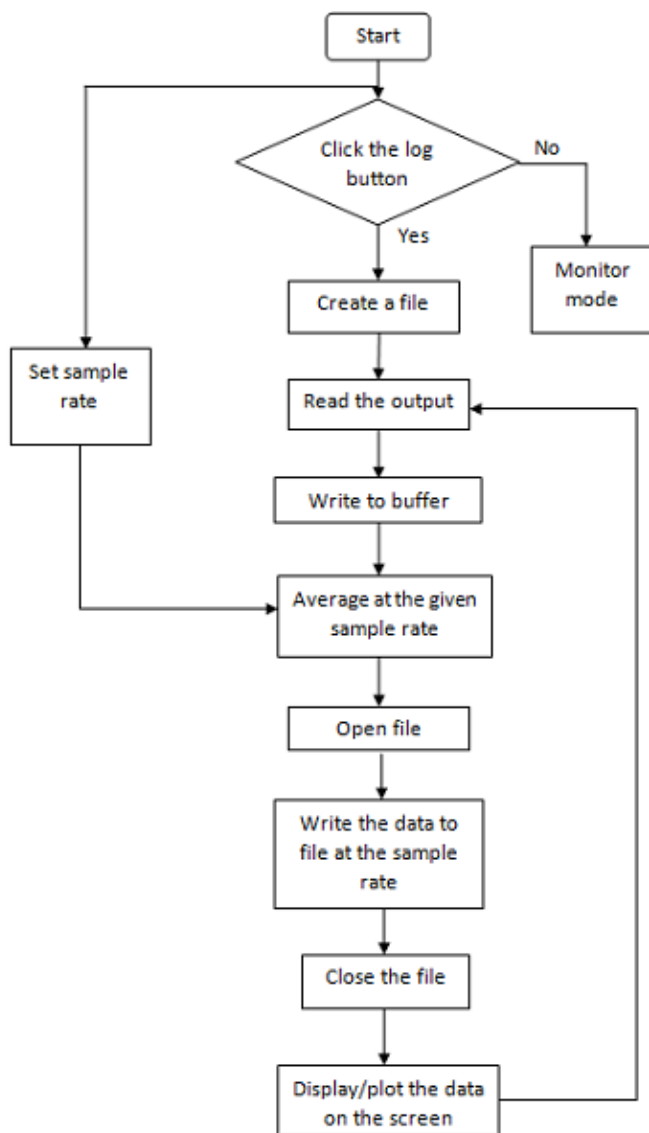


Figure 10: Flow chart of the program on the DAQ

2.2 Preliminary Tests

Several main issues were addressed in the testing of the system. The most basic one is the functioning of the sensor's electronic circuits. The sensor and amplifier systems were designed to give reasonable outputs according to the expected light

intensity and absorption. Also, the output voltages could be adjusted to the proper range through calibration involving both the SBC and the electronic circuits. A second key issue is the functioning of the overall system including the software and hardware. A series of system tests were designed to ensure proper software function and compatibility with the hardware. The system was to be tested under an actual algal-cultivation environment involving significant temperature variations, the potential for electrical interference from external sources, and other issues such as bio-fouling, which is likely to occur over long periods in a real production environment. Under these conditions, the sensor must be accurate and robust to guarantee it can be used in production control. Tests focusing on sensor and system stability over time only involved DI water and were mostly conducted in the Biological Engineering Sensor Technologies Laboratory (BEST lab) in the Department of Biological & Agricultural Engineering (BAEN), Texas A&M University (TAMU), College Station, TX. Tests focusing on sensor and system stability over time in the presence of significant temperature change and higher potential for external electrical interference were conducted with algae in a cultivation raceway in the lab of Dr. Ronald Lacey, BAEN, TAMU.

2.2.1 Initial Tests and Calibration Procedure

The prototype OD sensor system was initially tested in the BEST Lab. The system was powered with two 12 volts auto batteries in series and sharing the same ground in order to create a power range of -12 to +12 volts. The DAQ was powered by the AC adapter provided by the manufacturer. De-ionized (DI) water was pumped

through the flow cell first, and then the variable resistors were adjusted to tune the maximum output at approximately -3 volts on both NIR and Red channels measured with a digital multimeter. Shielded cables were used to reduce external noise.

After the variable resistor was adjusted, algae samples were prepared for calibrating the sensor to an appropriate absorption range. Algal suspensions were collected from raceways in lab of algae cultivation lab, BAEN, TAMU. The species of algae used was *Nannochloropsis oculata*, and the culture had been adapted to conditions in Pecos, Texas. For the test, 2.0 L of algal culture was bottled and sent to BEST Lab, and the sensor was calibrated according to the OD value of this algal culture. The calibration procedure was as follows: (1) one 0.39”x0.39” quartz cuvette (21/Q/10, Starna Cells, Atascadero, CA) filled with DI water was scanned for absorbance from 450 to 800 nm with a spectrophotometer (Cary 500 Scan UV-Vis-NIR, Varian, Palo Alto, CA) to provide a baseline spectrum with DI water only; (2) several algal samples from the initial culture were prepared at different OD levels by varying the proportions of algal suspension and DI water; (3) absorbance of each algal sample was measured by filling a cuvette with a small portion of the sample and scanning with the spectrophotometer; (4) the average absorbance from 745 to 755 nm (This referred to the document of OD measurement by ultraviolet-visible spectrophotometer by General Atomics) was calculated to serve as the reference OD₇₅₀ value for the given sample; (5) the rest of the same sample was pumped through the sensor’s flow cell to generate the output voltages, which were recorded on the Micro SD card by the DAQ; and (6) appropriate values were calculated for equation parameters to relate sensor output to

OD₇₅₀ reference values. Each sample was run through the system for 10 minutes to produce a stable signal.

2.2.2 Main Tests and Calibration Procedure

Main tests were conducted in Dr. Lacey's algae cultivation lab for relatively long periods of time in order to test the accuracy and stability of the sensor in the presence of significant temperature changes and potential electrical interference. The longest continuous test period was two weeks. The algae were cultivated in an indoor race way, where temperature was not regulated. Again, the species used was *N. oculata*. Each 24-hr period was considered a growth cycle regarding algal-culture light regulation, in which the light was on for 16 hours and off for 8 hours. The pH level was maintained below 9.1 with a pH controller that used CO₂ as the controlling agent.

The OD sensor was calibrated with the algal suspension from the raceway. The algal OD-measurement procedure for reference values followed the protocol used in Dr. Lacey's lab, which included a daily sampling and spectroscopic measurement: (1) one 1- x 1- cm cuvette with DI water was inserted in the spectrophotometer (Genesys 20, thermo scientific, Waltham, Massachusetts) and scanned at 750 nm as a blank to “zero the equipment;” (2) algal samples were prepared at different OD levels by diluting the original algal suspension from the raceway with DI water (Table 2), the total amount of each sample was around 100ml; (3) then, 10 ml of each algal sample was diluted 10 times with DI water and scanned with the spectrophotometer to avoid measurement inaccuracy at high concentrations; (4) the readings multiplied by the dilution factor —10 in this case – was treated as the reference OD₇₅₀ value at 750 nm for calibration. The rest

of the sample was pumped through the flow cell inside the sensor for 15 minutes, and the outputs of red and NIR channels were collected by the DAQ. The output-channel records were entered into a computer for analysis in statistical analysis software, the average of both channel outputs was used in the calibration for predicting OD₇₅₀. The calibration curve was developed based on multiple linear regression with the two output voltages as independent variables and the corresponding OD₇₅₀ value as the dependent variable. The data and calibration statistics were in the appendix B. The calibration curve parameters calculated in the analysis were entered into the program in the DAQ.

The sensor and DAQ box were placed by the raceway to test. The suction and exhaust tubes of the pump were installed in the raceway to hold them in position to withdraw and release back the algal culture, respectively. Once the sensor was turned on, the algae were pumped through the flow cell, and data were collected by the DAQ at 5-s intervals and stored in the Micro SD card.

Several of these tests were conducted from September to December, 2010. It is clear that the sensor output value is affected by variation of OD level in the algal culture that corresponds to light and dark cycles. The sensor also responds to sudden changes in algal culture concentration due to addition of growth media. Noise also appeared in the data. It was also apparent that the temperature changes caused drifting of the sensor output due to variations of day and night temperature.

2.2.3 Sensor System Temperature Stability Tests

From the initial tests, there was a strong indication that sensor output was influenced by ambient temperature. In order to investigate the influence of ambient

temperature on the sensor, a test was devised to exclude the effect of algal-culture temperature. This test was conducted in late December (2010) in algae cultivation lab so as to take advantage of temperature variation, and the sensor was positioned near the raceway. The sensor was activated, without turning the pump on, so that no liquid would flow through the flow cell. This test was conducted for 3 days. To add confirmation to the idea that temperature was the major influence on sensor output variation, the sensor was placed in an environment with stable ambient temperature at approximately 4.9°C in the BEST lab to be tested.

3. REDESIGNED SENSOR

3.1 Design and Construction of the Redesigned Sensor System

3.1.1 Overall Modifications

As shown in the previous results, the original sensor had issues of temperature drifting, instable and noisy output. Therefore, the sensor required an environment with regulated temperature to produce more stable output. The sensor would be redesigned and modified with the temperature control unit. As shown in Figure 11, the new sensor consisted of a temperature regulation module, temperature monitor feedback, an optical module, a hydraulic loop, an electronics module, and a data acquisition module.

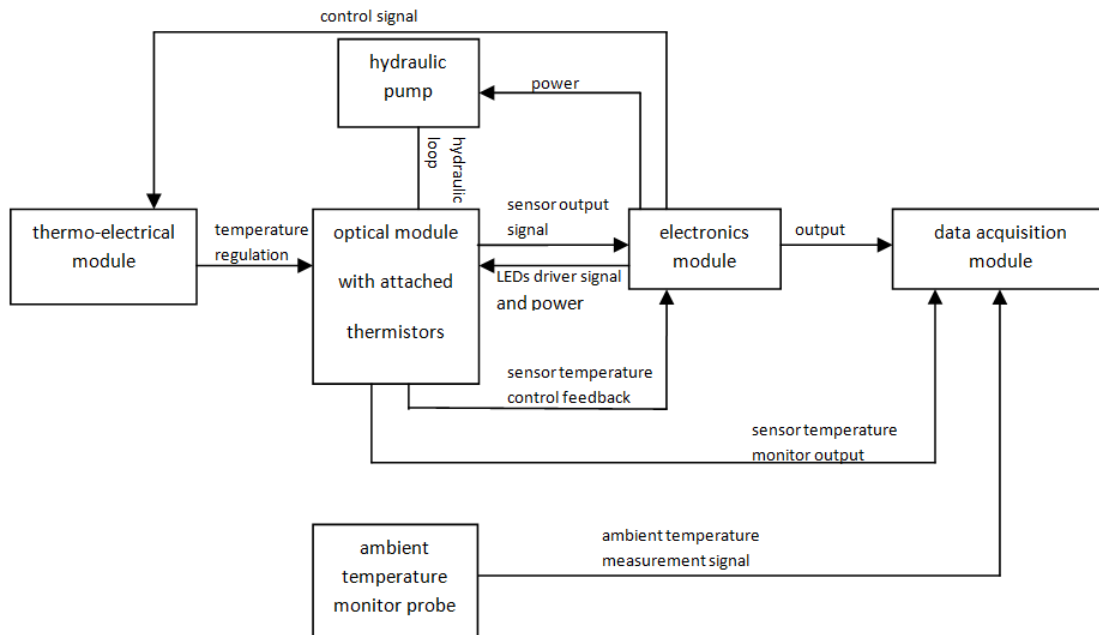


Figure 11: New sensor design block diagram (There are four major modules in the system: TEC module, optical module, electronics module, and DAQ)

Like the old sensor, the optical module would still include the two optical channels: NIR and red. The LEDs would also be at the same wavelength. And the detectors would also have been chosen with the similar response curve. The thermo-electrical cooling module (TEC) which is shown in the diagram is the temperature regulation element. While the control signal for the TEC is sent from the temperature control circuit in the electronics module, together with the feedback of the temperature monitor, a temperature regulation circuit is formed. Except for the TEC controller, the electrical module also would have the circuit for driving LEDs to send the signal to control the LEDs and a signal process circuit to prepare the signal from the detectors for the DAQ. The DAQ system would have the same functions as in the old system: displaying and recording the data.

3.1.2 Design of the Circuits

3.1.2.1 Temperature Effect on the LEDs and Detectors

As discussed in previous session, the ambient temperature had great influence on the output. Although all electronics have some temperature drift, the main parts affected by the temperature are LEDs and photodiodes. The radiant output and the peak emission wavelength of the LEDs will vary with the temperature, so the ambient temperature variation and the self-heating of the LEDs can be the reasons of drift in the output signal. Therefore, the LEDs are the primary goal of temperature regulation.

3.1.2.2 Temperature Control Method and Circuit

Results from the experiment showed that one temperature control unit should be added to regulate the temperature of those LEDs. One of the major requirements for the

temperature control device would be compact size, to fit into the sensor housing. To reduce the noise level of the whole system, a quiet and non-vibration device would be preferred. Also, there was not much power required for the system due to the low power LEDs and the temperature variation range of the operating environment. Thermoelectric cooling (TEC) module, which is based on the Peltier effect, is a solid-state heat pump. It is a small, flat device moving the heat from one side to another when a DC current is applied. With the current changing direction, the heat transfer direction would be reversed as well. Amount of the cooling is controlled by the magnitude of the current. A TEC (TE-31-1.0-2.0, TE Technology Inc., Traverse city, MI) module was chosen for this system. It had a maximum power of 5.6 watts together with maximum current of 2.3 amps and maximum voltage of 3.9 volts. There are two control methods for TEC. The first one is thermostatic method, which involves switching the current for the TEC between temperature set point. Therefore, the temperature would continually vary between those two points. The second method is steady state, where a feedback loop would be built to keep the temperature close to the set point [29].

Under this circumstance, the temperature needed to be stabilized at a specific set point to avoid temperature drift of the LEDs. Therefore, the second control method was chosen. In order to stabilize the temperature at a set point, first there would be a feedback loop to monitor the regulated temperature. Second, the TEC should be either cooling or heating, which requires the control circuit to be capable of driving the current in both directions. Therefore, a close loop temperature controller from a Texas Instrument application report was referred to and developed. Fundamentally, the control

circuit (Figure 12) consists of a control chip, an H-bridge driver, and a LC filter. A thermal feedback loop was added to set the steady temperature point. The fan is used to dissipate the heat from the heat sink in order to keep the TEC working as designed. Finally, there is a 12 volts power supply to power the whole system.

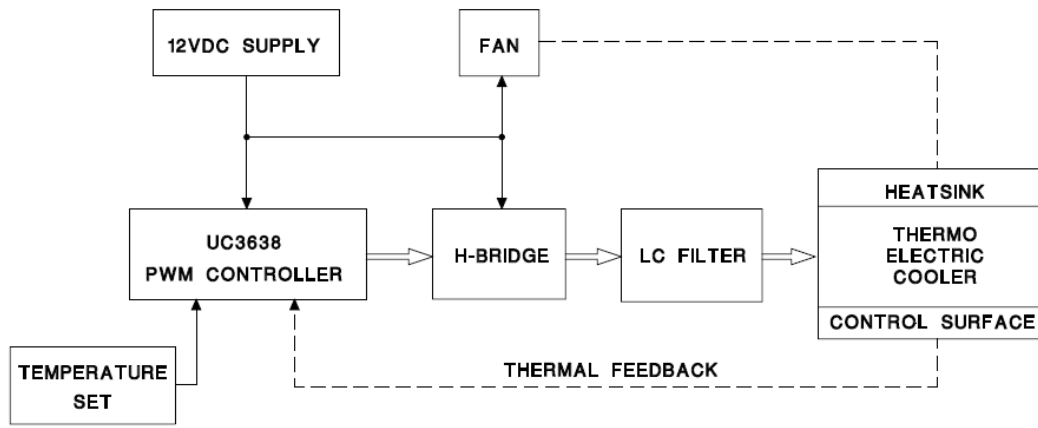


Figure 12: TEC control circuit block diagram

Due to the size of the TEC control circuit schematic, it was split into 3 parts. First part is the current limit circuit (Figure 13). The power module can provide up to 6-Amps current, while the TEC can draw more current than it is designed to. Therefore, a current limiter is needed to limit the current, which will go through the TEC module. The basic idea of this current limiter was: the voltage regulator VR1 provided a constant 1.25 voltage together with a high power resistor R16; therefore, a current limiter was formed. The current provided by the circuit follows the equation 6:

$$I = \frac{1.25 V}{R_{16}} \quad (6)$$

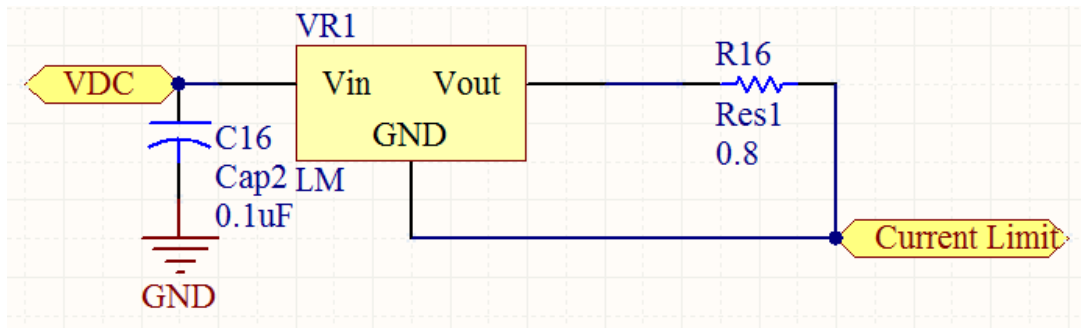


Figure 13: The current limit circuit schematic

The second part was the control chip and the temperature feedback loop (Figure 14). A pulse width modulation controller IC1 (UC 3638, Texas Instrument, Dallas, Texas) was employed to generate the pulse train to control the TEC. This is a controller which includes the required circuitry for closed loop PWM control such as a voltage reference, error amplifier, pulse width modulator, oscillator, current sense amplifier, and FET drivers. The PWM frequency was set 100 kHz by R15 together with C13.

A negative temperature coefficient (NTC) thermistor, RT1 (not shown in the schematic), was connected to H2 to form the feedback loop (Figure 14). The thermistor was placed in the hole in one side of the cold plate to monitor the temperature of the target surface. The resistor R7 is parallel with RT1 to linearize the output of the thermistor. The linear taper R9 is used to adjust the temperature set point. It was calibrated by using a thermocouple probe mounted on the cold plate to compensate the nonlinearity of the thermistor. Also, the set point of the controlled temperature was preset at a specific temperature by the thermocouple.

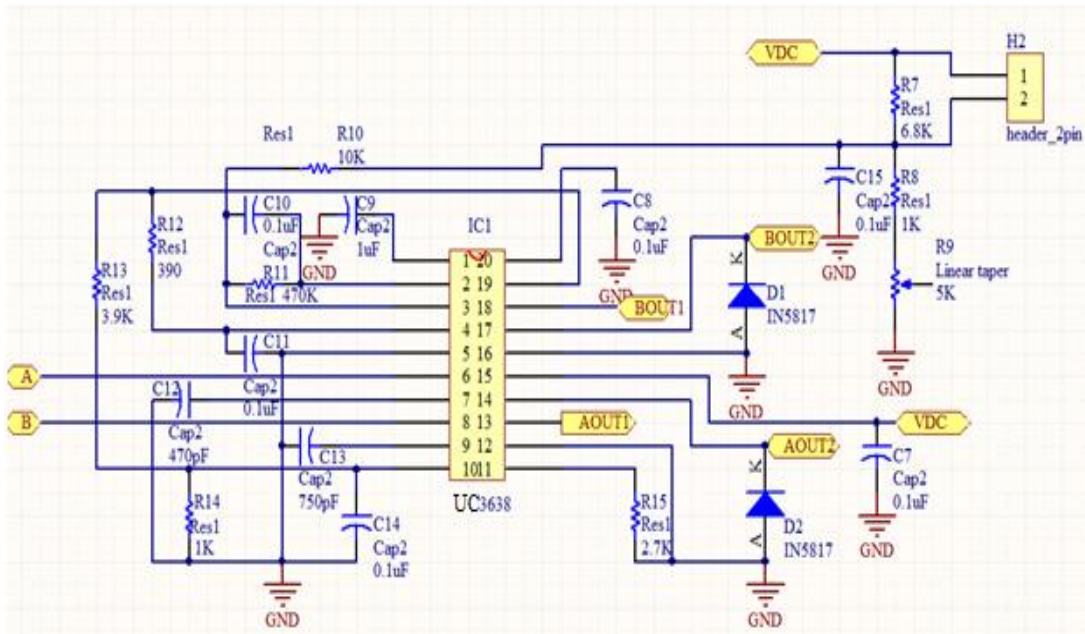


Figure 14: The control chip with its circuit and the feedback loop

In order to achieve the goal of stabilizing the target temperature at a set point, the H-bridge circuit (Figure 15) was designed for the bi-direction current driving for both cooling and heating. Metal-oxide-semiconductor field-effect transistors (MOSFET) Q1-Q4 form the H-bridge. The bipolar junction transistors (BJTs) Q5-Q8, which were connected to the AOUT1 and BOUT1, operate as the high side drivers. And the low sides of the MOSFETs are driven directly by AOUT2 and BOUT2. The basic operation idea of the circuit is described below. When the thermistor sends a temperature feedback signal to the control chip, a comparison is done with the set point provided by the linear taper R9, control signal is then sent to the H-bridge driver pins. When the signal on AOUT1 pin turns on the high side driver, Q1 is on and meanwhile, the AOUT2 pin would also send a signal to turn on the Q4. Therefore, the current would flow from the

power supply through Q1, the LC filter, the TEC and Q4 to the ground. When Q2, Q3 are turned on and Q1, Q4 are off, the current would go through the other direction. In this case, the TEC would be working both heating up and cooling down the cold plate under the control.

Because the ac ripples could potentially be damaging to the TEC module, the pulse output is converted to the dc voltage. Inductors L1, L2 together with capacitor C2-C6 form the LC filter (Figure 15), which would deliver a variable dc voltage up to ± 12 volts from the bridge.

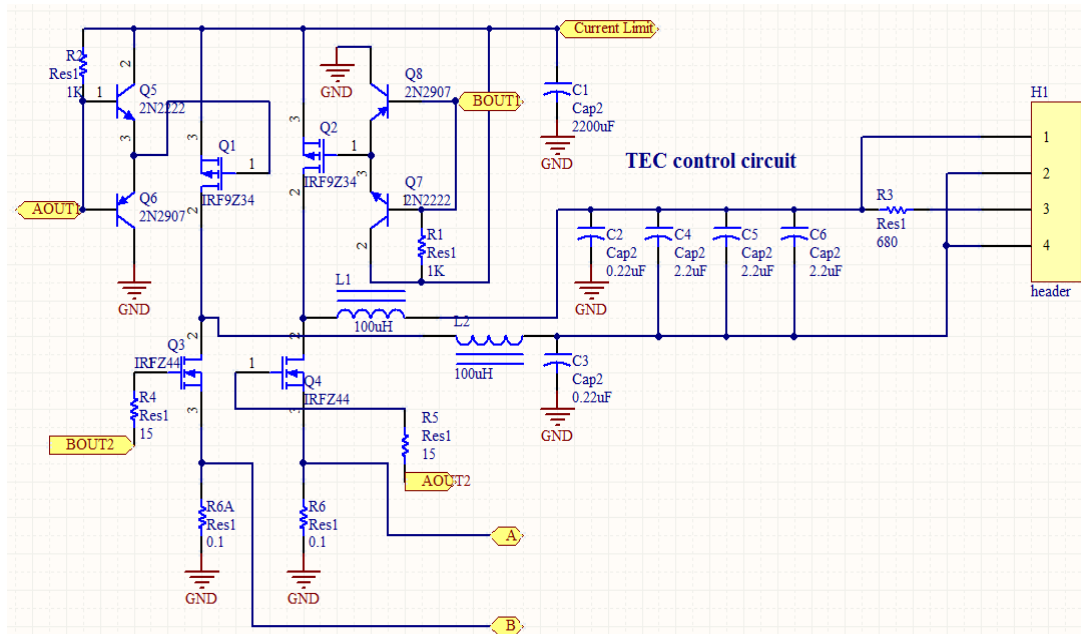


Figure 15: H-bridge circuit and LC filter circuit

3.1.2.3 Logarithmic Circuit for the Absorption Measurement

For the previous sensor, the detectors had a relatively small effective area, which was around 5.7 mm^2 . Under this situation, the signal generated by the photodiode would be very weak. The amplification coefficients for both channels were relatively large and the actual maximum current signal generated by the photo detector was around 0.017 mA for NIR channel and 0.0041 mA for red channel. The small current can cause low signal to noise ratio. Also, unstable output of the amplifier is possible if the noise current exceeded the signal current. The frequency response, which is related to the photodiode window size, would not be a main issue since the DC voltage was recorded by the data-acquisition system and used. Therefore, in the new design, the same series of photodiodes (S1337-1010BR, Hamamatsu Corporation, Hamamatsu, Japan) with a larger effective area were chosen.

In the previous design, the transimpedance amplifier was used simply to convert the current signal to voltage and amplify the signal. This time, a logarithmic (LOG102, Texas Instruments, TX) IC2 chip was used. The function of the logarithmic chip is to take log ratio of the reference signal and the sample signal and then provide a voltage output. The sample signal was the current generated by the photodiodes which received the light passed through the algal sample liquid. And the reference signal referred to the current signal generated by the photodiodes when light passed through the reference media. By constructing the housing of the reference and sample room in the same layout, based on the definition of the absorbance, ideally the output was the OD measured. But under the current situation, the layout of the reference and the sample housing would not

be exactly the same. The result would not be precisely absorption measurement.

Addition of this unit was aimed at increasing the linearity of the voltage output to get better prediction results. In figure 16, the IC2 is the log chip for the NIR channel. Pin1 is for the reference current signal and pin14 is for the sample current signal. The relation between the output and the input current signals is described in equation 7.

$$V_{log\ out} = (1V) * \log\left(\frac{I_{reference}}{I_{sample}}\right) \quad (7)$$

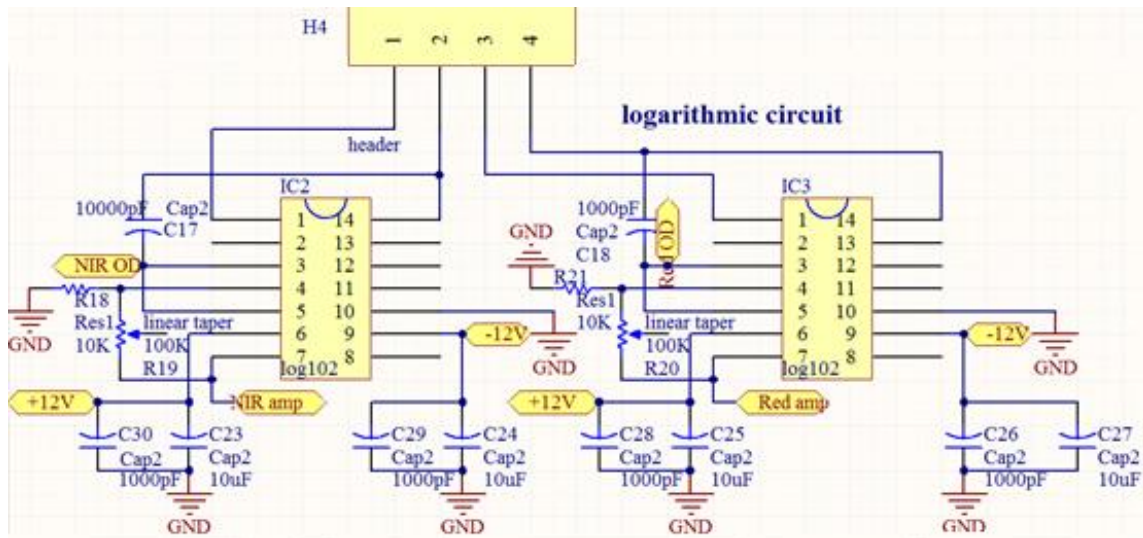


Figure 16: The logarithmic circuit schematic

The capacitor between pin14 and pin5 is the frequency compensation capacitor. The size of the capacitor was chosen from the Typical Characteristic Curves (Minimum Value of Compensation Capacitor) in the datasheet (Figure 17). The minimum value of this capacitor was determined by the maximum value of the input current from the sample detector I_{sample} and the minimum value of the input current from the reference

detector I_{sample} . The larger capacitor value would give a more stable output, but would reduce the frequency response. Due to the DC output signal, the value of the capacitor was chosen as the largest value in the curve to achieve more stable output. The following were the selection procedures: The basic idea was to build a circuit that can turn the current output of the detector into voltage and measure the current indirectly. Therefore, an amplification circuit as used in the old sensor was built. The maximum current output was archived when both LEDs in the same channel were turned on. And the minimum current output was when both LEDs for the same channel were turned off, which would be the dark current from the datasheet. For the gain of 8.38K of NIR channel, the output voltage was 4.038 Volts when the LEDs were on. The maximum input current for NIR channel was calculated to be at 0.46mA, and the minimum input current for NIR channel was 200pA from the datasheet. The same calculation was conducted on the red channel output. With the gain of 8.38K, the highest voltage output was 0.317 volts. Therefore, the maximum input current for red channel was around 0.038mA. The minimum input current value for red channel was also 200pA from the datasheet. According to the input current, from the curve, a 1000pF capacitor was chosen for the red channel and a 10000pF capacitor was chosen for the NIR channel.

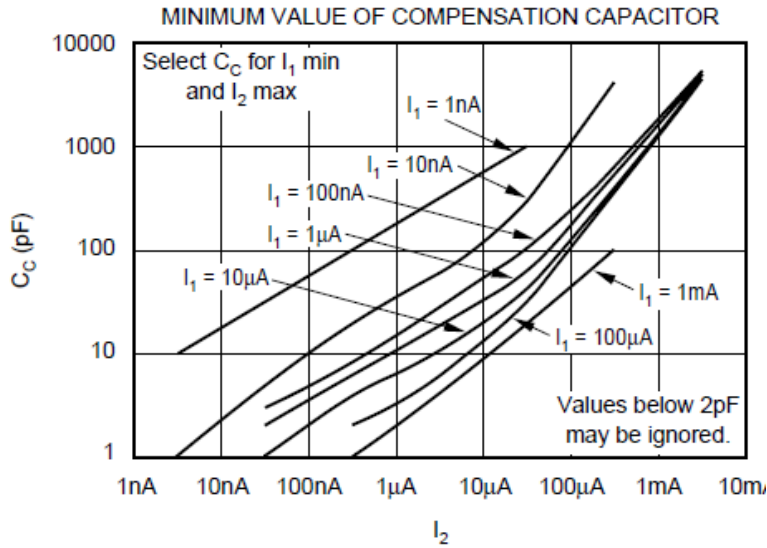


Figure 17: Minimum Value of Compensation Capacitor (the I_1 refers to the current signal from the reference detector and the I_2 is from the sample detector)

Capacitors in between the power line and the ground were positioned close to the LOG102 chip to reduce the lead inductance influence of the power supply line and noise. It was recommended in the datasheet that each of the power supply lines should be bypassed with a 10uF tantalum capacitor in parallel with another 1000pF ceramic capacitor.

Finally, there is a built in non-inverting amplifier in the LOG102 chip, the voltage output of pin7 is the output from pin3 amplified. This circuit can be used to tune the output into the range which can be accepted by the data acquisition box. The amplification gain can be adjusted according to the following equation 8 by increasing or decreasing the resistors ratio between pins 4 and 7:

$$V_{out\ amp} = \left(1 + \frac{R_{19}}{R_{18}}\right)V_{out\ OD} \quad (8)$$

In the equation, $V_{out OD}$ referred to the output from the log ration circuit; $V_{out amp}$ referred to the amplified output from $V_{out OD}$. And the equations for the both channels were the same.

3.1.2.4 LM317 Constant Current LED Driver

The previous LEDs driver circuit used voltage regulators to provide a stable forward voltage. Usually, LEDs illumination radiant output is not only closely related with the forward current provided by the power, but also varies with the temperature. The original circuit used a fixed 5-volts output voltage regulator and then a resistor was used for current and voltage limiting. With the voltage regulator which is a temperature dependent device, the output voltage would drift with the ambient temperature. Therefore, the LED illumination intensity would be varied with the current that is provided by the voltage regulator. The output of the sensor would also vary with the light intensity from the LEDs. In order to stabilize the output, this time a constant current LED driver was chosen. For this circuit, the first advantage is the stable current, which would reduce the temperature influence on the LEDs. The second advantage is the possibility of limiting forward current. In this case, there would be less chance for the current to exceed the maximum limit for the LEDs.

The LEDs driver circuit is shown in the following figure (Figure 18). A voltage regulator VR2 (LM317, STMicroelectronics, Geneva, Switzerland) was chosen as the constant current provider. It has a bandgap voltage, which is a temperature independent reference across the output and adjust pin. According to the 1.25V reference voltage, a resistor was chosen to generate the required forward current for the LEDs. The relation

between the reference voltage and the resistor is described in equation 9. Resistor R22 and R23 were chosen according to this equation. Capacitors for the power line are used to reduce the noise and stabilize the input power. Except for the values of R22 and R23, which are required by the different LEDs forward current in the two channels, the rest of the components share the same values and configuration for both channels.

$$R = \frac{1.25 V}{I_{forward}} \quad (9)$$

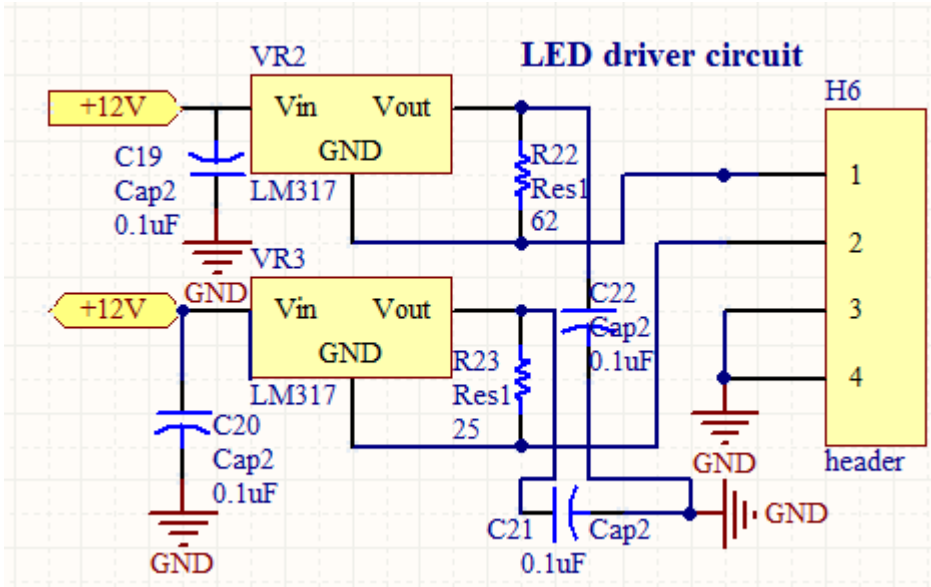


Figure 18: Constant current LED driver schematic

The whole circuit schematic, including the logarithmic circuit for the absorbance measurement, the constant current LED driver, TEC control circuit, power line and the headers, was attached in appendix E with the list of value of each component.

3.1.2.5 Printed Circuit Board

After the circuit was designed and tested on the prototype bread board, the printed circuit board (PCB) layout was designed in Altium Designer (Altium Limited, Shanghai, China). This layout has top and bottom layer with the same size of the power supply module for the convenience of enclosure. Also, the ground and power line of high power portion (TEC control) and low power part (LEDs driver and logarithmic circuit) were separated in order to reduce the interference between each part. Then the proper files had been generated to be imported in CircuitCam plotting program. In CircuitCam, the cutting route and cutting styles together with corresponding cutting tools were assigned for later use. Then a file was exported to be used in the BoardMaster program, which controls the computer numerical controlled (CNC) circuit board plotter (ProtoMat S42, LPKF Laser & Electronics, Hannover, Germany). This circuit plotter was used to manufacture final version of the PCB according to the layout. All components were soldered on the finished PCB (Figure 19) according to the schematic of the whole circuit. Also, the layout of the PCB is shown in the appendix D.

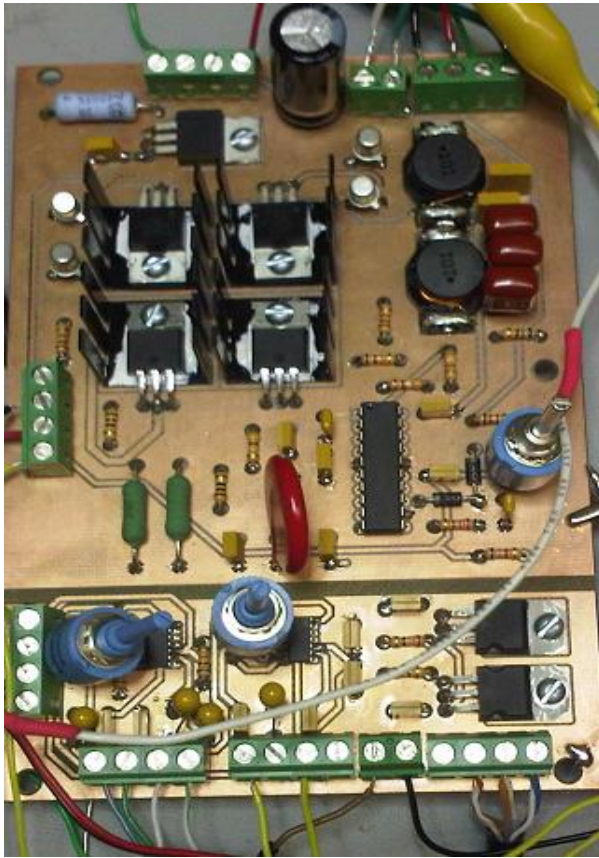


Figure 19: New printed circuit board (TEC control, LED driver and logarithmic circuit)

3.1.2.6 Thermistor Calibration

In order to record the regulated temperature of the cold plate, another thermistor identical to thermistor used in the feedback loop was added. This thermistor had to be calibrated before use. The calibration procedure was similar to the procedure for the thermistor used in the feedback loop. Temperature was varied by heating the water up inside a cup. Then the probe which used to monitor the water temperature and the thermistor were dipped inside the water together. Twelve volt power was provided for the thermistor. A linear taper, which was adjusted to 1.698-k Ω , was placed in series with

the thermistor. The temperature of the water was shown on the display in Celsius. Then, voltage across the thermistor was recorded and relationship was established with corresponding temperature (Figure 20).

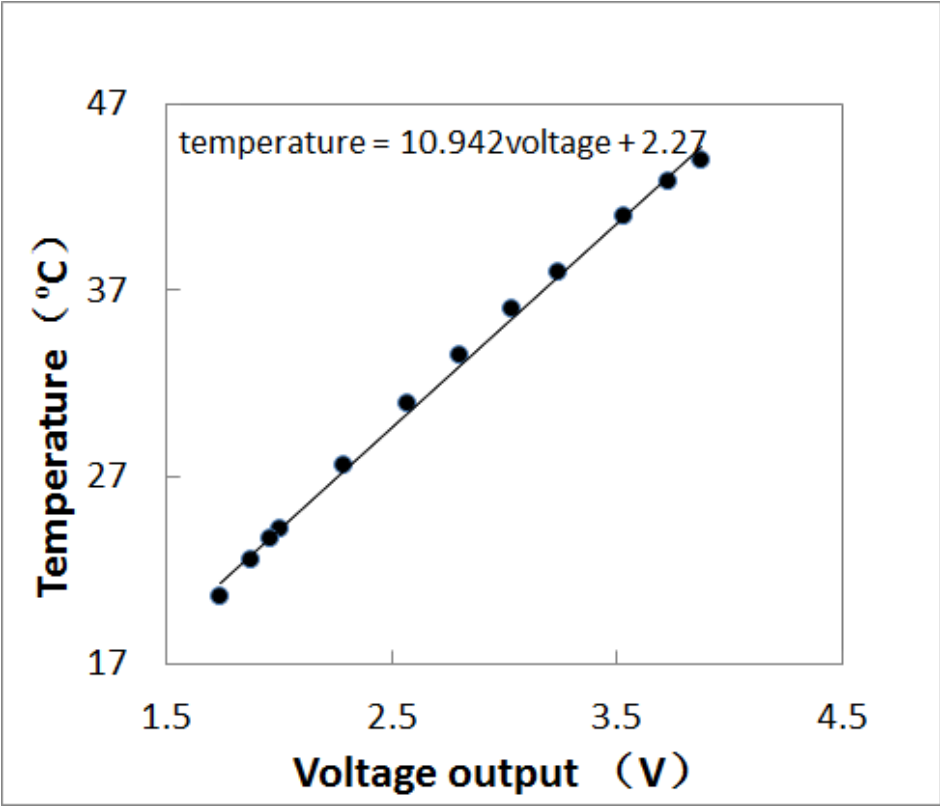


Figure 20: Calibration equation of the thermistor

3.1.3 Redesign and Assembly of the Sensor System Housing

3.1.3.1 Redesign of the Optical Module Sensor Housing

The TEC module was added to regulate the temperature for the sensor in order to reduce the temperature influence on the result; also, due to the change of the photodetectors, the configuration of the sensor optical housing would also be adjusted

accordingly. But the limitation lay in the dimension of the old sensor housing. The size of the old sensor housing was too small to fit any more parts in it. The housing had to be redesigned and rebuilt.

The basic idea on this sensor was not changed. The OD measurement taken by the sensor was still calculated according to the calibration curve which was based on the output of the two channel detectors. There were three points that required the change in the structure of the sensor: (1) to fit the new detectors that would be used for this sensor, larger windows would be used; (2) a reference layer would be added to the housing for the new circuit design and better alignment of the detectors and LEDs; and (3) extra space would be needed for the TEC module. Due to the size limitation of the old sensor, the temperature regulation unit was not able to be added in. So, in this design, the sensor housing was designed for easy installation and assembly of the thermal unit.

According to the new sensor requirement, the sensor housing has two levels. The bottom level is for the sample, there is a flow cell centered in the middle. The flow cell is secured by the top plate and limited by the two side covers. The side covers have holes for the flow cell fittings where the pump tubing connects. There are still two channels as in the previous sensor: NIR channel and red channel. Also, each channel includes two LEDs and one detector. The detectors and the LEDs are mounted on the detector plate and LED plate respectively. Also, an IR cutoff optical filter (NT55-237, Edmund Optics Inc., Barrington, NJ) at 700nm for red channel detector was mounted on the detector window of the sensor housing to prevent the detector from receiving the light from the NIR LEDs. At the red channel, there was a long pass filter (NT32-767, Edmund Optics

Inc., Barrington, NJ) at 780nm to block the light from the red LEDs. The detectors and the LEDs were placed facing each other with the flow cell positioned at the center in between them. When the algal samples are pumped through, the LEDs are emitting the light and the detectors receive the light that has passed through the algal sample in the flow cell. Then photodetectors generate current signals as output. The top level has the same layout as the bottom layer, but the slight difference is in the flow cell. DI water is used in the flow cell to generate reference signals. Following the idea and the layout mentioned above, the whole sensor housing was designed in AutoCAD (Figure 21). The dimension of the sensor housing is 2.5"x3.5"x3".

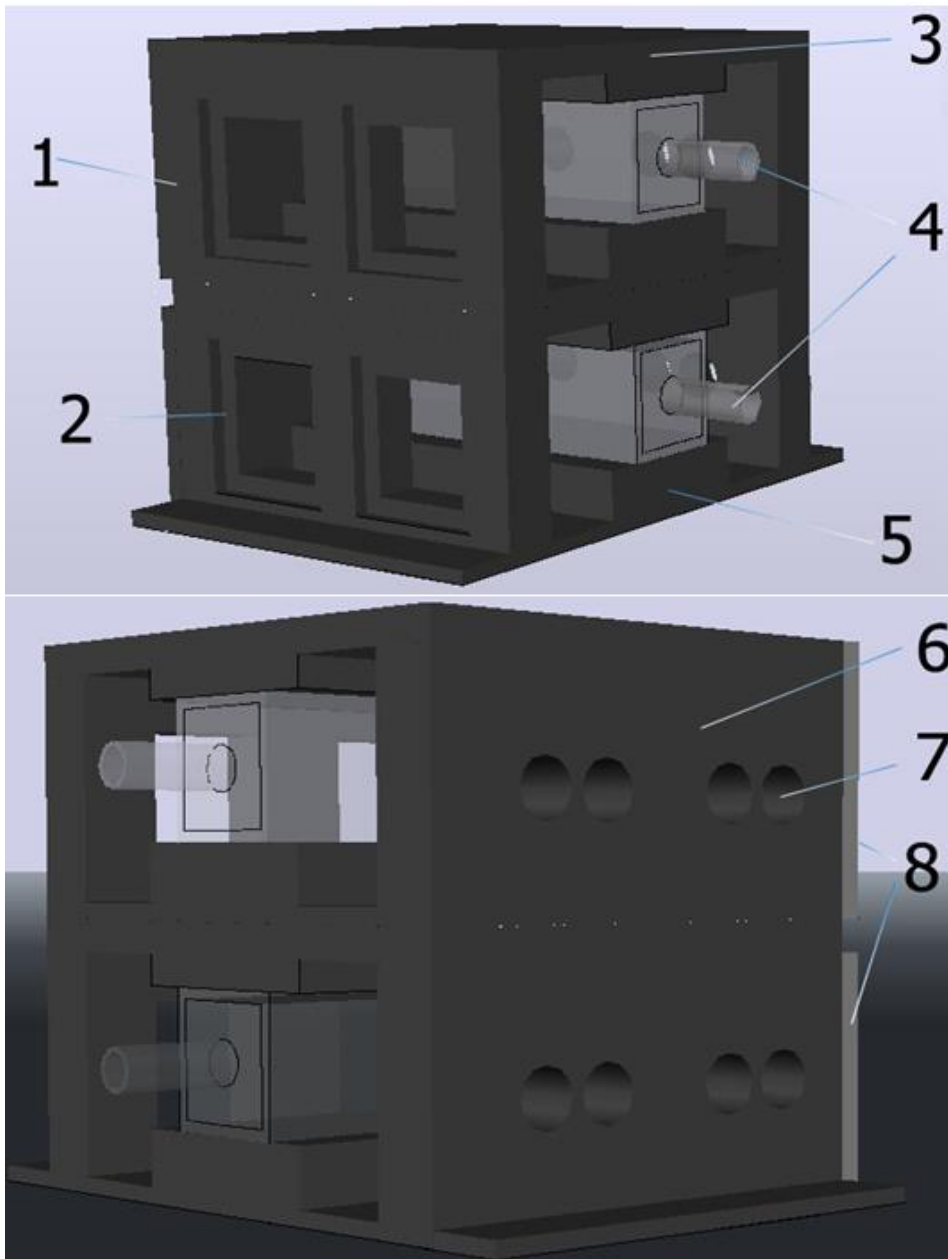


Figure 21: 3D design of the sensor housing in AutoCAD (Picture on the top is the left side view of the sensor housing: the top level is the reference housing and the bottom level is the sample level. Part 1 is the top level detector plate. Part 2 is the detector widow where detector mounted in. Part 3 is the top plate together with the Part 5 bottom plate to hold the flow cell which is part 4. The part numbers referred to different levels. Picture on the bottom is the right side view of the sensor housing. Part 6 is the LED plate which has Part 7 is LED holder to hold the LEDs in place. Part 8 are the back side plates which secure the flow cell in length. In the figure, the front side plates are not shown to give the better view of the flow cells.)

AutoCAD plotting was fabricated by Mathew Shimek in BAEN, TAMU, TX.

The sensor housing was made out of PVC material.

3.1.3.2 Optical Module Sensor Assembly

After the sensor housing of the optical module was completed, the LEDs, the detectors and the optical filters were placed in their corresponding positions. And the next step was to design the mounting of the thermal electrical cooler (TEC) module. The TEC has a cold side and a hot side. Usually, in order to work properly, the cold side has to be attached to a cold plate (a metal plate with high heat conductivity rate). Through the cold plate, the heat is conducted (removed) to (from) the objects more smoothly and consistently to maintain the even temperature. The hot side of the TEC is required to be attached to a heat dissipation device to disperse the heat generated. Because the TEC used in this sensor was not a high power unit, a 2.0" x 2.0" x 0.12" aluminum cold plate were used for the LEDs. A cold plate and a heat sink were also placed at the detector side, but no TEC was needed. The cold plates were drilled according to the position of the leads of the LEDs and the detectors. And then, the cold plates were put on the back of the LEDs and the detectors with thermal paste (Ceramique 2, Arctic Silver Incorporated, Visalia, CA) to achieve the maximum contact surface area. Following the cold plates, the TEC was placed between the back of the cold plate and the heat sink on the LED side to dissipate the heat. A Common computer AM2 socket heat sink was used together with a 45mm fan. Thermal compound was also used in between the cold plate and the cold side of the TEC. The back of the detectors were also attached to the other cold plate, and then attached to a computer heat sink. Figure 22 showed the assembly

view of the sensor housing with the TEC module. The dimension of the whole assembly with fans is 3"x5"x3.5".

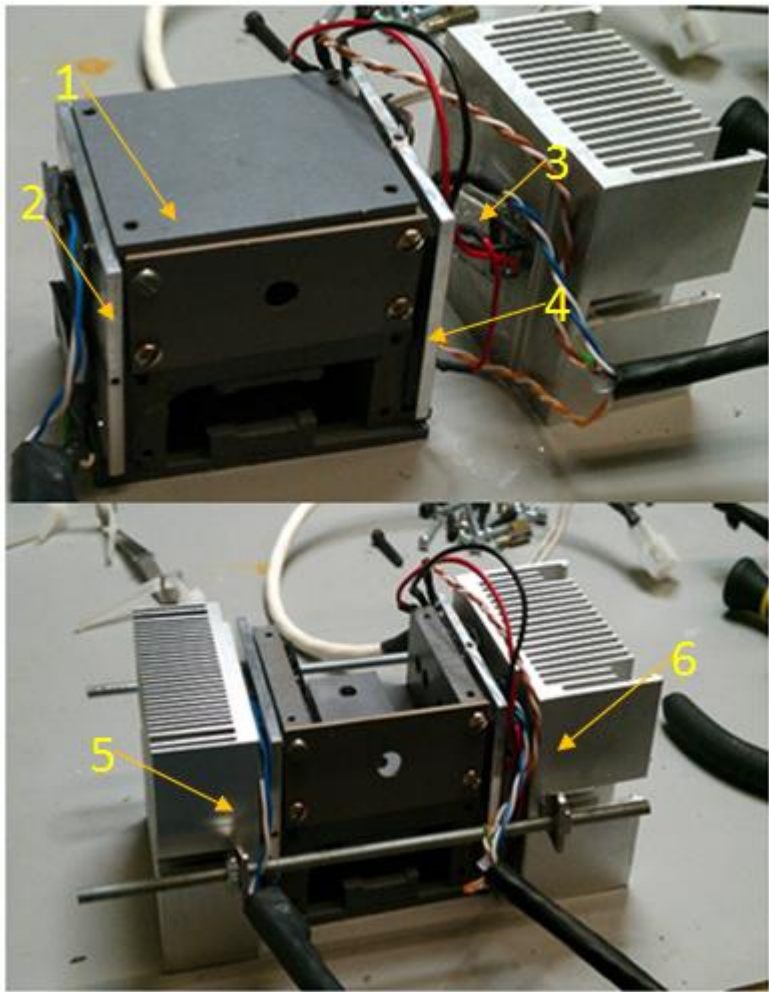


Figure 22: Sensor housing assembly with TEC and heat sink (1: Sensor housing; 2: Photodiodes side cold plate; 3: TEC module; 4: LED side cold plate; 5: Detector side heat sink; 6: LED side heat sink.)

3.1.3.3 Sensor System Enclosure

After the initial test of the sensor and the circuits in the BEST lab, there would be an enclosure assembled for the electronics and the sensor housing prior to the test in the practical environment. The design was aimed at separating the electronics and the sensor housing. Therefore, there were two separate parts: one part was for the electronics and the other part was for the whole sensor. Also, the electronics enclosure was placed above the sensor housing, under this situation, in case of a leak in the pump or tubing, the sample media would flow out without contaminating the electronics.

Enclosure for electronics was modified from an existing cast aluminum box (CU-5347, Bud Industries, Willoughby, OH) with the inner dimension of 7.08"x4.33"x3.00". To minimize the sensor size both, the power supply and the PCB board were a compact fit in the enclosure. According to the layout of the connection pin headers on the PCB board, there is LEDs driver pin header for powering the LEDs, detectors input pin header for the input current signal from the photodiodes, AC power input for supplying the AC power to the power supply, thermistor feedback pin header together with TEC power unit pin header, voltage output pin header, and the extra power source pin header for the fans, pumps and etc.. Therefore, there were a total of six connectors for this electronics box, six pin connectors (power connector, Molex, Lisle, IL) were used for the high power connection, and the standard Cat6 RJ45 connectors were chosen for the LEDs driver output and the detectors input, which were low power devices. Then, the positions and the shape of corresponding connectors for those pin headers was marked on the cover for fabrication purpose. Also, to dissipate heat generated by the MOSFET,

four large air vents were made on two narrow sides of the box. Extra dispersing air holes were drilled for the system. There were three extra tuning holes added for the three linear tapers located on the PCB board to adjust the temperature set point for TEC and the output gain. After the layout of the connectors, heat dissipation and the adjustment holes were designed, it was sent to be manufactured by Matt Shemick and then assembled with the help of Viktor Vlassov. Completed electronics enclosure is shown in the following figure (Figure 23).

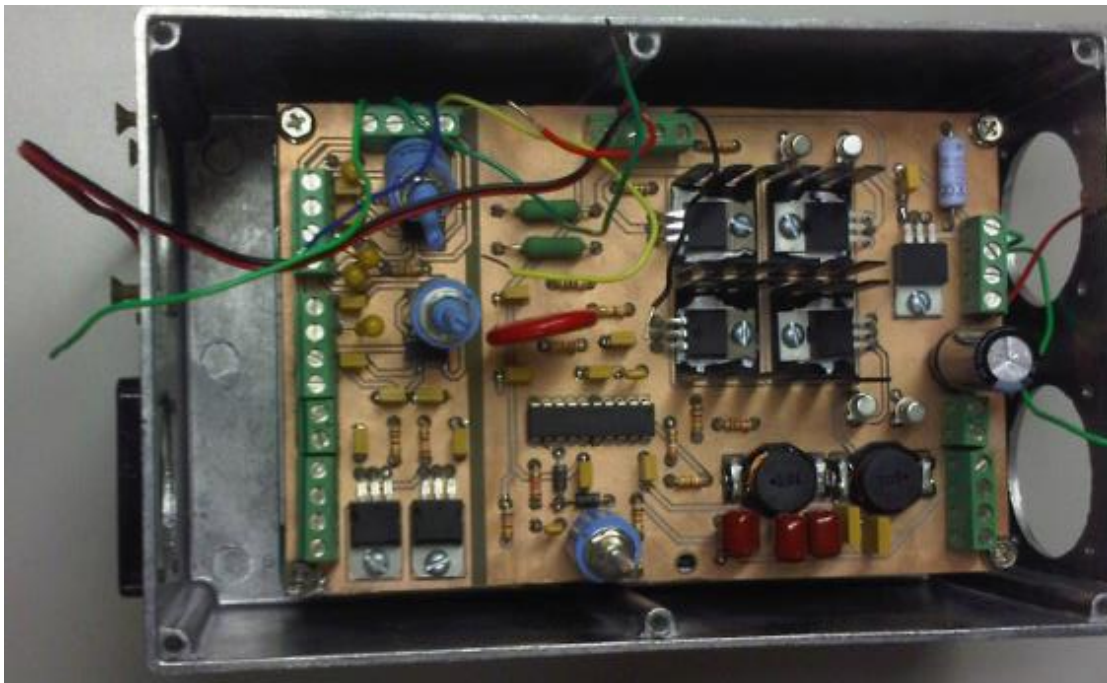


Figure 23: PCB and power supply module inside the electronics enclosure

The whole sensor enclosure was also modified from an 8"x8"x5" metal instrument case (1458D5, Hammond Manufacturing, Ontario, Canada). There was a

connector for the cable to send the voltage output and the temperature monitor voltage to the DAQ, one switch for the sensor system power and the other switch for the pump. As designed for the air ventilation, there were two small fans added, which blow air through the large air vents on the sides of the electronics box; also, there was a single 120mm fan added for cooling the whole system, especially for the TEC unit to dissipate the heat. Apart from things mentioned above, there were corresponding air vents for the fans, mounts for the pump, the temperature monitor unit and the indication LEDs holders. After the layout of all the things above was designed, the enclosure was modified by Matt Shemick and then assembled with the help of Viktor Vlassov. The enclosure (Figure 24) had electronics enclosure mounted above the sensor housing and on the bottom of the enclosure there were holes drilled for drain if needed in case of a water leak. The front panel has one connector, indication LEDs, a fuse, a large fan and switches. In the back, there is temperature monitor unit and the tubing holes for the pump. The mounting bracket for the pump and the small fans together with the air ventilation holes were on the two sides of the box.

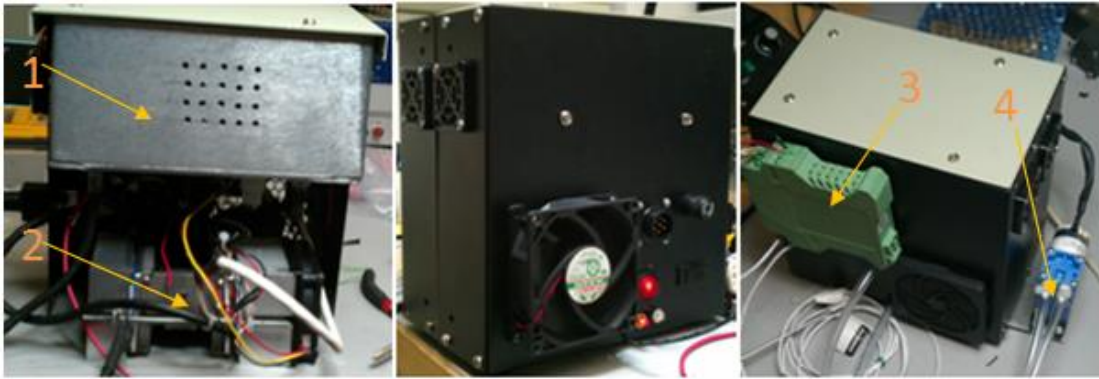


Figure 24: Whole sensor enclosure (left: Inside view; middle: Front view; right: Back view. 1: Electronics enclosure; 2: Sensor housing; 3: Ambient temperature monitor; 4: Pump)

3.1.4 Software

For the new sensor, most of the software remained the same as before. Still, the basic functions include: initiating and setting up the device, logging and storing the data, implementing calibration curve, and displaying the results. According to the output of the sensor, there were seven voltage output channels for the DAQ box: red channel after amplification, red channel raw data, NIR channel amplification, NIR channel raw data, ambient temperature channel, cold plate temperature channel and ground. Therefore, for the input of the DAQ, a seven pin connector was used. The expected output ranges would be different than before: NIR and red channels raw output range is from 0 to 2 volts; because the amplification coefficient was 5, the amplified output is 0 to 10 volts. Therefore, in the software, the code for the acceptable range was changed corresponding to each channel.

3.2 Tests of the Redesigned Sensor

3.2.1 Initial Test

After the sensor housing and the circuit were built, the circuit had to be tuned and tested with the sensor before enclosure. This test was done in the BEST lab. The LED driver and the logarithmic circuit on the PCB were connected through proper pins to the LEDs and the photodiodes, which were mounted on the sensor housing. The power was provided by a dual output power supply module. And the output data was collected by the data acquisition device (U3, LabJack Corporation, Lakewood, CO) and then stored in a computer (Figure 25). In this experiment, the sensor had been test with water and algae samples; also, the algal media had been diluted into different concentrations to examine the response of the sensor. The algae used in this test was coded P4B (*Nannochloropsis Salina*), which was collected, bottled and sent from Pecos microalgae research center (Pecos, TX). The ambient and cold plate temperatures were recorded to investigate the temperature stability of the sensor.

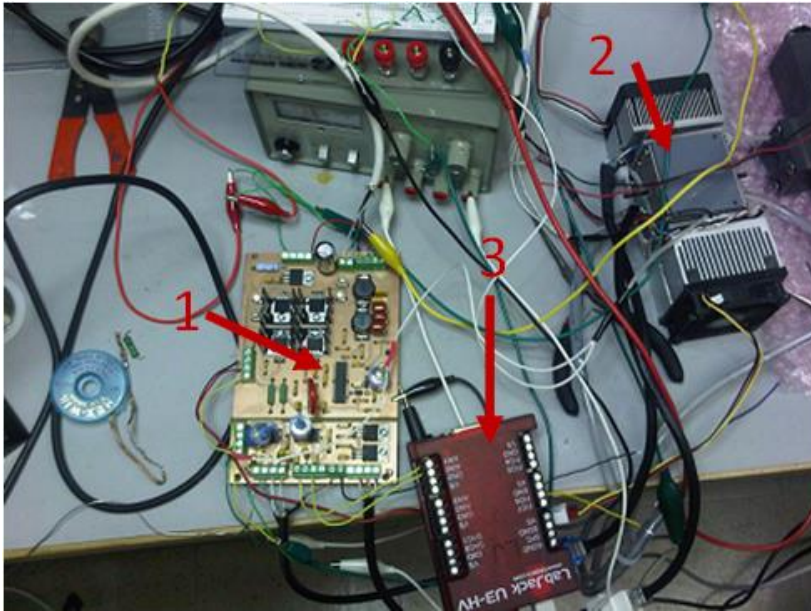


Figure 25: Sensor set up in BEST lab for initial test (1. PCB board; 2. Sensor housing; 3. Labjack DAQ system)

3.2.2 Test of the Sensor Temperature Stability in BEST Lab

After the sensor was fully assembled, it was first set to test the electronics to explore the long term temperature performance of the sensor. This time the sensor was set up on the electrical bench in BEST lab with the variation of the ambient temperature. This test was conducted for seven days. The sensor was activated without a running pump. Therefore, there was no algae culture involved in the test. The test was aimed at evaluating the temperature stability of the whole sensor system only. The ambient temperature and the channels outputs were recorded through Labjack on the computer.

3.2.3 Main Tests and Calibration Procedure of the Redesigned Sensor

The initial experiment on the performance of the sensor was as before, conducted in Dr. Lacey's algae cultivation lab (BAEN, TAMU, College Station, TX). This time the

algae species under test was *Nannochloropsis salina*. The cultivation was in a forty gallon raceway; while at the time of the test conducted around 20-25 gallons of algae were raised in the raceway. Algae in the raceway were circulated by an electrical paddle at the speed of 13.5 rpm/min. The temperature was regulated between 20°C to 28°C. And the pH was controlled from 7.9 to 8.5. Finally, each 24-hr period was separated by 8-hr light on period, which was during the night with 1000 watts florescence light illumination and 16-hr light off, which was in the day without the light illumination. During the dark cycle, the raceway was covered by the dark curtain to shield as much as possible light to control the growth rate of the algae culture.

This test was conducted from 06-02-2012 to 06-23-2012. The sensor was turned off for one day on 06-12-2012. In the first 2 to 3 days, the sensor was pumping the sample through flask, which held sample from the raceway to make sure that the speed of the pump would not break the algal cells. Then, the sensor was placed by the raceway (Figure 26) with the tubing from the pump secured to the top of the raceway wall by a clamp. Then the sensor continuously kept pumping the algae culture from the raceway to the flow-through cell and then back to the raceway again. The DAQ was placed near the sensor to record the ambient temperature, regulated temperature and both channels output voltage.

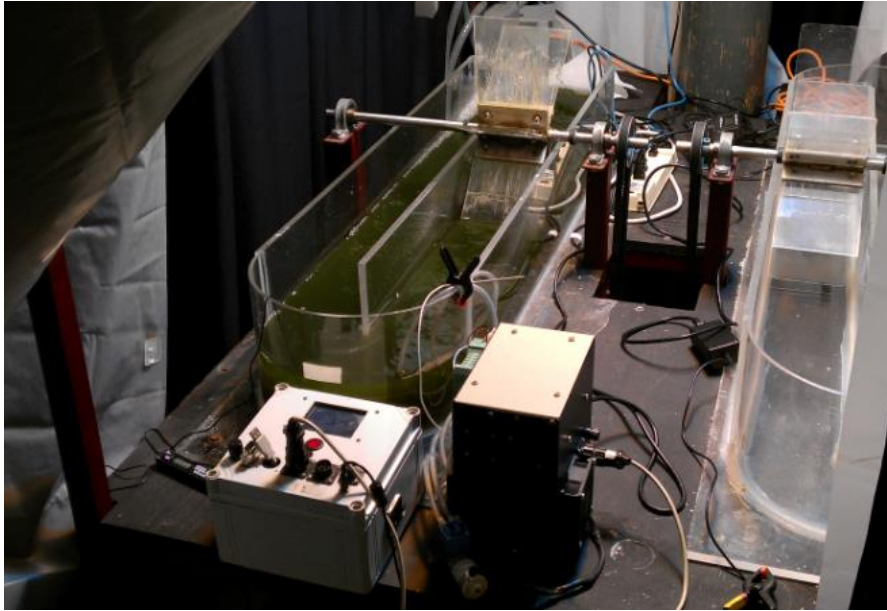


Figure 26: Main test of the redesigned sensor set up in Dr. Lacey's lab by the raceway

For the new sensor, calibration was based on post calibration with the spectrophotometer (Genesys 20, thermo scientific, Waltham, Massachusetts). The algae media were collected from the raceway to be prepared for the calibration. Approximately 1 ml of algae sample was taken from the raceway by a pipette; then, it was diluted by DI water into 10-ml in a sample tube (60819-761, VWR International, Radnor, PA). A 1- x 1- cm cuvette (97000-584, VWR International, Radnor, PA) was filled up with DI water and then inserted into the sample holder of the spectrometer to be scanned as the baseline. After the sample was made evenly, it was transferred to the same cuvette and then scanned with the same spectrometer at the wavelength at 750-nm. In the meantime, the output of both channels was recorded correspondingly. During the test, a total of 63

such samples were taken, yielding 63 referenced OD₇₅₀ measurements together with the channels voltage outputs.

After the test, the data was transferred to a computer to process in Excel. The 63 data points were divided into 2 sets: (1) the calibration set, which was to generate the proper curve between the channels voltage output and the spectrometer OD₇₅₀ measurements; (2) the validation set, which would compare the predicted OD₇₅₀ from the calibration curve to the spectrometer OD₇₅₀ measurement to show the accuracy of the sensor. The 63 data points were randomized in the Excel. Then 40 data points were selected for the calibration set. A multiple linear regression line equation was generated with the NIR channel output as a factor and red output as another factor; the spectrometer OD₇₅₀ measurements as predictor. For the rest of the 23 data points, both channels outputs were fitted into the linear equation to get the 23 predicted OD₇₅₀ values from the calibration equation. The calibration statistics are shown in the appendix C.

4. RESULTS

4.1 Tests Results of the Original Sensor

For the original version of the sensor, there were different stages of tests to pinpoint the performance and the issues. Except for the initial test of the sensor response in the BEST lab, most main tests with algae were conducted in the algae cultivation lab to investigate stability and repeatability. Then, the sensor had been moved back to BEST lab to test in the temperature stable environment to explore the temperature influence on the sensor output. Almost all those tests mentioned above occurred from August to December, 2010. All those tests were different in length, which varied from 2-3 days to 2 weeks.

4.1.1 Results of Initial Tests in BEST Lab

The initial tests were conducted in the BEST lab. During the tests, the main purpose was to examine the basic function of the whole system and tune the circuit to have the proper output. Algae samples which diluted in different concentrations were pumped through the sensor. . The relationship between the output voltage and the reference OD_{750} value (Figure 27) showed that the sensor's detectors responded almost linearly in the OD_{750} range from 0 to 1.2. Data beyond this range were not collected due to the limitation of the original algal culture's density. Also, trends in the output voltage showed that the voltage output response was decreasing as the OD values increased. Results confirmed the basic absorbance rule that the denser the algal culture was: the more light was absorbed by the algal suspension.

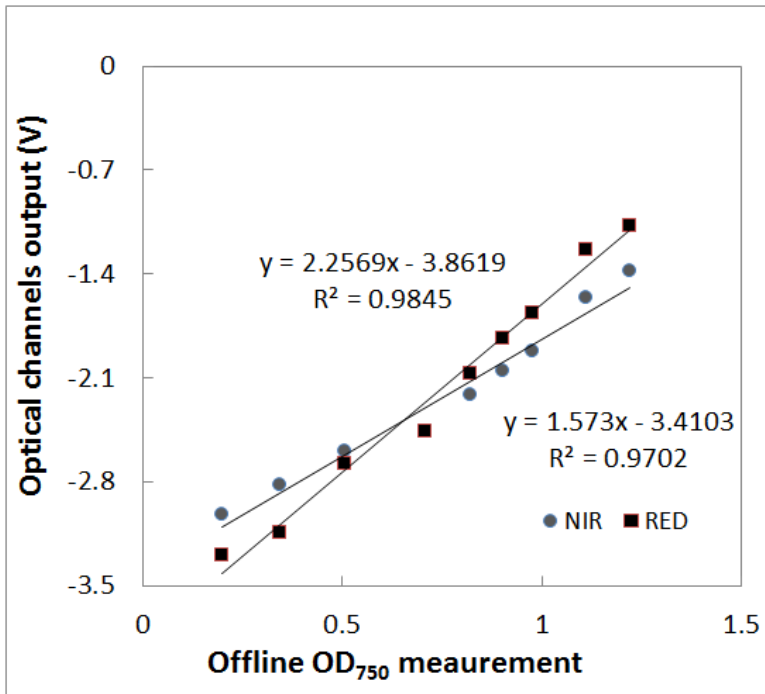


Figure 27: Optical channels voltage output vs. offline OD measurement (Test in the BEST lab with algae *Nannochloris oculata* in different concentrations)

Except the basic sensor response, the sensor was also been tested for a short period to investigate the stability and the noise of the output. *Nannochloris oculata* was bottled from algae cultivation lab. The Following figures were from one of the tests, which were performed in approximately 40 minutes. The algae culture used in the test had a fixed concentration. First, there was a 15 minute stabilization time for the sensor. The voltage output of The NIR optical channel was at -1.4 volts after stabilization (Figure 28), while the red channel had a voltage output at -0.9 volts (Figure 28). The sensors predicted OD from the calibration equation was around 0.17 (Figure 28). Though the noise was obvious in the red optical, the predicted OD appeared to be stable at approximately 0.17 (Figure 28) and the trend can be observed easily.

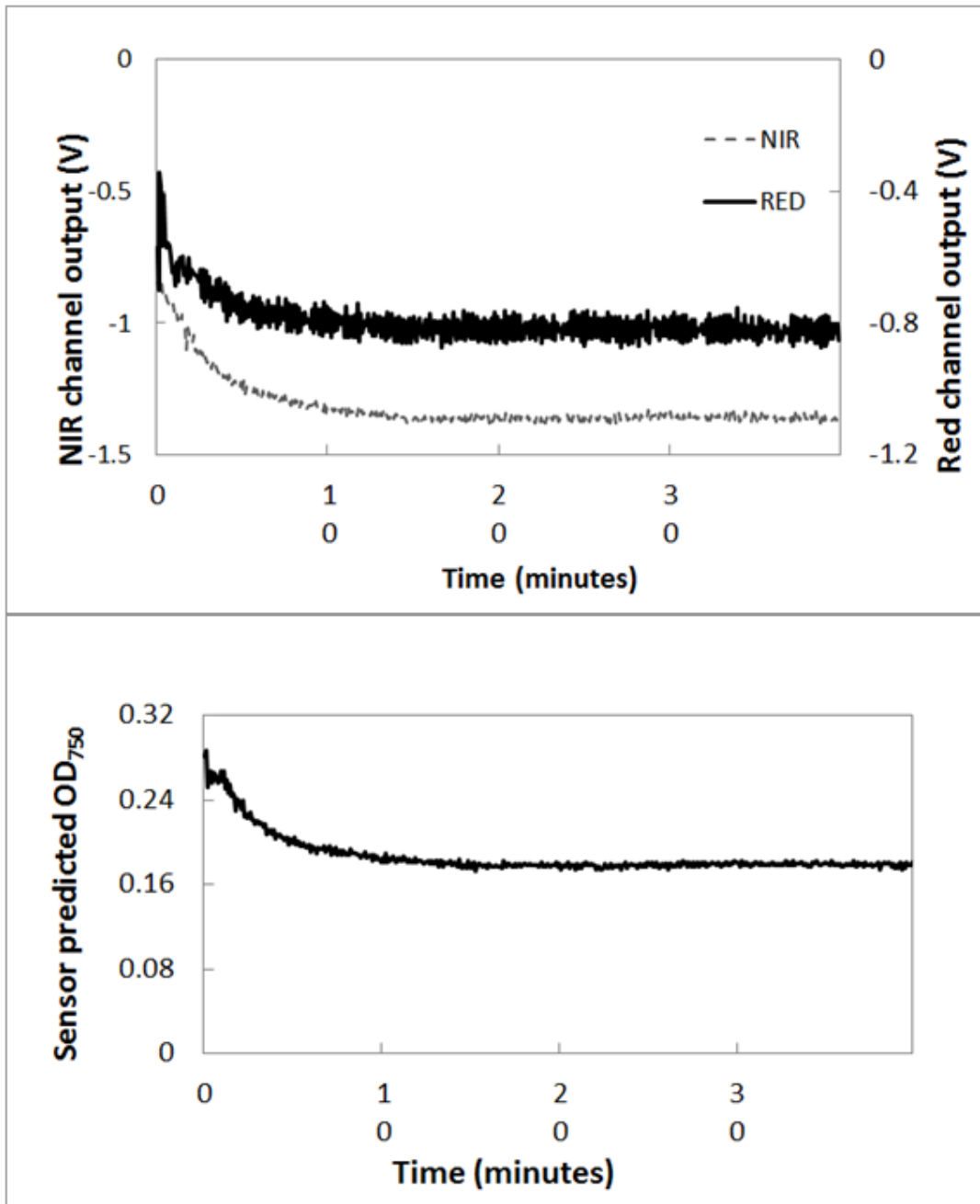


Figure 28: Initial sensor test result with fixed concentration of algal sample in BEST lab (Above: optical channels output during the 40 minutes test; blow: sensor predicted OD at 750 nm during the 40 minutes test.)

4.1.2 Results of the Main Tests in Algae Cultivation Lab

The first main test was conducted from 10/18/2010 to 10/20/2010. The sensor was tested in algae cultivation lab to monitor the algal density inside the raceway. Six offline spectrometer data points were taken to compare to the sensor estimated OD₇₅₀. The test results have shown the growth trend of the algae in a two day period. When the light was on, the fast growth period can be seen on the graph (Figure 29). After dilution with water at approximately 19 hour mark, there is corresponding sharp curve (Figure 29) indicating fast growth of algae. Then the stagnant period when the light was off from around 31 to 40-hr with a more flat curve (Figure 29) indicated that the algae were not growing. Also, the response to the sudden changes in the culture media was shown in the graph (Figure 29) at around 19-hr when 10-L of water was added in the raceway. The interference of the cultivation procedures such as aeration is shown in this graph (Figure 29) at around 29-hr. During the test period noise was detected in the output. Some of the severe and random noise was due to the heavy load machines switching on or off in the power line. The 6 offline spectrometer data points were compared to the corresponding sensor readings, which were recorded at the same time as the offline measurements (Figure 30). This comparison was aimed at evaluating the accuracy of this sensor. Following from the results, R² was 0.84 and root mean square error (RMSE) of 0.061. The results show that this sensor respond to algae media at different OD levels with a fair accuracy.

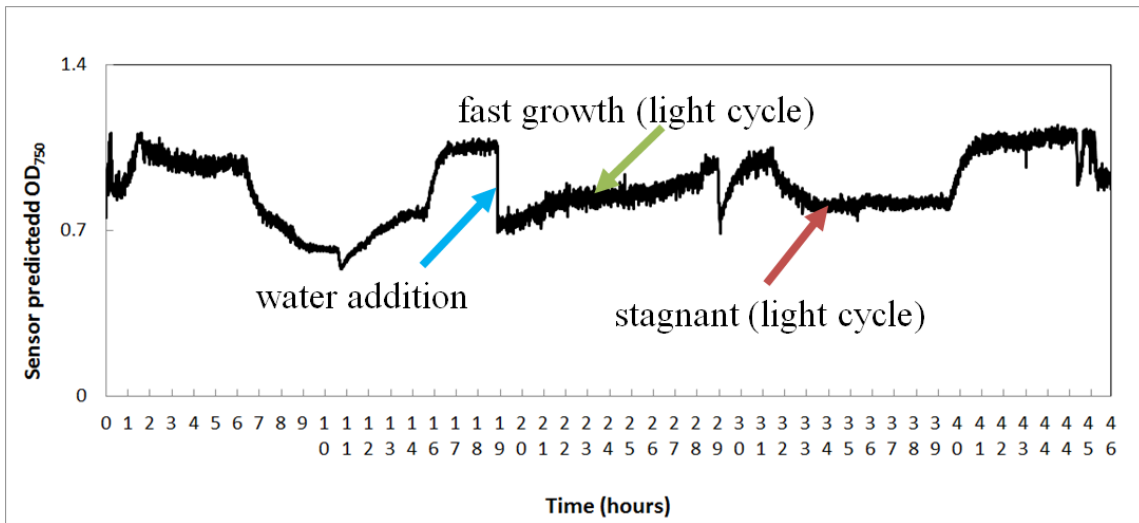


Figure 29: Sensor predicted OD vs. time during test in algae cultivation lab for around 2 days (from 10/18/2010 to 10/20/2010)

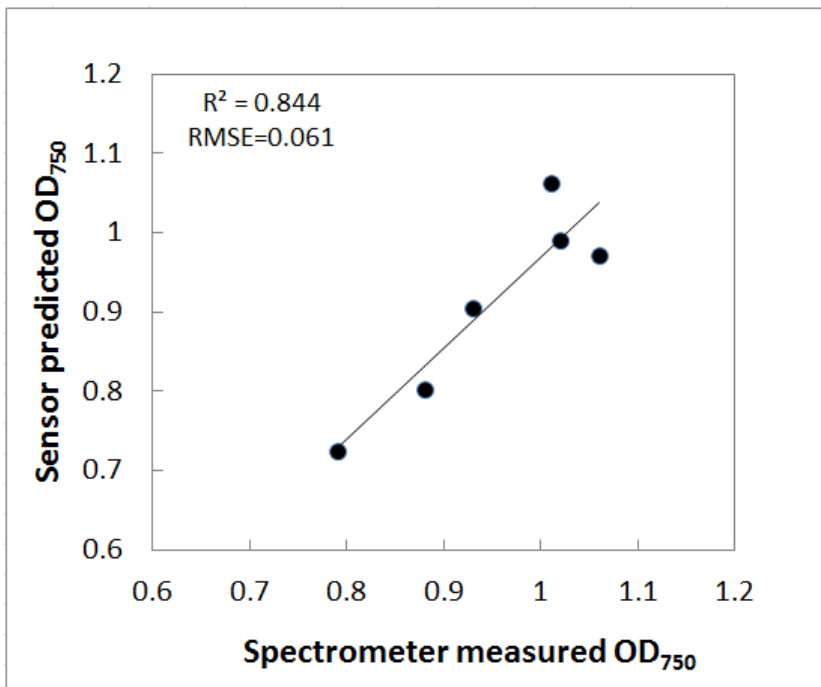


Figure 30: Comparison of sensor measured OD and the offline spectrometer OD measurement of the main test on 10/18/2010 in algae cultivation lab

The test discussed above shows one of the best results among the tests for the original sensor. The following test shows results that were the worst among all the original sensor tests. From the 11/22/2010 to 11/28/2010, the sensor was again positioned by the raceway in the algae cultivation lab as mentioned above with the algae culture continuously pumped through. Under this scenario, the sensor was not stable in the first three and a half days. The output (Figure 31) was swinging in 2.5 OD unit range and did not show any trends for this noise that could be observed. The guess for this unstable swing was caused by sudden exterior interference on the electronics of this sensor and the parasitic capacitances and inductances which existed in the prototype materials and components. But at around 3.5 days, the results started to become stable and normal. Then, during the rest of the days, even with the remaining noise, the growth trend of the algae was observed (Figure 31). The fast growth with illumination (red arrows) and stagnant period (green arrows) without illumination are shown (Figure 31). This result confirmed that the sensor had to be improved on the electronics and noise resistance as well.

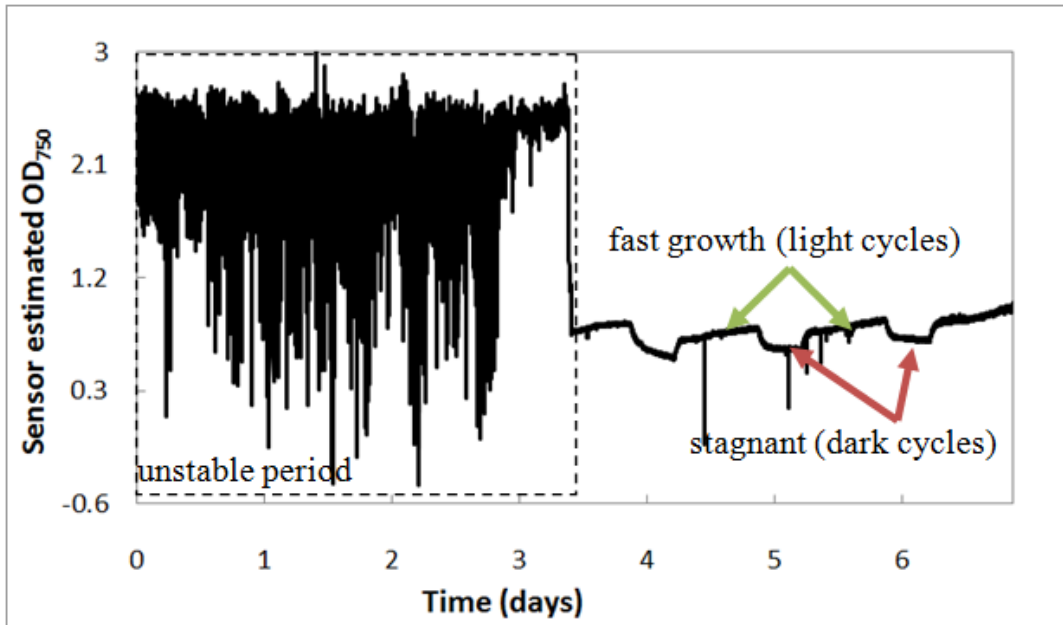


Figure 31: Plot of the sensor estimated OD in 7 days period from test on 11/22/2010 with the algal culture in the algae cultivation lab (showing the unstable output)

4.1.3 Results from Sensor System Temperature Stability Tests

The following experiment was conducted in the BEST lab after the temperature probe was installed in 10/14/2010. The aim of this test was originally to find out whether the temperature monitor probe was functioning or not. Therefore, in this short test, the sensor was placed on the electrical bench with DI water in a flask pumping through. Data was recorded at 20 s intervals for this time. From comparing the temperature output to the sensor estimated OD, the evidence showed that they had the same trends, which indicated the output was drifting with the temperature. When the temperature dropped and then became stable, the sensor estimated OD also dropped and then became constant for next 3 hrs. The temperature reached the lowest point at the same time as the sensor estimated OD. After that, both the temperature and the output were rising. This result

indicates that the output of the sensor was strongly influenced by the ambient temperature.

From the previous tests, there was a strong indication that sensor output was influenced by ambient temperature. In order to investigate the influence of ambient temperature on the sensor, a test was devised to exclude the effect of algal culture temperature. This test was conducted in 12/17/ 2010 in algae cultivation lab so as to take advantage of temperature variation, and the sensor was positioned near the raceway. The sensor was activated, without turning the pump on, so that no liquid would flow through the flow cell. This test was conducted for 3 days, and results showed that the output voltages of both optical channels varied with ambient temperature. And the output temperature drift was 0.1 volts for the red channel (Figure 32) and 0.07 volts for the NIR with 5°C change (Figure 32). The comparison of the sensor predicted OD₇₅₀ (Figure 32) to the ambient temperature graph (Figure 32) shows that they have the same pattern. Due to the temperature drift of the optical channels, there was a variation of 0.25 in the OD measurement (Figure 32) curve, which is a function of two optical channels. Direct evidence shows correlation between two optical channel outputs and the temperature. Two linear equations were fitted respectively for each optical channel in the graph with a R² of 0.33 (Figure 33) for red and 0.86 for NIR (Figure 33). Also, the fitted lines indicated that the temperature drift of the NIR optical channel was 0.0143 volts/°C (Figure 33) and the red channel was 0.008 volts/°C (Figure 33). All the results show that the temperature had a direct and strong influence on the output.

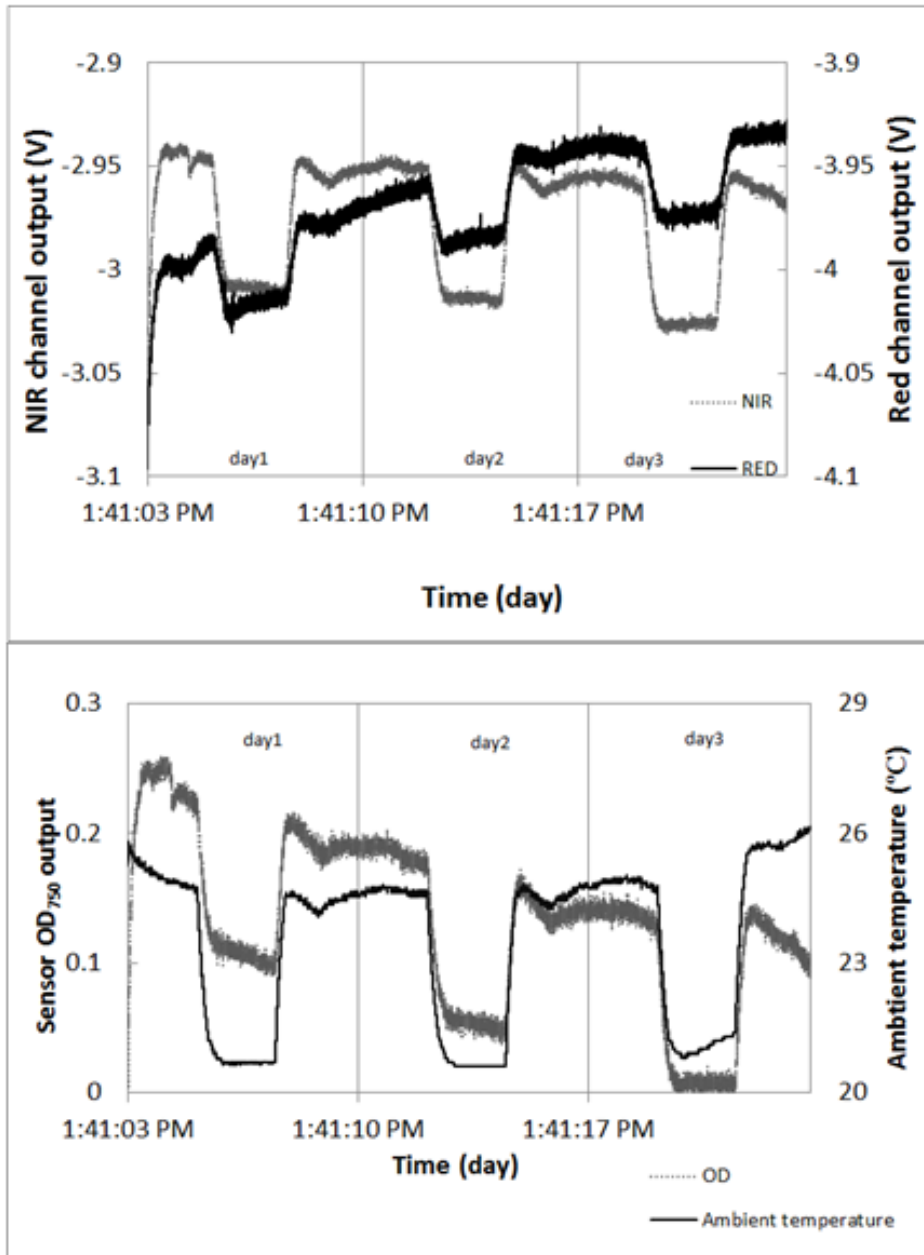


Figure 32: Results from the test of sensor system temperature stability tests in algae cultivation lab without algae culture (Top: optical channels output during the 3 days test; bottom: Sensor estimated OD₇₅₀ graph for 3 days during the test in algae cultivation lab)

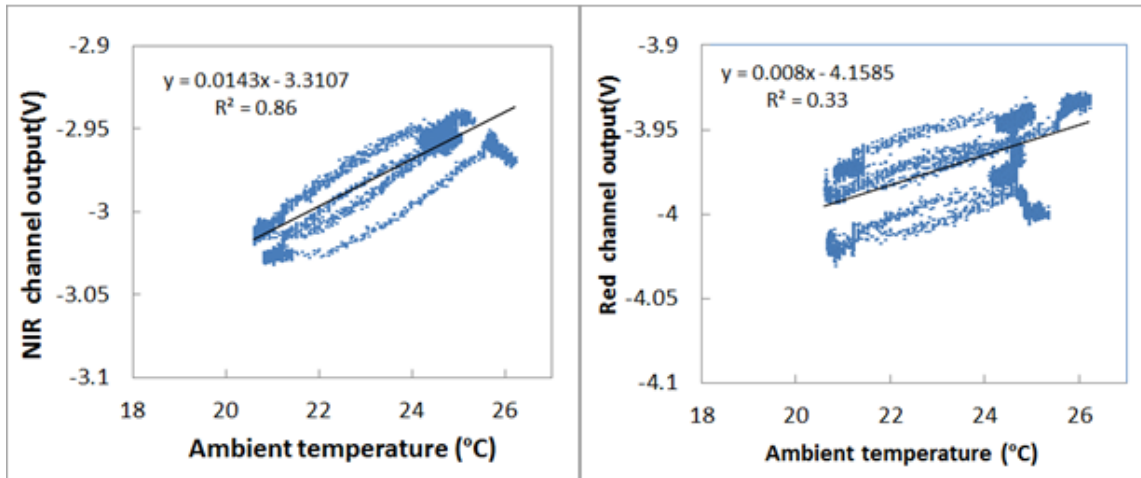


Figure 33: Correlation between optical channels output and ambient temperature during the temperature stability test in algae cultivation lab for 3 days (Left: NIR channel output vs. ambient temperature; right: red channel output vs. ambient temperature)

To add confirmation to the idea that temperature was the major influence on sensor output variation, the sensor was placed in an environment with stable ambient temperature at approximately 4.9°C. This test was conducted from 03/28/2011 to 03/30/2011 in the BEST lab. The sensor body was placed in the freezer of a refrigerator to achieve an environment with a stable ambient temperature. The sensor was activated without any liquid pumping through. The reduction in output variation was evident in both channels; there were approximately 0.04 volts variations in the signal output in the NIR channel and 0.015 volts in the red.

4.2 Tests Results of the Redesigned Sensor

4.2.1 Results of the Redesigned Sensor Initial Tests in the BEST Lab

These tests were conducted in the BEST lab with bottled algae culture P4B as mentioned in the previous session. Test results were plotted in the following figures. The

sensor response to different levels of algal concentration is shown (Figure 34). As the concentration increases, the output increases accordingly. High linear correlation can be seen between the algae media concentration level and output voltage with a R^2 of 0.989 for the red channel (Figure 34) and 0.989 for the NIR channel (Figure 34). Under ideal situation, where LEDs and photodiodes are identical in performance and with identical layout of the reference and sample chamber, the output would be 0 volts when the same media is in both of the flow cells. However, due to the fabrication errors of the sensor housing and misalignments of the optics, there was 0.15 volts systematic error in red channel output and 0.07 volts in NIR channel output. For the first 0.5 hours, from the start till around 2.5 hours, the sensor had DI water in both reference and sample flow cells, initially with the pump turned on and then shut off. There was a difference of 0.03 volts in the red channel (Figure 35) and 0.012 volts in the NIR channel (Figure 35) between pump being on and off due to the noise generated by the pump. This noise could be caused by the vibration of the pump and the small bubbles in the flowing media. The spike periods in the graph indicate the time when the sample flow cell was drained and different concentration algal suspension samples were under testing (Figure 35). The pump was turned off from 5 hour mark until 25 hour mark with the algal media in the flow cell. Due to precipitation of algae cells inside the sample suspension, the output voltage in both channels had a small drop (Figure 35). Algae media of fixed concentration were kept flowing through the sample to test the sensor long term stability. As shown in the graph, the output of the red channel remained approximately at 0.57 volts (Figure 35) and the NIR channel remained at 0.25 volts for the rest of the 20 hour

test (Figure 35). Also, the ambient temperature during the test varied from 16.5°C to 19.5°C (Figure 35) while the regulated temperature variation was at 0.8°C (Figure 35). This result shows a much improved temperature stability with the new sensor under the regulation of the TEC module.

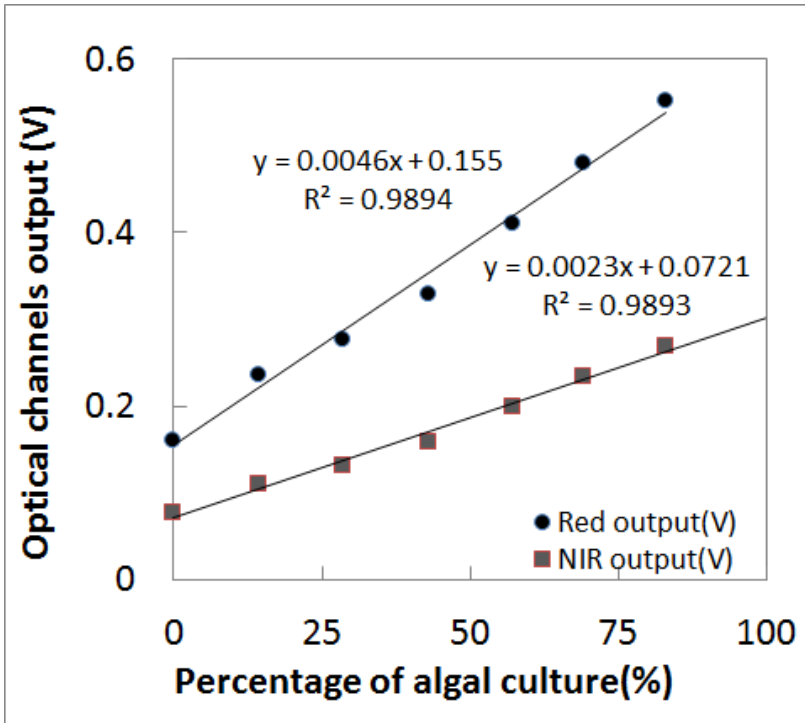


Figure 34: Optical channels response to the different concentration of algal samples test in BEST lab with P4B

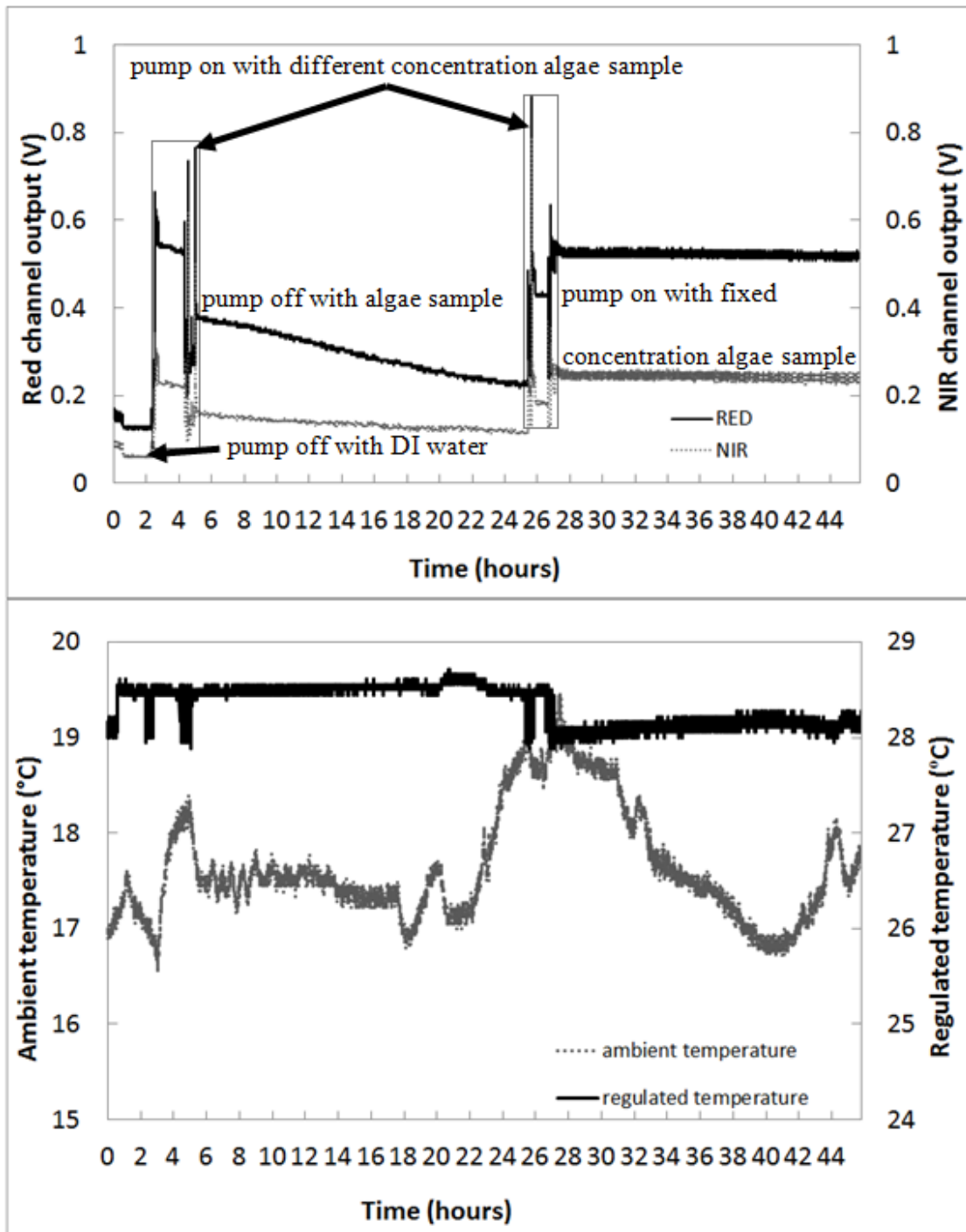


Figure 35: Results of the sensor initial test with different concentration of P4B algal culture in the BEST lab (Top: optical channels long term response under different situations; bottom: temperature long term response)

4.2.2 Results of Redesigned Sensor System Temperature Stability Tests

As all the results showed that the original sensor had issues in temperature stability and external noise resistance, the sensor housing, the LED driver circuit and the signal processing circuit were then redesigned and rebuilt. In the redesign, a temperature control unit was added to regulate the LED temperature. After the sensor with electronics enclosure had been assembled, the first test for the stability of the new sensor was conducted in the BEST lab. Due to the lack of algae culture in the BEST lab, the sensor was set up on the electronics bench in the lab without any liquid pumping through. This test was aimed at the temperature and noise stability of the sensor. The period of the test started from 04/01/2012 and it lasted for about 36 hours. Because there was no pre-calibration for this sensor by this time, the estimated OD is not shown in the graph. During the test, the ambient temperature varied from 20°C to 23.5°C (Figure 36), while the regulated temperature had a variation of 0.3°C, which was from 27.7°C to 28°C (Figure 36). With the regulated temperature, the red channel output had a variation of 0.03 volts (Figure 36) and no particular temperature drift can be observed; the NIR channel had a variation of 0.025 volts (Figure 36) and also, no obvious temperature drift was observed. Then the comparison of the optical channels output and the ambient temperature was plotted. Two linear equations were fitted. Compared to the original sensor output with a R^2 of 0.86, this time the NIR channel had a R^2 of 0.285 (Figure 37). The red channel had improved also with a R^2 of 0.269 (Figure 37) compared to 0.33. And the fitted lines indicated that the temperature drift of the NIR optical channel was 0.0033 volts/°C (Figure 37) and the red channel was 0.0039 volts/°C (Figure 37). Also,

the temperature drifts of both channels were greatly reduced compared to results with the original sensor. These results clearly show that the sensor has a better temperature performance and had more stability over the original design.

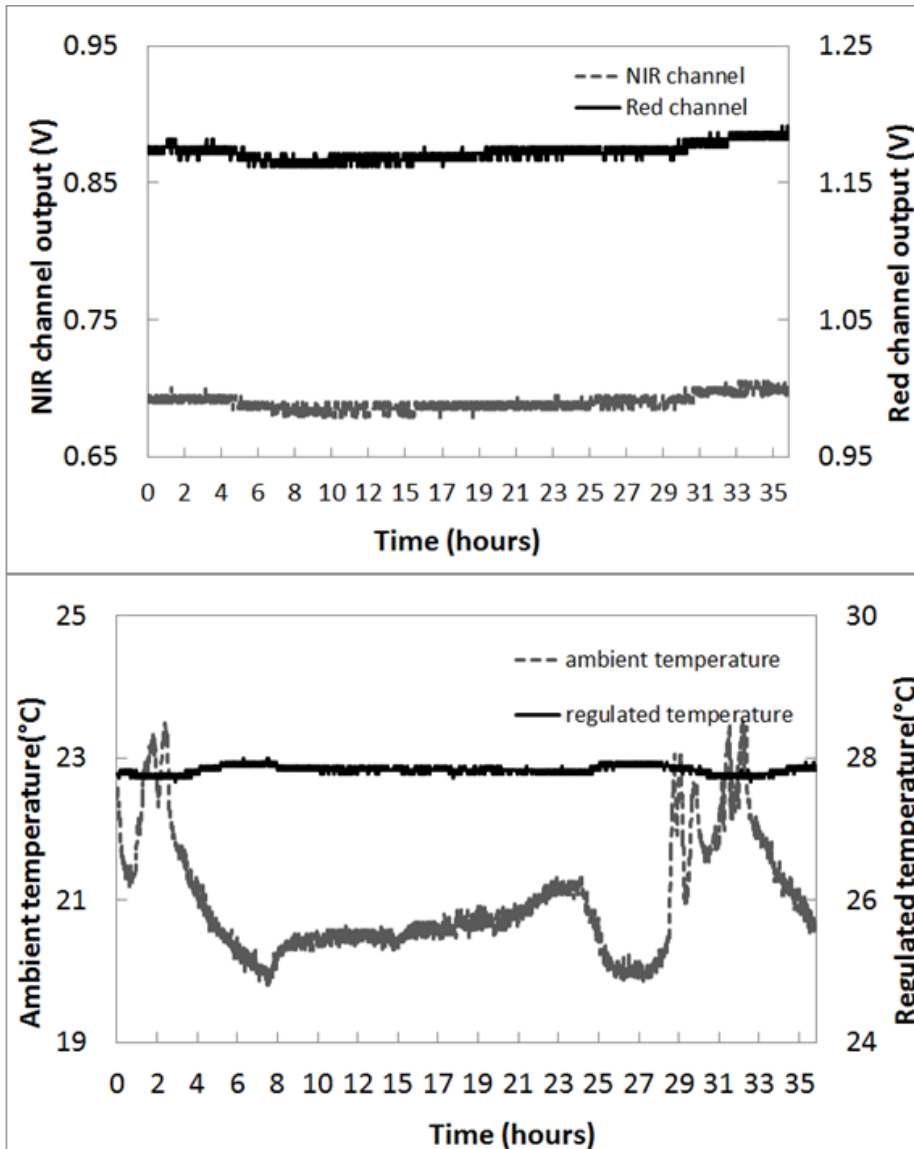


Figure 36: Results of the redesigned sensor temperature stability test without any algal culture in the BEST lab (Top: optical channels long term response during the test period; bottom: temperature long term response during the test period)

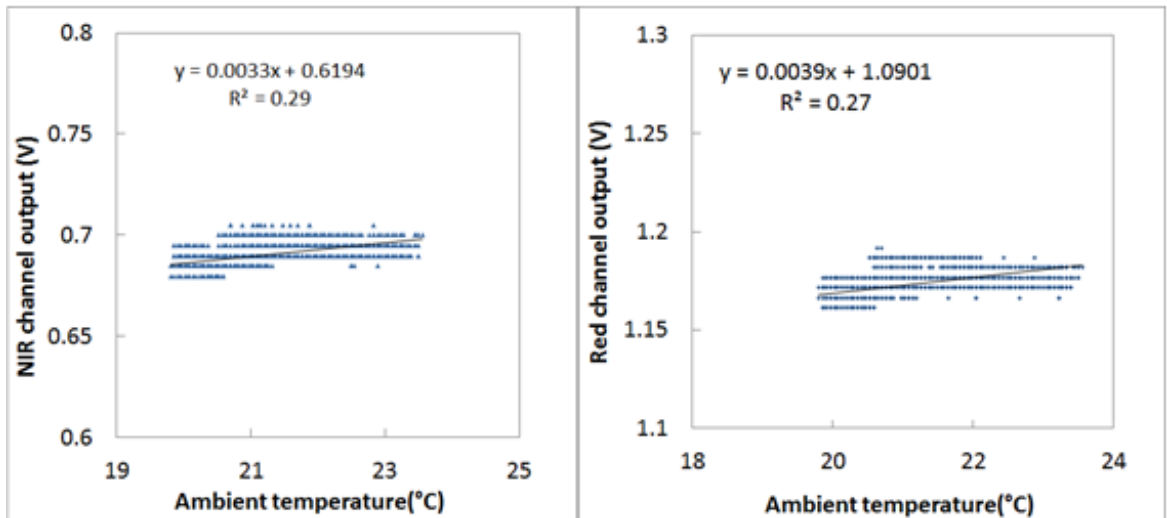


Figure 37: Correlation between optical channels output and ambient temperature during the temperature stability test in the BEST lab (Left: NIR channel output vs. ambient temperature; right: red channel output vs. ambient temperature)

4.2.3 Main Tests Results of Redesigned Sensor

As mentioned in the material and methods session, the sensor was put on to test from 06/02/2012 to 06/23/2012 in the algae cultivation lab (BAEN, Hobgood building, TAMU, College Station, TX). This test was with algae culture grown in the raceway. Ambient temperature, red and NIR optical channel output before and after amplification, and regulated temperature (cold plate on the back of the LEDs) were recorded at 20s time interval. Also, this test was separated into two periods: the first was from 06/02/2012 to 06/11/2012; the second was from 06/13/2012 to 06/24/2012. On 06/12/2012, there was an adjustment for the software for the DAQ, therefore, on that day the sensor was off. Also, for the first three days, the pump was tested to ensure safe operation for the algae. The OD range for this test was from 0.5 to 1.2 OD units, which was limited by the density of the algae culture under test.

As described in the previous session, total of 63 spectrometer OD₇₅₀ measurement points were taken. The corresponding readings from the two optical channels were recorded at the same time. First the comparisons of the optical channels output with the spectrometer OD₇₅₀ measurement were plotted. With the increasing OD level, both channels outputs had obvious increment. Also, there was strong linear relationship between the spectrometer OD₇₅₀ measurement and both optical channel outputs, for the red channel with a R² of 0.96 (Figure 38) and NIR channel with a R² of 0.94 (Figure 38). Then, as mentioned before, the 63 data points were split into a calibration set with 40 data points and a validation set with 23 data points. After the calibration equation was generated with multiple linear regression method, the remaining 23 NIR and red channel data points were fitted get the predicted OD₇₅₀ values. Then the predicted OD₇₅₀ data were compared to the spectrometer OD₇₅₀ measurement from the validation set. The strong linear relationship (Figure 43) was shown between the sensor predicted OD₇₅₀ and the spectrometer OD₇₅₀ measurement. The accuracy of the sensor was evaluated by the R² and the root mean square error (RMSE). And the results showed that the sensor was showing predicted OD with a R² of 0.98 and the RMSE of 0.034.

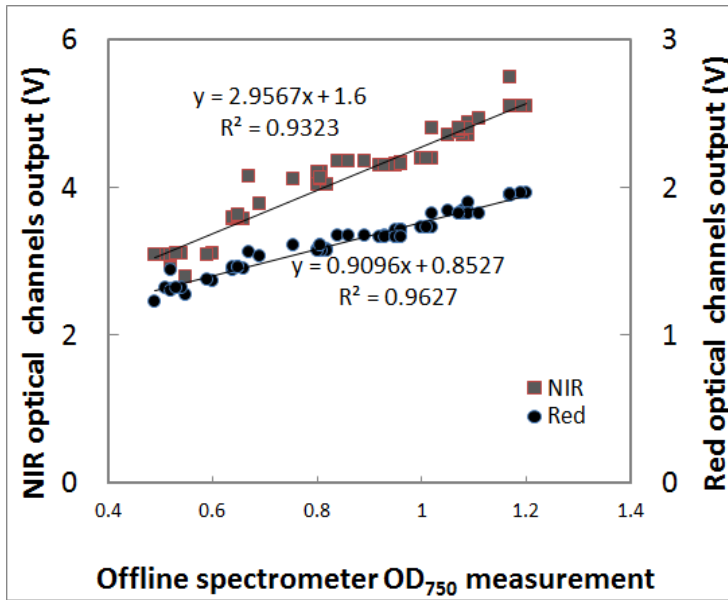


Figure 38: Optical channels output response compared to measured offline OD₇₅₀ sample values (test in algae cultivation lab 06/04/2012)

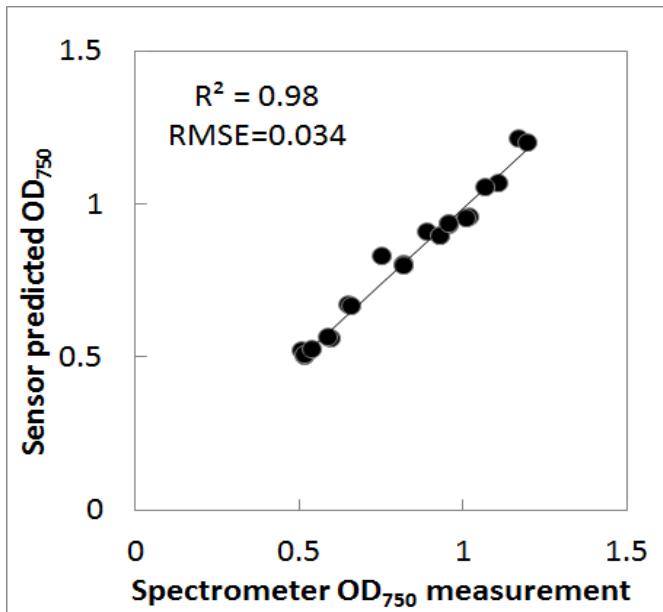


Figure 39: Sensor predicted OD₇₅₀ values compared to spectrometer OD₇₅₀ measurement (test in algae cultivation lab 06/04/2012 with algal culture from the raceway)

The performance of each channel output was evaluated. These were the results of the first period of test from 06/04/2012 to 06/11/2012. For the seven and half days test, the signal from each channel was stable. Also the noise was reduced significantly compared to the original sensor. Each optical channel responded to the algae culture changes well. Fast growth periods (green arrows) were corresponding to the curves with the rising slopes, while stagnant periods (red arrows) were corresponding to the flat curves in between those sharper curves (Figure 40). During the test, the ambient temperature had a variation of 8°C, which was from 31°C to 23°C (Figure 40), while the temperature of the regulated cold plate had varied from 26.1°C to 26.5°C (Figure 40). The temperature regulation device was able to provide more stable temperature environment. All the data in the seven and half days of the test were also fitted into the calibration curve to obtain the sensor predicted OD₇₅₀ (Figure 40). For the long term response on the sensor, the fast growth periods (green arrows) when the light was on (light cycle) and the stagnant periods (red arrows) when the light was off (dark cycle) can be observed in the graph. Similar to the long term growth trend, the sensor also responded well to the cultivation activities (Figure 40), such as water, media addition (blue arrow) or algae transfer (orange arrow). Algae transfer was done when the algae in the raceway stopped growing, half of the algae were taken out and the remaining algae were diluted up to the existing volume with culture medium. Also, the red dots in the figure (Figure 40) represent the spectrometer OD₇₅₀ measurements, and the data show good match with the sensor predicted OD₇₅₀. The new sensor has an obvious improvement in the temperature stability and a great reduction in the noise.

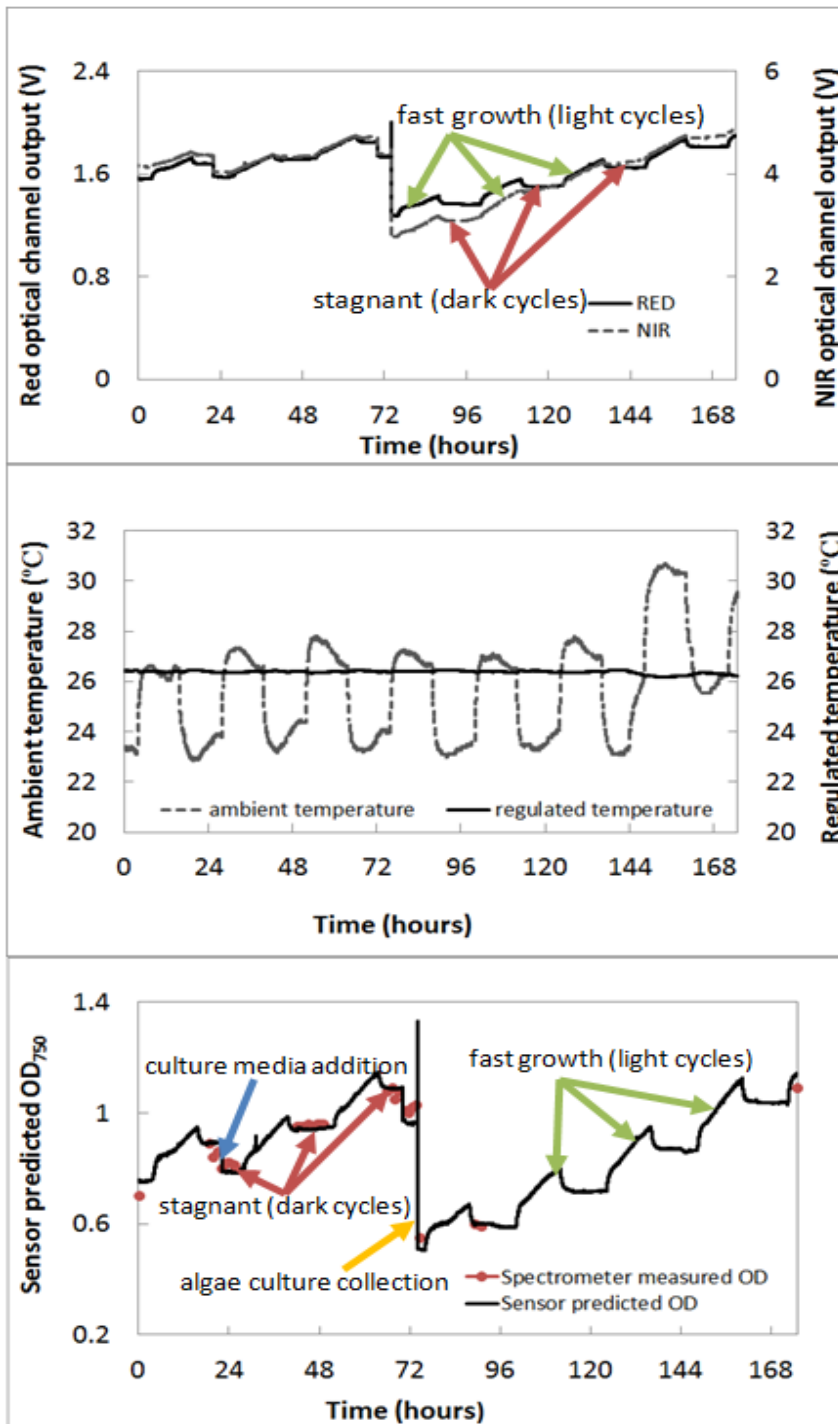


Figure 40: Test results from the main test in algae cultivation lab with the algal culture from the raceway on 06/04/2012 (Top: optical channels output response during the test period; middle: ambient temperature and regulated temperature during the test period; bottom: sensor predicted OD₇₅₀ during the whole test time)

The test from 06/13/2012 to 06/25/2012 was also plotted below. The red and NIR optical channel outputs have shown the trend of the algae growth (Figure 41). As previous tests, the growth pattern and the culture activities can be observed from the graph (Figure 41). The obvious noise had appeared during testing in between day2 and day3. There were three probable reasons for this noise: (1) algae culture in the raceway was not homogeneous; (2) possible external interference on the electronics; (3) water in the reference cell evaporated and the air bubble was left inside. If the sensor was moved, the bubble would have changed its position relative to the LEDs and detectors so that signal would be varied due to the different light paths through the DI water or air bubble. During the remaining four days, the data was not normal without any specific trend. There was one possible reason for that. Due to the vibrations of the pump, the hose clamp which secured the hose to the hose fitting on the flow cell was loose. The hose started to fall off and the pump began to pump air mixed with the sample. Eventually, the pump had failed completely. The temperature regulation worked well in this test. When the ambient temperature (Figure 41) swung from 21°C to 28°C, the regulated temperature (Figure 41) only varied from around 27.2°C to 27.5°C. Finally, both red and NIR optical channels output data were fitted into the calibration curve to get the sensor predicted OD₇₅₀. The results (Figure 41) show the trend of the light and dark cycles in the long term algae growth. And the sudden changes of the media also could be found in the plot due to the cultivation activities (Figure 41). The offline measurement (red dots) were also close to the sensor predicted OD₇₅₀. But due to the failure of the pump as mentioned above, the data in the last three and half days did not follow any trend.

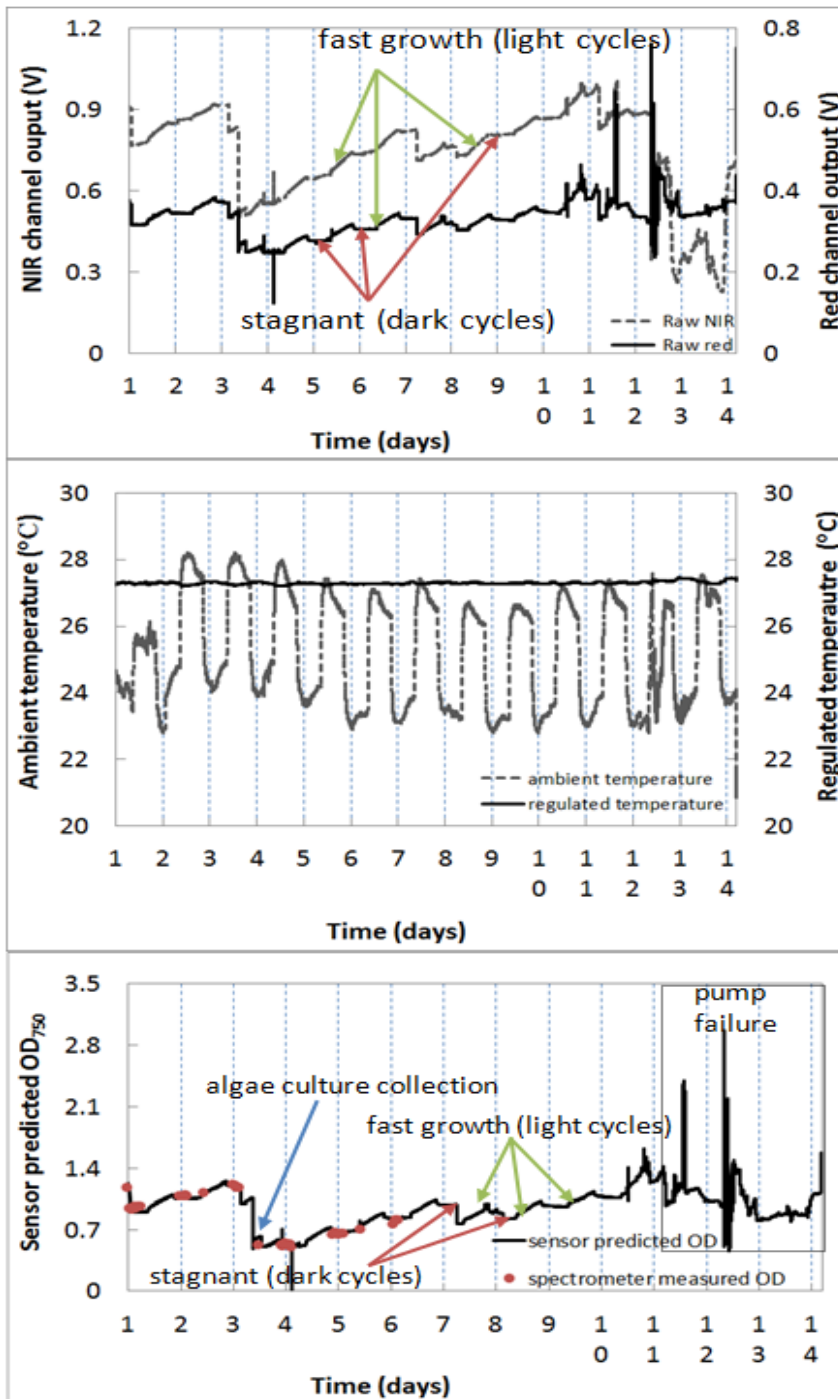


Figure 41: Test results from the main test in algae cultivation lab with the algal culture from the raceway from 06/13/2012 to 06/25/2012 (Top: optical channels output response during the test period; middle: ambient temperature and regulated temperature during the test period; bottom: sensor predicted OD₇₅₀ during the whole test time)

5. CONCLUSIONS AND DISCUSSIONS

5.1 Original Sensor

For the original sensor, the basic current to voltage converter, the LEDs driver and the supply of the system power were designed, built and tested. The signal from the photodetector was processed to be received by the DAQ system. Also, the program for this sensor was coded for the DAQ system. Then the sensor was tested under both lab and raceway environments to evaluate the performance. Calibration curves were developed according to the two optical channel outputs and the offline OD measurement during the tests. The correlation between sensor predicted OD and the spectrometer OD measurement was good with an R^2 of 0.8443 and compared to the offline spectrometer OD measurement with a RMSE of 0.0613 under the raceway environment. The sensor met the basic requirement of estimating OD. While during the later test, the temperature monitor unit was added in and more issues were discovered, such as temperature drift, unstable output signal, and noise problems.

5.2 Redesigned Sensor

The new version of sensor was developed since then. For the new sensor, the LEDs driver was designed as a constant current to increase the temperature and overall stability. A simple transimpedance amplifier was replaced by the logarithmic circuit based on the Beer-Lambert law to improve the linearity, accuracy and reduce the noise. Also, a temperature control unit was added in this circuit to regulate the LEDs operation temperature to increase the stability. Larger detectors were used for increasing signal to noise ratio. Then, the program was modified accordingly. Also, the sensor housing was

redesigned and rebuilt according to the change in the circuit and to achieve the maximum efficiency of the optical components. This new sensor was also tested both in the lab and raceway environments. The results showed that the new sensor was improved in temperature stability with lower R^2 of the output vs. ambient temperature than the original sensor. Also, the temperature drift per Celsius was reduced. The sensor responded well both to the long term algae growth and short term OD change in the cultivation media. Finally, it showed higher accuracy and better linearity with a R^2 of 0.98 and RMSE of 0.034 under the raceway environment.

5.3 Practical Application

This sensor is suitable for the online monitoring of the OD of algae culture. OD could be directly related to the biomass concentration and then according to it, the algae density from the culture media could be calculated. Therefore, it would be a very important parameter in algae cultivation. This sensor will provide continuous real time OD information, which can save human labor and reduce costs in large scale algae production systems. For example, after the sensor is calibrated with the offline OD measurement, it will record and display the algal culture OD on the DAQ system for monitoring the algae growth trend. Also, the signal can be received either by the operator or the devices that can be used to control the algae density. When the OD reached the set point, the signal would be sent to the control pump to add culture media in order to keep an optimal density for the algae to grow. Under the test in the algae cultivation lab, when the algae stopped growing at OD of close to 1.2, the value was shown on the screen of the DAQ and read by the operators. It indicated that the algae

need to be transferred or to be harvested. In addition, the sensor can also show the sudden change in the cultivation media to indicate the cultivation activities. In a word, the sensor will and can provide the key parameters in automatic large scale algae production systems.

5.4 Issues Regarding Usage of the System

As discussed before, the DI water in the reference flow through cell had a temporary seal; therefore, the air bubbles would be left in the cell after water evaporated. Then, when the sensor is moved around, the bubble would not stay at the same position due to the uneven surface, thus, the output which was the log ratio of the reference and sample signal would be change suddenly. This required a better seal method for the flow cell and will require the refill of water every 2 or 3 weeks.

The second issue is in regards to biofouling. Even though the sample flow cell is made of quartz glass and was highly polished, the algae would still accumulate on the inside surface. This would also cause the sensor to lose accuracy and increase the noise level. The solution for this is to rinse the sample flow cell every 2 or 3 weeks with a cleaning detergent.

The pump could be the third possible problem with the sensor. The pump for this sensor has too much vibration when it was activated. For the last test of the sensor, due to the vibration of the pump, the hose fell off the fitting of the flow cell, which caused pump failure. Also, when the algae culture is pumping through the flow cell, lots of small air bubbles can be observed. That would reduce the sensor's accuracy. The solution for this issue would be to switch to a pump with less vibration and with controllable

pumping volume. After the pump sends specific amount of algae into the flow cell, then the pump will be in the off position and the OD can be measured after the algae liquid in the flow cell degassed.

5.5 Future Research

Regarding this sensor, the prototype was developed and tested in the lab production raceway. There were still some improvements to be done. First, in the future, tests under the large outdoor raceway would be conducted to evaluate the sensor performance in the real production environment. The temperature performance will be the most important performance, because the outdoor environment would have larger temperature variation, which would be a challenge to the capabilities of the temperature control unit. The noise resistance would be another challenge for outdoor large scale raceway, since there would be more interference in the outdoor raceway than indoor. Also, due to the technology limitation in the lab, the sensor was relatively heavy and large in size. For the practical manufacture purpose, the standardized smaller scale of the electronic components and the multi-layer PCB would be used to shrink the size down and to provide a more stable signal. In that way, the sensor will be more acceptable in the market.

REFERENCES

1. Sjors van Iersel, Liliana Gamba, Andrea Rossi, Sacha Alberici, Bart Dehue, Jasper van de Staij and Alessandro Flammini. 2009. © FAO. Algae-based biofuels: A review of challenges and opportunities for developing countries (Page 1).
3. M. Aguilera-Morales, M. Casas-Valdez, S. Carrillo-Domínguez, B. González-Acosta, and F. Pérez-Gil. 2005. Chemical composition and microbiological assays of marine algae *Enteromorpha spp.* as a potential food source. *Journal of Food Composition and Analysis* 18: 79–88.
2. Katsumi Yamaguchi, Hiroshi Nakano, Masahiro Murakami, Shoji Konosu, Osamu Nakayama, Midori Kanda, Akihiro Nakamura and Hiroaki Iwamoto. 1987. Lipid Composition of a Green Alga, *Botryococcus braunii*. *Agric. Biol. Chem.* 51(2): 493-498.
4. Catherine M. Gatenby, David M. Orcutt, Daniel A. Kreeger, Bruce C. Parker, Vanessa A. Jones and Richard J. Neves. 2003. Biochemical composition of three algal species proposed as food for captive freshwater mussels. *Journal of Applied Phycology* 15: 1–11.
5. Kalpesh K. Sharma, Holger Schuhmann and Peer M. Schenk. High Lipid Induction in Microalgae for Biodiesel Production. *Energies* 2012, 5, 1532-1553.
6. T.J. Lundquist, I.C. Woertz, N.W.T. Quinn, and J.R. Benemann. 2010. A Realistic Technology and Engineering Assessment of Algae Biofuel production (Page 3-13)
7. Daniel Chaumont. 1993. Biotechnology of algal biomass production: a review of systems for outdoor mass culture. *Journal of Applied Phycology* 5: 593-604.
8. Patrick Lavens and Patrick Sorgeloos. 1996. Manual on the Production and Use of Live Food for Aquaculture. FAO FISHERIES TECHNICAL PAPER 361. ISBN 92-5-103934-8. (2.5-Use of micro-algae in aquaculture)
9. Oilgae team (C3B, Anugraha Apartments, 41 Nungambakkam High Road, Chennai, Tamilnadu, India). Oilgae guide to algae-based wastewater treatment – a sample report.
10. Chun-Yen Chen, Kuei-Ling Yeh, Rifka Aisyah, Duu-Jong Lee, and Jo-Shu Chang. 2011. Cultivation, photobioreactor design and harvesting of microalgae for biodiesel production: A critical review. *Bioresource Technology* 102: 71–81
11. Kazuhisa Miyamoto. 1997. Renewable biological systems for alternative sustainable energy production. ISBN 92-5-104059-1. FAO Agricultural Services Bulletin - 128. (Chapter 6-oil production)

12. Stefan Bringezu, Helmut Schütz, Meghan O'Brien, Lea Kauppi, Robert W. Howarth and Jeff McNeely. 2009. United Nation Environment Programme. ISBN: 978-92-807-3052-4
13. Colin M. Beal, Colin H. Smith, Michael E. Webber, Rodney S. Ruoff and Robert E. Hebner. 2011. A Framework to Report the Production of Renewable Diesel from Algae. *Bioenergy Resource* 4: 36–60.
14. Laurent Lardon, Arbaud Hélias, Bruno Sialve, Jean-Philippe Steyer, and Olivier Bernard. 2009. Life-Cycle Assessment of Biodiesel Production from Microalgae. *Environmental Science and Technology* 43 (17): 6475–6481.
15. Brian J. Krohn, Clayton V. McNeff, Bingwen Yan, and Daniel Nowlan. 2011. Production of algae-based biodiesel using the continuous catalytic Mcgyan® process. *Bioresource Technology* 102: 94–100.
16. Michael A. Borowitzka. 1999. Commercial production of microalgae: ponds, tanks, tubes and fermenters. *Journal of Biotechnology* 70: 313–321.
17. Anatoly A. Gitelson, Yury A. Grits, Dror Etzion, Zou Ning, and Amos Richmond. 2000. Optical properties of *Nannochloropsis* sp and their application to remote estimation of cell mass. *Biotechnology and bioengineering*, Vol. 69(5): 517-525.
18. Hung Lam and Yordan Kostov. 2009. Optical instrumentation for bioprocess monitoring. *Advanced Biochemistry Engineering/Biotechnology* 116: 1–28.
19. P. J. Baxter, G. D. Christian and J. Růžička. 1994. Rapid determination of total biomass from a yeast fermentation using sequential injection. *Analyst*, 119: 1807-1812.
20. Bernhard Sonnleitner, Georg Locher and Armin Fiechter. 1992. Biomass determination. *Journal of Biotechnology* 25: 5-22.
21. K. Kiviharju, K. Salonen, U. Moilanen, E. Meskanen, M. Leisola, and T. Eerikäinen. 2007. On-line biomass measurements in bioreactor cultivations: comparison study of two on-line probes. *Journal of industrial microbiology & biotechnology* 34(8): 561-566.
22. Optek-Danulat, Inc. (N118 W18748 Bunsen Drive Germantown, WI). Product information brochure - AS16-N single channel NIR absorption probe. Page: 10-11.
23. Buglab, LLC (3350 Clayton Road, Suite 220, Concord, CA). BE2100 Sensor datasheet.
24. Mettler-Toledo, LLC (1900 Polaris Parkway, Columbus, OH 43240). Product brochure - InPro8000 sensor series.

25. Luís A. Meireles, José L. Azevedo, João P. Cunha, and F. Xavier Malcata. 2002. On-line determination of biomass in a microalgae bioreactor using a novel computerized flow injection analysis system. *Biotechnology Progress* 18: 1387-1391.
26. J.M. Sandnes, T. Ringstad, D. Wenner, P.H. Heyerdahl, T. Källqvist, and H.R. Gislerød. 2006. Real-time monitoring and automatic density control of large-scale microalgal cultures using near infrared (NIR) optical density sensors. *Journal of biotechnology* 122: 209-215.
27. Ladislav Nedbal, Martin Trtílek, Jan Červený, Ondřej Komárek, and Himadri B. Pakrasi. 2008. A photobioreactor for precision cultivation of photoautotrophic microorganisms and for high-content analysis of suspension dynamics. *Biotechnology and Bioengineering* 100(5): 902-910.
28. Thomasson, J. A., R. Sui, Y. Yao, and Y. Ge. 2010. Toward on-line measurement of algal properties. ASABE Paper No. 1009395. St. Joseph, Mich.: ASABE.
29. Dave Salerno. 2001. Closed-Loop Temperature Regulation Using the UC3638 H-Bridge Motor Controller and a Thermoelectric Cooler. Texas Instruments application report.

APPENDIX A

DATA ACQUISITION PROGRAM SOURCE CODE

[MainFrm.vb]

Option Explicit On

```
Public Class MainForm
    '----Variable declaration----
    Dim _RLCHandleAnalog As IntPtr
    Dim _IsLOG As Boolean = False
    Dim _LogFileCreated As Boolean = False
    Dim _Channel(3) As Byte
    Dim _Data(1) As Byte

    'Variables for NIR and Red channel
    Dim _RawData_NIR As Integer
    Dim _RawData_Red As Integer
    Dim _Read_Analog_NIR As Double
    Dim _Read_Analog_Red As Double
    'Variables for Channel 3 (Air Temp) and Channel 5 (Water Temp)
    Dim _RawData_TempAir As Integer
    Dim _RawData_TempWater As Integer
    Dim _Read_Analog_TempAir As Double
    Dim _Read_Analog_TempWater As Double
    'Variables for Channel 2 (Power Supply V+) and Channel 4 (Power
Supply V-)
    Dim _RawData_Vplus As Integer
    Dim _RawData_Vminus As Integer

    Dim _Read_Analog_Vplus As Double
    Dim _Read_Analog_Vminus As Double

    Dim _ProgramCounter As Long = 0
    Dim _LogCounter As Long = 0
    Dim _GraphCounter As Integer = 0
    'Define the graphing area
    '=====
    Const _RectLeft As Integer = 10           'Left
    Const _RectTop As Integer = 45           'Top
    Const _RectWidth As Integer = 243       'Width
    Const _RectHeight As Integer = 150      'Height
    Const _PtoP As Integer = 3              'the length of line
joining to points
    Const YDiv As Integer = 3
    'the length of the history array
    'e.g., Int(243/3)-1 = 80, from 0 to 80, has a total of 81
elements
    Dim ArrayLength As Integer = Int(_RectWidth / _PtoP) - 1
```

```

'=====
Dim _NIR_Sum As Double = 0.0           'Stores the accumulated
NIR reading
Dim _Red_Sum As Double = 0.0          'Stores the accumulated
Red reading
Dim _NIR_Avg As Double = 0.0          'Stores the averaged NIR
reading
Dim _Red_Avg As Double = 0.0          'Stores the averaged Red
reading
Dim _TempAir_Sum As Double = 0.0      'Stores the accumulated
air temperature channel measurement
Dim _TempWater_Sum As Double = 0.0    'Stores the accumulated
water temperature channel measurement
Dim _TempAir_Avg As Double = 0.0      'Store the average air
temperature (raw data, not calibrated)
Dim _TempWater_Avg As Double = 0.0    'Store the average water
temperature (raw data, not calibrated)
Dim _Vplus_Sum As Double = 0.0        'Store the accumulated V+
reading
Dim _Vplus_avg As Double = 0.0        'Store the accumulated V-
reading
Dim _Vminus_Sum As Double = 0.0       'Store the averaged V+
reading
Dim _Vminus_avg As Double = 0.0       'Store the averaged V-
reading
'=====
Dim _OD As Double                     'Stores the instantaneous
OD measurement
Dim _maxOD As Double = 1.0            'stores the max OD in the
history for graphic purpose
Dim _yhistory(ArrayLength) As Double  'For graphic
purpose, Y coordinates
Dim bm_Config As Bitmap
Dim bm_Start As Bitmap
Dim bm_Pause As Bitmap
Dim bm_Exit As Bitmap
Dim bm_Calib As Bitmap
Dim VLine1 As Integer = 0
Dim VLine2 As Integer = -CInt(_RectWidth / _PtoP / YDiv) 'This is
based on the current division of X axis in the graph
Dim VLine3 As Integer = -2 * CInt(_RectWidth / _PtoP / YDiv)
Dim VLineStr1 As String
Dim VLineStr2 As String
Dim VLineStr3 As String

'----End of variable declaration----

Private Sub picExit_Click(ByVal sender As Object, ByVal e As
System.EventArgs) Handles picExit.Click
    Dim _result As Integer = MsgBox("Exit Program?",
MsgBoxStyle.YesNo, "Exit")

```

```

If _result = vbYes Then
    If _LogFileCreated Then          'If there is a log File
        _rawdata.Close()           'Close the log file
    End If
    Application.Exit()              'Exit the application
End If
End Sub

Private Sub Timer1_Tick(ByVal sender As Object, ByVal e As
System.EventArgs) Handles Timer1.Tick
    '----Read Channel NIR, which is connected to PIN5----
    _Channel(0) = 1
    _Channel(2) = 3                  'range from -10v to +10v
    DeviceIoControl(_RLCHandleAnalog, IOCTL_RLC_ANALOGIN1, _
        _Channel, _Channel.Length, _Data, _Data.Length, Nothing,
Nothing)
    _RawData_NIR = BitConverter.ToInt16(_Data, 0)
    '----Current hardware setting has negative channel outputs
    '----Therefore the AIN was setup as the +- 5V full range
    If (_RawData_NIR And &H800) = &H800 Then
        _RawData_NIR = _RawData_NIR Or &HFFFFFF00
    End If
    _Read_Analog_NIR = (_RawData_NIR * 20) / 4096
    '----End of read channel NIR----

    '----Read Channel RED, which is connected to PIN4----
    _Channel(0) = 0
    _Channel(2) = 3                  'range from -10v to
+10v
    DeviceIoControl(_RLCHandleAnalog, IOCTL_RLC_ANALOGIN1, _
        _Channel, _Channel.Length, _Data, _Data.Length, Nothing,
Nothing)
    _RawData_Red = BitConverter.ToInt16(_Data, 0)
    If (_RawData_Red And &H800) = &H800 Then
        _RawData_Red = _RawData_Red Or &HFFFFFF00
    End If
    _Read_Analog_Red = (_RawData_Red * 20) / 4096
    '----End of read channel RED----
    'Add the code for temperature sensor reading
    'Channel 3 is connected to the sensor in air
    'Chaneel 5 is connected to the sensor in water
    _Channel(0) = 3
    _Channel(2) = 3
    DeviceIoControl(_RLCHandleAnalog, IOCTL_RLC_ANALOGIN1, _
        _Channel, _Channel.Length, _Data, _Data.Length, Nothing,
Nothing)
    _RawData_TempAir = BitConverter.ToInt16(_Data, 0)
    If (_RawData_TempAir And &H800) = &H800 Then

```

```

_RawData_TempAir = _RawData_TempAir Or &HFFFFFF00
End If
_Read_Analog_TempAir = (_RawData_TempAir * 20) / 4096

_Channel(0) = 5
_Channel(2) = 3
DeviceIoControl(_RLCHandleAnalog, IOCTL_RLC_ANALOGIN1, _
_Channel, _Channel.Length, _Data, _Data.Length,
Nothing, Nothing)
_RawData_TempWater = BitConverter.ToInt16(_Data, 0)
If (_RawData_TempWater And &H800) = &H800 Then
_RawData_TempWater = _RawData_TempWater Or &HFFFFFF00
End If
_Read_Analog_TempWater = (_RawData_TempWater * 20) / 4096

'Add the code for power supply voltage
'Channel 2 is connected to power supply Raw Nir
'Channel 4 is connected to power supply Raw Red
'The measurement range for these two channels is -10 to +10

_Channel(0) = 2
_Channel(2) = 1
DeviceIoControl(_RLCHandleAnalog, IOCTL_RLC_ANALOGIN1, _
_Channel, _Channel.Length, _Data, _Data.Length,
Nothing, Nothing)
_RawData_Vplus = BitConverter.ToInt16(_Data, 0)

If (_RawData_Vplus And &H800) = &H800 Then
_RawData_Vplus = _RawData_Vplus Or &HFFFFFF00
End If
_Read_Analog_Vplus = (_RawData_Vplus * 10) / 4096

_Channel(0) = 4
_Channel(2) = 1
DeviceIoControl(_RLCHandleAnalog, IOCTL_RLC_ANALOGIN1, _
_Channel, _Channel.Length, _Data, _Data.Length,
Nothing, Nothing)
_RawData_Vminus = BitConverter.ToInt16(_Data, 0)
If (_RawData_Vminus And &H800) = &H800 Then
_RawData_Vminus = _RawData_Vminus Or &HFFFFFF00
End If
_Read_Analog_Vminus = (_RawData_Vminus * 10) / 4096

_ProgramCounter = _ProgramCounter + 1

If (_IsLOG = False) Then

Dim _MoniStr As New System.Text.StringBuilder
_MoniStr.Append("Monitor: NIR ")
_MoniStr.Append(_Read_Analog_NIR.ToString("F3"))
_MoniStr.Append("[V] | RED ")

```

```

_MoniStr.Append(_Read_Analog_Red.ToString("F3"))
_MoniStr.Append("[V]")
lblTitle.Text = _MoniStr.ToString()

ElseIf (_IsLOG = True) Then

    _LogCounter = _LogCounter + 1

    _NIR_Sum = _NIR_Sum + _Read_Analog_NIR
    _Red_Sum = _Red_Sum + _Read_Analog_Red
    _TempAir_Sum = _TempAir_Sum + _Read_Analog_TempAir
    _TempWater_Sum = _TempWater_Sum + _Read_Analog_TempWater
    _Vplus_Sum = _Vplus_Sum + _Read_Analog_Vplus
    _Vminus_Sum = _Vminus_Sum + _Read_Analog_Vminus

    If (_LogCounter >= _LogIntvlShort * _SampleRate) Then 'e.g.,
20Hz * 20s = 400 readings

        _NIR_Avg = _NIR_Sum / (_LogIntvlShort * _SampleRate)
        _Red_Avg = _Red_Sum / (_LogIntvlShort * _SampleRate)
        _TempAir_Avg = _TempAir_Sum / (_LogIntvlShort *
_SampleRate)
        _TempWater_Avg = _TempWater_Sum / (_LogIntvlShort *
_SampleRate)
        _Vplus_avg = _Vplus_Sum / (_LogIntvlShort * _SampleRate)
        _Vminus_avg = _Vminus_Sum / (_LogIntvlShort *
_SampleRate)

'=====
'Apply the calibration equation here
_OD = 1
lblRed.Text = "Red[V]: " & _NIR_Avg.ToString("F3")
lblNIR.Text = "NIR[V]: " & _Red_Avg.ToString("F3")
lblOD.Text = "OD: " & _OD.ToString("F2")

'Apply the temperature equation here
'=====
'=====
'=====

lblAir.Text = "Amb: " & _TempAir_Avg.ToString("F3")
'change string added to the log
lblWater.Text = "CP: " & _TempWater_Avg.ToString("F3")
lblV1.Text = "RNIR: " & _Vplus_avg.ToString("F2")
lblV2.Text = "RRED: " & _Vminus_avg.ToString("F2")

'---- Log the readings into the log file-----
'Use stringbuilder is faster
Dim _RecStr As New System.Text.StringBuilder

_RecStr.Append(_NIR_Avg.ToString("F4"))

```

```

_RecStr.Append(",")
    _RecStr.Append(_Red_Avg.ToString("F4"))
    _RecStr.Append(",")
    _RecStr.Append(_OD.ToString("F4"))
    _RecStr.Append(",")
    _RecStr.Append(_TempAir_Avg.ToString("F4"))
    _RecStr.Append(",")
    _RecStr.Append(_TempWater_Avg.ToString("F4"))
    _RecStr.Append(",")
    _RecStr.Append(_Vplus_avg.ToString("F3"))
    _RecStr.Append(",")
    _RecStr.Append(_Vminus_avg.ToString("F3"))
    _RecStr.Append(",")
    _RecStr.Append(Now.ToLongTimeString)
    _rawdata.WriteLine(_RecStr.ToString())

'Needs to close and reopen the file to make sure the data are not
lost due to power down or other unexpected errors
    If (_ProgramCounter Mod (_SampleRate * _LogIntvlShort *
10) = 0) Then
        _rawdata.Close()
        _rawdata = IO.File.AppendText(_DataFileFullPath)
    End If

End If

End Sub

Private Sub picLog_Click(ByVal sender As Object, ByVal e As
System.EventArgs) Handles picLog.Click
    If Not _IsLOG Then
        '----For the first time hit this button in the program
        '----The log file needs to be created in the data
directory
        '----Directory & file operation----
        If Not _LogFileCreated Then

            If IO.Directory.Exists(_wd) = False Then 'If the
directory cannot be created
                Try
                    IO.Directory.CreateDirectory(_wd)
                Catch ex As Exception
                    Dim _result As Integer = MsgBox("Failed to
create the data folder, Continue into monitor mode?",
_MsgBoxStyle.YesNo + MsgBoxStyle.Critical, "Error 0")
                    If _result = vbNo Then
                        Application.Exit()
                    End If
                End Try
            End If
        End If
    End If

```

```

Dim _filenum As Integer = 1
    Dim _Moment As Date = Now
    Dim _tempdata As String = _wd & CStr(_Moment.Month) &
    "-" & CStr(_Moment.Day) & "-" & CStr(_Moment.Year) & "-" &
    CStr(_filenum) & ".txt"

    Do While IO.File.Exists(_tempdata) = True
        _filenum = _filenum + 1
        _tempdata = _wd & CStr(_Moment.Month) & "-" &
    CStr(_Moment.Day) & "-" & CStr(_Moment.Year) & "-" & CStr(_filenum) &
    ".txt"
    Loop

    _DataFileName = CStr(_Moment.Month) & "-" &
    CStr(_Moment.Day) & "-" & CStr(_Moment.Year) & "-" & CStr(_filenum) &
    ".txt"
    _DataFileFullPath = _tempdata

    Try
        _rawdata = IO.File.CreateText(_DataFileFullPath)
        _rawdata.WriteLine("RED[V],NIR[V],OD,
    AirTemperature, Cold PlateTemperature, Raw RED, Raw NIR, TIME")
        _LogFileCreated = True
        _IsLOG = True
        picLog.Image = bm_Pause
        lblTitle.Text = "Logging: " & _DataFileName
        _LogCounter = 0

        '-----
        VLineStyle1 = Now.ToShortTimeString()
        '-----

    Catch ex As Exception
        Dim _result As Integer = MsgBox("Fail to create the
    data log file, Continue into monitor mode?", _MsgBoxStyle.YesNo +
    MsgBoxStyle.Critical, "Error 1")
        If _result = vbNo Then
            Application.Exit()
        Else
            _LogFileCreated = False
            _IsLOG = False
        End If
    End Try

    '----End of creating directory & log file operation----
    ElseIf _LogFileCreated Then

    Try
        _rawdata = IO.File.AppendText(_DataFileFullPath)
        _IsLOG = True
        picLog.Image = bm_Pause
        lblTitle.Text = "Logging: " & _DataFileName
        _LogCounter = 0

```

```

Catch ex As Exception
    Dim _result As Integer = MsgBox("Fail to reopen the
data log file, Continue into monitor mode?", _MsgBoxStyle.YesNo +
MsgBoxStyle.Critical, "Error 2")
    If _result = vbNo Then
        Application.Exit()
    Else
        _IsLOG = False

        picLog.Image = bm_Start
        lblTitle.Text = "Monitoring"
        _LogCounter = 0
    End If
End Try

End If

ElseIf _IsLOG Then 'If the status is LOGGING and the start/stop
button pressed

    _rawdata.Close()           'Close the log file
    picLog.Image = bm_Start
    _IsLOG = False             'Set the _IsLOG flag to false
    _LogCounter = 0            'Reset the _LogCounter
    lblTitle.Text = "Monitoring"
    _NIR_Sum = 0.0             'Reset the _NIR_Sum
    _Red_Sum = 0.0             'Reset the _Red_Sum
    _TempAir_Sum = 0.0
    _TempWater_Sum = 0.0
    _Vplus_Sum = 0.0
    _Vminus_Sum = 0.0

End If
End Sub

Private Sub MainFrm_Load(ByVal sender As Object, ByVal e As
System.EventArgs) Handles MyBase.Load

    '----Open up the Analog Input Channels----
    _RLCHandleAnalog = CreateFile("RLC1:", &HC0000000, 0, 0, 3, 0,
0)

    If _RLCHandleAnalog = INVALID_HANDLE_VALUE Then
        Dim _result = MsgBox("Fail to open analog ports, please
retry", MsgBoxStyle.OkOnly + MsgBoxStyle.Exclamation)
        If _result = vbOK Then
            Application.Exit()
        End If
    End If
End If

```



```

'-----
'_Channel(2) = 1    'Set the measurement as +- 5V full range
Timer1.Interval = 1000 / _SampleRate
Timer1.Enabled = True

bm_Calib = New Bitmap(My.Resources.Calib)
picCalib.Image = bm_Calib

bm_Config = New Bitmap(My.Resources.Config4)
picSetting.Image = bm_Config

bm_Start = New Bitmap(My.Resources.Start4)
picLog.Image = bm_Start

bm_Pause = New Bitmap(My.Resources.Pause4)

bm_Exit = New Bitmap(My.Resources.Exit4)
picExit.Image = bm_Exit

End Sub
Private Sub picSetting_Click(ByVal sender As Object, ByVal e As
System.EventArgs) Handles picSetting.ClickSettingFrm.ShowDialog()
End Sub

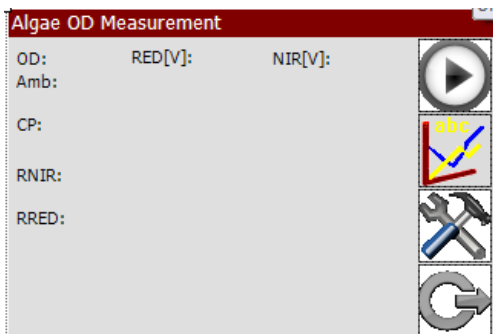
Private Sub picCalib_Click(ByVal sender As Object, ByVal e As
System.EventArgs) Handles picCalib.ClickCalibFrm.ShowDialog()
End Sub

Private Sub lblV1_ParentChanged(ByVal sender As System.Object,
ByVal e As System.EventArgs) Handles lblV1.ParentChanged

End Sub
End Class

```

Design:



[Module1.vb]

Module Module1

```
Public _wd As String = "\SDCard\Algae\" 'the working
directory
Public _rawdata As IO.StreamWriter 'stream write for the
datafile
Public _DataFileName As String 'the data file name
for current data collection as "6-2-2010-01"
Public _DataFileFullPath As String 'the full path of the
file name as "\SDCard\Algae\6-2-2010-02.txt"
Public _SampleRate As Integer = 20 'Define the sampling
rate of analog inputs, default is 25 Hza
Public _LogIntvlShort As Integer = 20 'Define the short
data log interval, default is every 60 second
Public _ODRange As Double = 1.0 'Measurement Range,
defined on the graphic Y axis
Public _RedCoef As Double
Public _NIRCoef As Double
Public _Intercept As Double
Public _Offset As Double = -0.12
Public Const _LowerEnd = -0.05 'For graphic purpose,
set the lower end as -0.05
Public XDivTime(3) As Date
'Public _RLCHandlerRS485 As IntPtr 'variable for RS485(COM2) on
the RLC mainboard
Public Declare Function DeviceIoControl Lib "coredll.dll" _
    (ByVal hDevice As IntPtr, _
    ByVal dwIoControlCode As Int32, _
    ByVal lpInBuffer As Byte(), _
    ByVal dwInBufferSize As Int32, _
    ByVal lpOutBuffer As Byte(), _
    ByVal dwOutBufferSize As Int32, _
    ByRef lpBytesReturned As Int32, _
    ByVal lpOverlapped As IntPtr) As Boolean
Public Declare Function CreateFile Lib "coredll.dll" _
    (ByVal lpFileName As String, ByVal dwDesiredAccess As
Int32, _ByVal dwShareMode As Int32, ByVal lpSecurityAttributes As
IntPtr, _ByVal dwCreationDisposition As Int32, ByVal
dwFlagsAndAttributes As Int32, _ByVal hTemplateFile As IntPtr) As
IntPtr

Public Declare Function CloseHandle Lib "coredll.dll" _
    (ByVal hObject As IntPtr) As Boolean

Public Const IOCTL_RLC_ANALOGIN1 = &H4 'To use the analog
inputs on Micropod
Public Const IOCTL_RLC_SERIALMODE = &H16 'To use serial port in
RS485 protocol
Public Const INVALID_HANDLE_VALUE = -1&
End Module
```

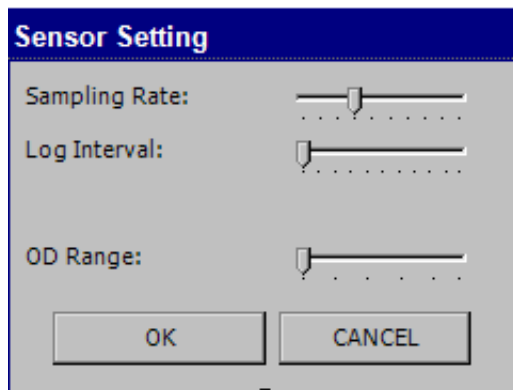
[SettingFrm.vb]

```
Public Class SettingFrm

    'Dim _SetSmplRt As Integer
    'Dim _SetIntvlShort As Integer
    'Dim _SetIntvlLong As Integer
    'Dim _SetODRange As Double

    Private Sub btnCancel_Click(ByVal sender As Object, ByVal e As
System.EventArgs) Handles btnCancel.ClickMe.Close()
    End Sub
    Private Sub SettingFrm_Load(ByVal sender As Object, ByVal e As
System.EventArgs) Handles MyBase.Load
        TrckBarSR.Value = _SampleRate
        lblSR.Text = "Sampling Rate: " & _SampleRate.ToString()
        TrckBarLogShort.Value = _LogIntvlShort
        lblLogShort.Text = "Log Short: " & _LogIntvlShort.ToString()
        TrckBarRange.Value = _ODRange * 10
        lblODRange.Text = "OD Range: " & _ODRange.ToString("F1")
    End Sub
    Private Sub btnOK_Click(ByVal sender As Object, ByVal e As
System.EventArgs) Handles btnOK.Click
        _SampleRate = TrckBarSR.Value
        _LogIntvlShort = TrckBarLogShort.Value
        _ODRange = CDb1(TrckBarRange.Value / 10)
        MainFrm.Invalidate()
        MainFrm.Timer1.Interval = Int(1000 / _SampleRate)
        Me.Close()
    End Sub
    Private Sub TrckBarSR_ValueChanged(ByVal sender As Object, ByVal
e As System.EventArgs) Handles TrckBarSR.ValueChanged
        lblSR.Text = "Sampling Rate: " &
(TrckBarSR.Value).ToString()
    End Sub
    Private Sub TrckBarRange_ValueChanged(ByVal sender As Object,
ByVal e As System.EventArgs) Handles TrckBarRange.ValueChanged
        lblODRange.Text = (TrckBarRange.Value / 10).ToString("F1")
    End Sub
    Private Sub TrckBarLogShort_ValueChanged(ByVal sender As Object,
ByVal e As System.EventArgs) Handles TrckBarLogShort.ValueChanged
        lblLogShort.Text = "Log Short: " &
(TrckBarLogShort.Value).ToString()
    End Sub
End Class
```

Design:



APPENDIX B

DATA USED FOR CALIBRATION AND VALIDATION OF THE ORIGINAL
SENSOR AND REDESIGNED SENSOR

Table 2: Calibration data set for the original sensor (calibrated on 08/16/2010)

NIR (volts)	RED (volts)	Spectrometer measured OD (10 dilution factor)
-2.438	-2.879	0.018
-1.977	-2.186	0.040
-1.627	-1.694	0.061
-1.540	-1.558	0.067
-1.331	-1.297	0.096
-1.165	-1.136	0.117
-1.054	-1.057	0.105
-0.752	-0.894	0.183

Table 3: Validation data set for the original sensor (test on 10/18/2010)

Spectrometer measured OD (10 dilution factor)	Sensor estimated OD
0.106	0.972
0.079	0.725
0.088	0.802
0.093	0.905
0.101	1.064
0.102	0.990

Table 4: Original recorded offline OD measurement and two channels output (test from 06/04/2012 to 06/24/2012 of the redesigned sensor)

date	light condition	time	Offline OD measurement	Red channel output (V)	NIR channel output (V)
04-06-12	d	15:30	0.67	1.562	4.153
05-06-12	d	10:30	0.89	1.678	4.365
	d	11:30	0.84	1.678	4.359
	d	12:30	0.86	1.678	4.354
	d	13:30	0.80	1.578	4.041
	d	14:30	0.82	1.578	4.033
	d	15:30	0.82	1.577	4.034
	d	16:48	0.81	1.573	4.207
	d	17:41	0.80	1.573	4.207
06-06-12	d	09:39	0.96	1.715	4.335
	d	10:45	0.96	1.711	4.331
	d	11:35	0.96	1.709	4.326
	d	12:35	0.96	1.709	4.327
	d	13:45	0.95	1.709	4.327
	d	14:45	0.96	1.711	4.333
	d	15:43	0.96	1.712	4.336
	d	16:35	0.96	1.715	4.340
07-06-12	d	09:40	1.08	1.846	4.706
	d	10:48	1.09	1.846	4.709
	d	11:44	1.05	1.846	4.710
	d	12:40	1.08	1.847	4.714
	d	14:10	1.01	1.731	4.387
	d	15:10	1.00	1.730	4.391
	d	16:10	1.02	1.734	4.396
	d	17:10	1.01	1.732	4.390
	d	18:10	0.55	1.275	2.789
08-06-12	d	08:50	0.60	1.368	3.103
	d	10:20	0.59	1.376	3.082
11-06-12	l	21:40	1.09	1.898	4.874
12-06-12	d	10:30	1.17	1.948	5.503
	d	11:30	0.93	1.671	4.293
	d	12:30	0.92	1.669	4.295
	d	13:30	0.95	1.667	4.299
	d	14:30	0.93	1.669	4.305

date	light condition	time	Offline OD measurement	Red channel output (V)	NIR channel output (V)
	d	15:30	0.95	1.669	4.305
	d	16:30	0.96	1.669	4.321
13-06-12	d	10:30	1.07	1.822	4.740
	d	11:30	1.08	1.829	4.793
	d	12:30	1.09	1.829	4.810
	d	13:30	1.07	1.820	4.811
	l	21:30	1.11	1.820	4.926
14-06-12	d	10:40	1.20	1.967	5.109
	d	11:35	1.19	1.963	5.109
	d	12:33	1.17	1.953	5.103
	d	13:30	1.17	1.953	5.110
	l	22:30	0.52	1.441	2.983
15-06-12	d	08:40	0.52	1.309	3.077
	d	09:30	0.51	1.321	3.096
	d	10:40	0.54	1.324	3.105
	d	11:30	0.52	1.301	3.084
	d	12:30	0.53	1.325	3.109
	d	13:30	0.49	1.229	3.090
16-06-12	d	08:07	0.64	1.446	3.582
	d	09:06	0.66	1.456	3.580
	d	10:00	0.65	1.458	3.587
	d	11:00	0.64	1.458	3.593
	d	12:00	0.65	1.457	3.606
	d	13:00	0.65	1.459	3.624
	l	21:10	0.69	1.537	3.781
17-06-12	d	12:10	0.76	1.607	4.110
	d	13:10	0.81	1.609	4.117
	d	14:10	0.81	1.610	4.132
21-06-12	d	17:00	1.02	1.821	4.800

Table 5: Calibration data set for the redesigned sensor (test from 06/04/2012 to 06/24/2012)

Spectrometer OD measurement	Red channel output (V)	NIR channel output(V)
0.52	1.441	2.983
0.80	1.578	4.041
0.96	1.711	4.331
1.09	1.898	4.874
0.95	1.667	4.299
0.81	1.610	4.132
1.17	1.953	5.103
0.86	1.678	4.354
0.92	1.669	4.295
1.00	1.730	4.391
0.65	1.457	3.606
1.08	1.846	4.706
1.17	1.953	5.110
0.69	1.537	3.781
1.08	1.829	4.793
0.96	1.709	4.326
0.64	1.458	3.593
1.05	1.846	4.710
0.55	1.275	2.789
1.19	1.963	5.109
0.53	1.325	3.109
0.64	1.446	3.582
0.84	1.678	4.359
0.67	1.562	4.153
1.01	1.731	4.387
1.07	1.820	4.811
0.81	1.609	4.117
0.95	1.709	4.327
0.95	1.669	4.305
1.09	1.846	4.709
0.96	1.669	4.321
0.8	1.573	4.207
1.02	1.821	4.800
0.81	1.573	4.207
0.96	1.709	4.327

Spectrometer OD measurement	Red channel output (V)	NIR channel output(V)
1.08	1.847	4.714
0.49	1.229	3.090
1.09	1.829	4.810
0.96	1.712	4.336
0.65	1.459	3.624

Table 6: Validation data set for the test of the redesigned sensor (test from 06/04/2012 to 06/24/2012)

Offline OD measurement	Sensor predicted OD
1.17	1.214
0.76	0.830
0.60	0.559
1.02	0.956
0.82	0.800
0.51	0.519
0.52	0.502
0.89	0.908
0.96	0.936
0.59	0.564
1.01	0.954
0.65	0.669
0.96	0.932
0.93	0.896
0.93	0.896
1.20	1.201
0.66	0.666
1.11	1.066
1.07	1.054
0.52	0.508
0.54	0.522
0.96	0.936
0.82	0.800

Table 7: RTD temperature probe calibration data points for the ambient air temperature

Temperature (°C)	voltage (V)
40	3.953
39	3.873
38	3.783
37	3.700
36	3.605
35	3.502
34	3.431
33	3.332
32	3.241
31	3.151
30	3.060
29	2.972
28	2.880
27	2.792
26	2.680
25	2.606
24	2.515
23	2.427
22	2.337
21	2.245
20	2.155
19	2.064
18	1.973
17	1.882
16	1.792
15	1.695
14	1.610
13	1.519
12	1.427
11	1.338
10	1.247
9	1.156
8	1.065
7	0.975
6	0.884
5	0.793

Table 8: RTD temperature probe calibration data points for the algal culture temperature

Temperature (°C)	Voltage (V)
37.1	3.720
35.8	3.600
34.8	3.510
33.8	3.419
32.8	3.329
31.8	3.238
30.7	3.138
29.8	3.056
28.6	2.946
27.8	2.874
26.7	2.774
25.4	2.656
22.7	2.410
21.8	2.327
20.8	2.236
19.8	2.145
18.5	2.026
17.7	1.962
16.2	1.816
15.7	1.771
14.6	1.670
13.6	1.579
12.4	1.469
11.0	1.342
10.3	1.277
9.3	1.186
8.3	1.095
7.3	1.004
6.4	0.922
5.2	0.813

Table 9: Thermistor calibration data points for monitoring the regulated temperature

Temperature (°C)	Voltage (V)
44.0	3.880
42.8	3.730
41.0	3.536
38.0	3.244
36.0	3.040
33.5	2.803
30.9	2.571
27.6	2.292
24.2	2.002
23.7	1.967
22.5	1.874
20.6	1.738

APPENDIX C
MULTIPLE LINEAR REGRESSION STATISTICS FOR BOTH ORIGINAL AND
NEW SENSOR

Table 10: Regression statistics of the original sensor calibration on 08/16/2010

Regression Statistics	
Multiple R	0.98
R Square	0.97
Adjusted R Square	0.95
Standard Error	0.01
Observations	8

Table 11: Coefficients for the calibration of the original sensor on 08/16/2010

	Coefficients	Standard Error	t statistic	p-value
Intercept	0.249	0.015	16.916	1.3205E-05
NIR channel output(V)	0.249	0.047	5.3513	0.003
Red channel output(V)	-0.130	0.038	-3.457	0.018

Table 12: Regression statistics of the redesigned sensor calibration from the test from 06/04/2012 to 06/24/2012

Regression Statistics	
Multiple R	0.98
R Square	0.95
Adjusted R Square	0.95
Standard Error	0.04
Observations	40

Table 13: Coefficients for the calibration of the from 06/04/2012 to 06/24/2012 (tests of the redesigned sensor)

	Coefficients	Standard Error	t statistic	p-value
Intercept	-0.800	0.081	-9.918	5.75E-12
Red channel output(V)	0.827	0.166	4.974	1.53E-05
NIR channel output(V)	0.0734	0.052	1.399	0.170

APPENDIX D

LAYOUT OF THE PCB IN THE NEW SENSOR

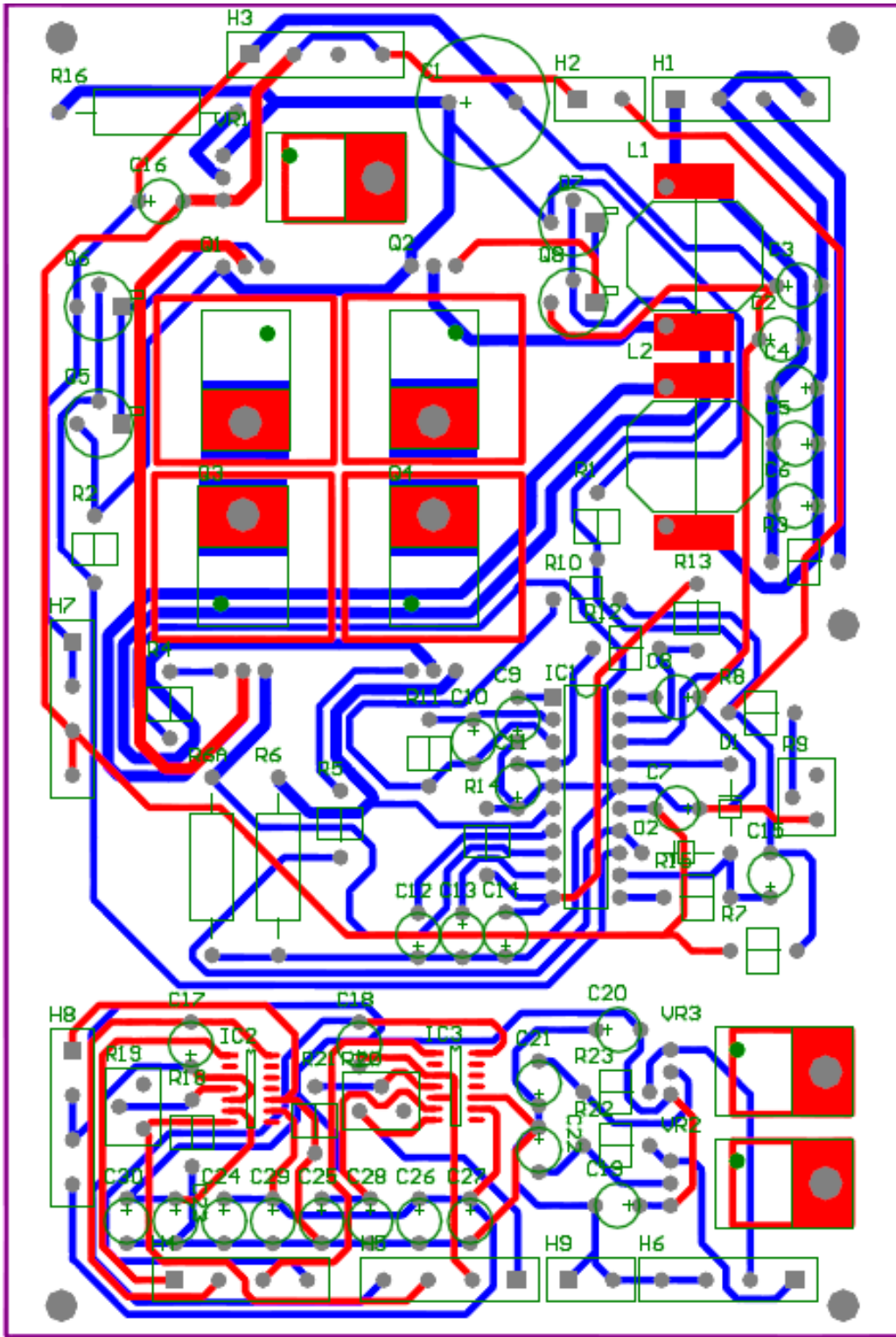


Figure 42: The PCB layout of the whole electronic circuit for the new sensor

APPENDIX E

WHOLE SCHEMATIC OF THE CIRCUITS (LED DRIVER, LOGARITHMIC
CIRCUIT AND TEC CONTROL CIRCUIT) AND THE VALUE OF EACH
COMPONENT

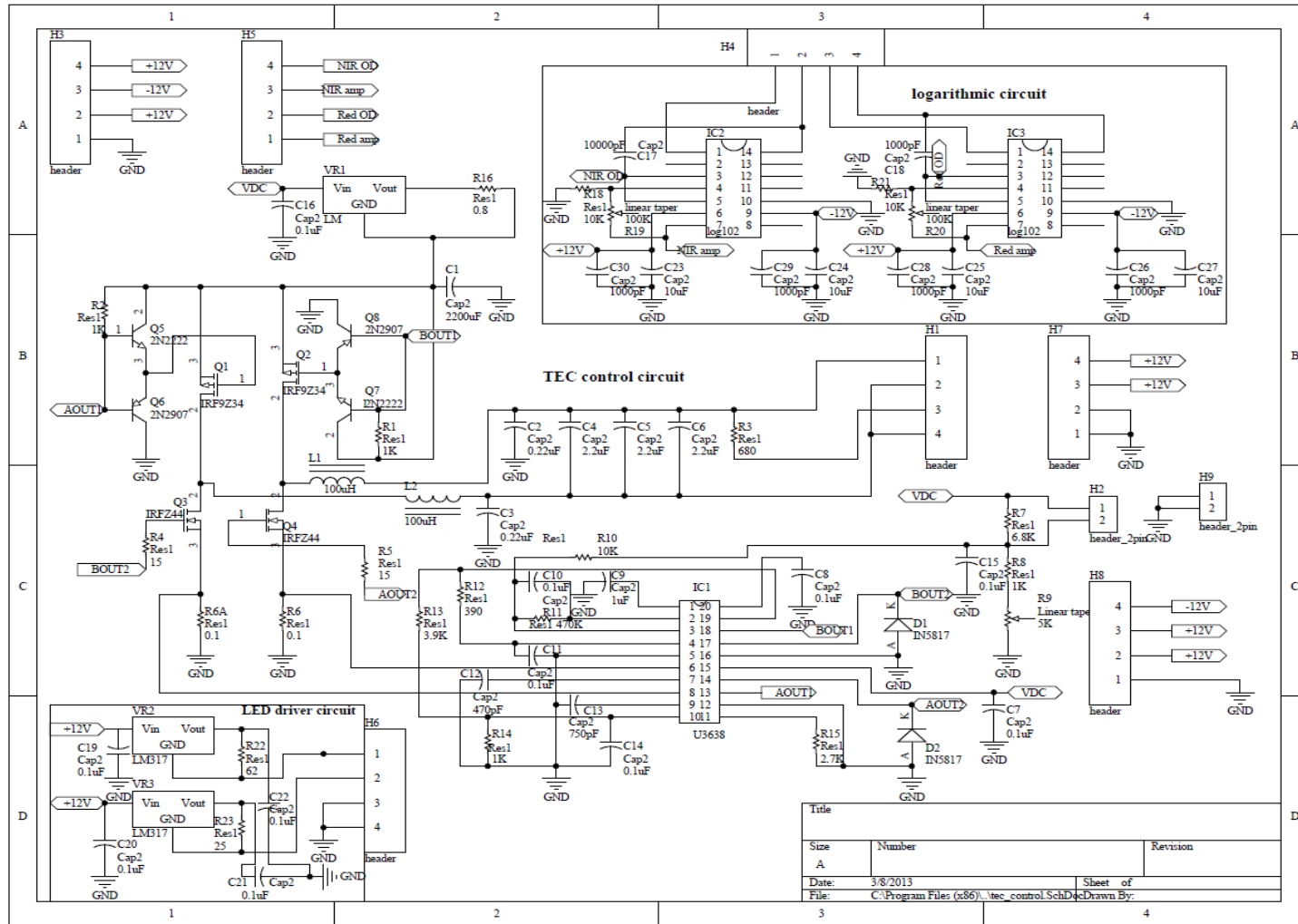


Figure 43: Whole schematic of the new sensor circuits including TEC control circuit, LED drivers and logarithmic circuit